First publ. in: Reviews in Mineralogy and Geochemistry 47 (2002), pp. 615-700

14 Noble Gases in Lakes and Ground Waters

Rolf Kipfer[1,2], Werner Aeschbach-Hertig[1,3], Frank Peeters[1], and Marvin Stute[4]

[1]*Department of Water Resources and Drinking Water*
Swiss Federal Institute of Environmental Science and Technology, EAWAG
8600 Dübendorf, Switzerland
rolf.kipfer@eawag.ch

[2]*Institute for Isotope Geology and Mineral Resources*
[3]*Environmental Physics*
Swiss Federal Institute of Technology, ETH Z
8092 Zürich, Switzerland

[4]*Barnard College, Columbia University*
New York, New York

INTRODUCTION

In contrast to most other fields of noble gas geochemistry that mostly regard atmospheric noble gases as 'contamination,' air-derived noble gases make up the far largest and hence most important contribution to the noble gas abundance in meteoric waters, such as lakes and ground waters. Atmospheric noble gases enter the meteoric water cycle by gas partitioning during air / water exchange with the atmosphere.

In lakes and oceans noble gases are exchanged with the free atmosphere at the surface of the open water body. In ground waters gases partition between the water phase and the soil air of the quasi-saturated zone, the transition between the unsaturated and the saturated zone. Extensive measurements have shown that noble gas concentrations of open waters agree well with the noble gas solubility equilibrium according to (free) air / (free) water partitioning, whereby the aquatic concentration is directly proportional to the respective atmospheric noble gas abundance (Henry law, Aeschbach-Hertig et al. 1999b).

In applications in lakes and ground waters the gas specific Henry coefficient can simplifying be assumed to depend only on temperature and salinity of the water. Hence the equilibrium concentrations of noble gases implicitly convey information on the physical properties of the water during gas exchange at the air / water interface, i.e., air pressure, temperature and salinity of the exchanging water mass. The ubiquitous presence of atmospheric noble gases in the meteoric water cycle defines a natural baseline, which masks other noble gas components until their abundance is sufficiently large that these components can be separated against the natural atmospheric background. For most classical geochemical aspects this typical feature of natural waters may look at first sight as a disadvantage. In fact it turns out to be advantageous because in most cases the noble gas abundance in water can be understood as a binary mixture of two distinct noble gas components—a well-constrained atmospheric component and a residual component of non-atmospheric origin.

Only very few processes are able to fractionate atmospheric noble gases. All these processes are controlled by well-understood physical mechanisms, which in consequence constrain air-derived noble gases and any other component completely. In addition to atmospheric noble gases basically two non-atmospheric noble gas components are present in most natural waters: *radiogenic* noble gases and *terrigenic* noble gases from different geochemical compartments of the Earth.

Radiogenic noble gases are generated by all kinds of disintegrations of radioactive

precursors and succeeding nuclear reactions (see Ballentine and Burnard 2002 in this volume). Only $^{4}He_{rad}$, $^{3}He_{rad}$, occasionally $^{40}Ar_{rad}$, and very rarely $^{21}Ne_{rad}$ have sufficiently large production yields that these isotopes can be observed in natural waters. Whereas rocks and minerals generate all four isotopes, ^{3}He (as tritiogenic $^{3}He_{tri}$) is also produced by the decay of atmospheric tritium (^{3}H, half-life: 4500 d, Lucas and Unterweger 2000) that is bound in meteoric water molecules. On the one hand the combined analysis of tritiogenic $^{3}He_{tri}$ and ^{3}H allows the quantitative dating of young waters having residence times of up to 50 years (e.g., Tolstikhin and Kamenskiy 1969; Schlosser et al. 1988; Solomon and Cook 2000). On the other hand radiogenic $^{4}He_{rad}$ generally yields qualitative ages for old ground waters recharging on millennium time scales (e.g., Solomon 2000).

Terrigenic noble gases denote as a collective term noble gases originating from well-defined geochemical reservoirs with a distinct geochemical composition. In meteoric waters two terrigenic components can be found: noble gases of crustal and of mantle origin. Terrigenic fluids are defined by the characteristic isotopic composition of He. The particular $^{3}He/^{4}He$ ratio is a defining feature of the respective terrigenic component. The continental crust is dominated by isotopically heavy He that is produced *in situ* by nuclear reactions in crustal rocks and minerals ($^{3}He/^{4}He < 10^{-7}$, Mamyrin and Tolstikhin 1984, Ballentine and Burnard 2002 in this volume). Note that in the literature crustal He is often identified by radiogenic He. Here, we distinguish between He that is produced by nuclear processes ('radiogenic He') and He that originates from a geochemical reservoir ('terrigenic He'). The Earth mantle contains besides newly produced He relicts of isotopic light He inherited during planet formation ($^{3}He/^{4}He > 10^{-5}$, Mamyrin and Tolstikhin 1984; see Porcelli and Ballentine 2002 and Graham 2002 in this volume).

In summary, in most cases the noble gas concentrations in meteoric waters can be understood as a mixture of *atmospheric* noble gases (He, Ne, Ar, Kr, Xe) with variable amounts of *radiogenic* and / or *terrigenic* He. The noble gas concentrations in meteoric waters can be translated into

1. climatic conditions during air / water exchange (*atmospheric noble gas component*),
2. water-residence times and renewal rates (*radiogenic noble gas component, mainly He*), and
3. geochemical fingerprints and the origin of non-atmospheric fluids (*terrigenic noble gas component, mainly He*).

In lakes and young ground waters the determination of water residence times by ^{3}H-^{3}He dating in order to study transport and mixing processes has been the prevalent use of noble gas isotopes (e.g., Torgersen et al. 1977; Schlosser et al. 1988). Recent applications in lakes also used the concentrations of atmospheric noble gases to reconstruct possible lake level fluctuations in the past recorded as change of the partial pressure of the (noble) gases due to variation of the altitude of the lake surface (Craig et al. 1974; Kipfer et al. 2000).

Similarly, the dependence of noble gas solubility equilibrium on the physical conditions during gas exchange, in particular the sensitivity of the Henry coefficients on temperature, has successfully been used in ground-water studies to reconstruct the soil temperature prevailing during ground-water recharge. If an aquifer contains ground waters that recharged during different climatic conditions in the past, noble gas concentrations provide information about the past temperature evolution (Mazor 1972; Andrews and Lee 1979). This approach has been applied to reconstruct the continental temperature regime of the Pleistocene / Holocene transition in the tropics (e.g., Stute et al. 1995b; Weyhenmeyer et al. 2000) as well as in mid latitudes (Stute et al. 1995a; Beyerle et al. 1998; Stute and Schlosser 2000; Aeschbach-Hertig et al. 2002b).

Results of all these studies were hampered by the common observation that ground waters in contrast to surface waters always contain atmospheric (noble) gases in excess, i.e., the measured dissolved noble gas concentrations are usually significantly larger than the expected solubility equilibrium. Such noble gas excesses, being characteristic for ground waters, are known in the literature as 'excess air' (Heaton and Vogel 1981). Despite experimental evidence that showed that the elemental composition of the noble gas excess is 'air-like', the formation processes responsible for the observed gas excess in ground waters remain unclear. Only recently, new concepts have been developed that link the formation of excess air with the physical processes that control air / water partitioning at the transition between the unsaturated and the saturated zone in soils. In particular two models, the partial re-equilibration and closed system equilibration model, are now available, which describe the relative abundances of dissolved atmospheric noble gases as well as the possible fractionation relative to pure air (Stute 1989; Stute et al. 1995b; Aeschbach-Hertig et al. 2000).

Apart from lakes and ground water, noble gases are also useful in the study of other continental water reservoirs, such as pore waters in sediments and rocks. However, little work has been done in these areas so far. The one 'aqueous' system that has received considerable attention in recent years is ice. The polar ice sheets have proven to be excellent archives of past environmental conditions, and noble gases as conservative tracers play a role in extracting information from these archives. A short review of recent applications of noble gases in ice is therefore included at the end of this chapter.

ANALYTICAL TECHNIQUES

The determination of noble gases in water can be divided into three successive analytical steps: (1) noble gas extraction from the water, (2) purification and separation of the extracted noble gases, and (3) quantitative (mass spectrometric) analysis. For extended discussions of methods for noble gas analysis in waters (and other terrestrial fluids) the readers are referred to Clarke et al. (1976), Rudolph (1981), Bayer et al. (1989), Stute (1989), Gröning (1994), Ludin et al. (1997), and Beyerle et al. (2000a).

Following the classical approach (Rudolph 1981; Stute 1989; Gröning 1994) the dissolved noble gases are degassed from a water sample typically collected in copper tubes (10-45 cm^3 volume) by vacuum extraction. To extract the dissolved gases the copper tubes are connected to an extraction vessel mounted on an ultra-high vacuum extraction / purification system. After pumping down the head space of the extraction vessel ($<10^{-4}$ Torr) the copper tube is opened and connected over a capillary to cold traps that are filled with adsorbent media, such as char coal or zeolite, and cooled by an acetone / dry-ice mixture or by liquid nitrogen. Vigorous shaking or stirring of the water facilitate the liberation of the volatile gases into the gas phase. The liberated gases including water vapor are transported through the capillary in the direction of the cold traps where the condensable fluids are adsorbed. The capillary limits, like a bottleneck, the amount of water being transported. The velocity of the gas stream increases to such an extent that the extracted non-condensable gases over the cold traps are prevented from back diffusion into the extraction vessel. Experiments demonstrate that a degassing procedure of about 5 min extracts more than 99.995% of the dissolved gases, but only about 0.5 g of water. As a result the extraction leads to the virtually complete separation of the gas from the water phase. If required, the degassed water can be transferred back into the original copper tube or a glass bulb and sealed off again to allow ingrowth of tritiogenic $^3He_{tri}$ for a later ^3H determination (Bayer et al. 1989; Beyerle et al. 2000a).

In the classical analytical procedure the extracted gases are dried and cleaned by passing various getter pumps. Finally a cryostatic cold trap entirely adsorbs the purified

noble gases from where they are released sequentially element by element by progressive heating. Each noble gas element is expanded into an appropriate sector and/or quadrupole mass spectrometer for final determination. The mass spectrometer and especially the set up of the ion source are tuned to guarantee long term stability and reproducibility of the noble gas analysis. Commonly the most abundant noble gas isotopes are determined on Faraday cups. The rare ^{3}He isotope is counted on an electron multiplier. The ^{3}He measurement is carried out in parallel with the measurement of the abundant ^{4}He to determine a precise ^{3}He/^{4}He ratio.

Although the classical approach is analytically fairly robust and yields reliable results for the elemental abundance of noble gases in waters, there are some experimental difficulties that are delicate to deal with. The most critical point is the element specific gas release from the cryostatic cold trap. In particular the elemental selectivity of cryostatic cold traps is too coarse to completely isolate Ar from Kr. As common ion-sources are tuned to maximum sensitivity their response to different gas amounts is not only highly non-linear, but also depends on the relative presence of all components in the rest gas. Hence the Ar residual in the Kr determination may cause analytical problems, because of the overwhelming atmospheric Ar abundance.

The problem of cryostatic separation can be circumvented by a gas preparation / purification procedure that operates without any separation of the heavier noble gases, as developed by Beyerle et al. (2000a). According this analytical method the gas phase containing the heavy noble gases is diluted to such an extent that Ar does not interfere with the measurement of the other noble gases, and Ar, Kr and Xe can be analyzed in a single measuring cycle.

According to the Beyerle et al. (2000a) extraction scheme a first series of traps cooled by liquid nitrogen adsorbs all condensable gases being extracted from a water sample. The free gas phase, that contains all the He and Ne, is cleaned and expanded for the consecutive ^{3}He, He and Ne measurement. To analyze the heavy noble gases the water vapor and the rest of the condensable fluids are released by heating up the cold traps. The wet gas phase is dried by passing a zeolite trap and expanded into a large reservoir (~2000 cm^3) from which small aliquots (~1 cm^3) are taken, cleaned and prepared for the final simultaneous mass spectrometric analysis of Ar, Kr and Xe (Beyerle et al. 2000a).

Advantages of the approach 'dilution instead of separation' are that the reactive components, mainly N_2, O_2, CH_4 and CO_2, are removed easily and that repeated measurements of a particular sample are possible. Most importantly, however, the dilution step can be adjusted such, that the Ar does not perturb the Kr and Xe detection. All three heavy noble gases can be determined in one single measurement: Ar is detected on a Faraday cup, whereas Kr and Xe are counted on an electron multiplier.

As Xe concentrations depend most sensitively on the temperature during air / water exchange, an additional gas split can be prepared for a more precise Xe measurement. Note that there is no requirement of complete or even reproducible elemental separation, only the quantitative Xe trapping has to be guaranteed.

The mass spectrometric systems and the extraction procedures are regularly calibrated against air (0.4-2 cm^3 STP), a high quality noble gas standard and/or an internal water standard (Beyerle et al. 2000a). Deep water of lakes is suggested for the use as long-term water standard, because of the stable physical conditions and the virtually constant stable noble gas concentrations of such deep-water bodies. As lake waters contain reasonable tritium amounts (e.g., Torgersen et al. 1977, 1981; Aeschbach-Hertig et al. 1996a; Hohmann et al. 1998; Peeters et al. 2000a) the water standard can

even be used for ^{3}H calibration.

The experimental methods for the analysis of the noble gases in meteoric water achieve an overall precision—expressed as relative error of an individual concentration —of about 1%. Selected elemental (He/Ne, Ar/Kr, Kr/Xe) and isotopic ratios ($^{3}He/^{4}He$, $^{20}Ne/^{22}Ne$, $^{36}Ar/^{40}Ar$) have errors of less than 0.6% (Beyerle et al. 2000a).

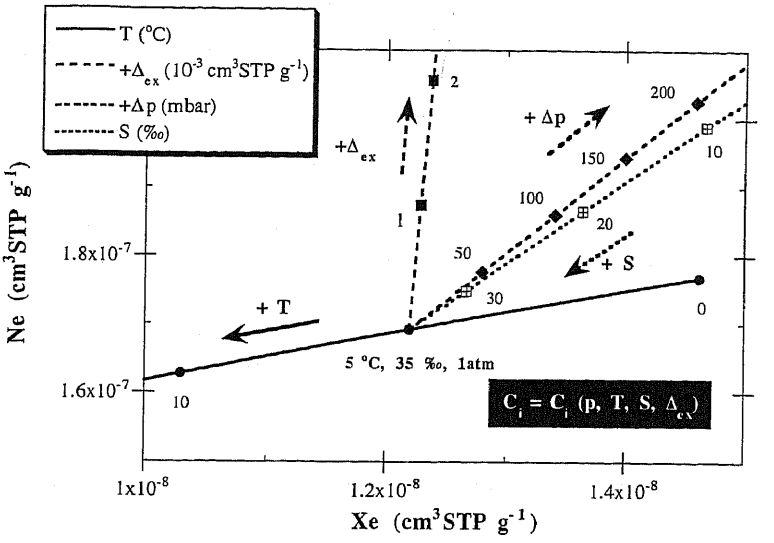

Figure 1. Effect of pressure (p), temperature (T), salinity (S), and excess air (Δ_{ex}) on gas / partitioning of Xe and Ne. Arrows indicate the increase of the noble gas concentrations in reaction to an increase of the respective property. The symbols mark the concentrations $C_i[p, T, S, \Delta_{ex}]$ being calculated for the physical conditions indicated by the numbers. Xe reacts sensitively to T changes but remains almost unaffected by injection and dissolution of air ($+\Delta_{ex}$). Ne behaves in the opposite way. Changing either pressure ($+\Delta p$) or salinity (S) has almost the same effect on all (noble) gases. Changes of the physical conditions prevailing gas exchange are imprinted and retained the specific noble gas pattern, which in turn can be back-translated in a most direct manner into information on environmental change.

NOBLE GAS COMPONENTS IN WATER

Atmospheric noble gases 1: Solubility equilibrium

Open waters with a free interface to the atmosphere tend to dissolve atmospheric gas until the concentrations of the gas and the water phase are in a thermodynamic equilibrium. The kinetic aspects of the air / water exchange are beyond the scope of this chapter. An extended review is given by Schwarzenbach et al. (1993). Gas exchange at the lake / air interface can saturate a water layer at a rate of about 1 m per day, i.e., the controlling gas transfer velocities are on the order of 10^{-5} m s^{-1}. As gas exchange phenomena are fairly fast, the surface water of open water bodies is expected to have atmospheric noble gases in equilibrium with the atmosphere at the physical conditions prevailing (Fig. 1, Table 1). This axiomatic statement is supported by experimental evidence (Craig and Weiss 1971; Aeschbach-Hertig et al. 1999b) and holds accordingly for all atmospheric gases that have neither additional sources nor sinks and hence are bio-geochemically conservative.

Gas partitioning at the free air / water interface can be described reasonably well by Henry's law, which assumes that the concentrations in the two phases are directly proportional to each other:

$$C_i^{gas} / C_i^{water} = H_i^{'}\left(T, C_j^{water}, ...\right) \approx H_i^{'}(T,S) \tag{1}$$

where C_i^{gas}, C_i^{water} denote the concentrations of gas i in the gas and in the water phase, respectively, and H_i is the 'dimensionless' Henry constant that depends on temperature T and the concentrations of all dissolved species C_j (see also Ballentine and Burnard 2002; Ballentine et al. 2002—both in this volume). For most applications, the dependence of H_i on the chemical interaction between solutes can be neglected because the concentrations of natural waters are sufficiently low that dissolved atmospheric (noble) gas species behave as ideal gases. Hence the total effect of solutes on the dissolution of a single gas can be expressed by the cumulative dependence of H_i on the salinity, S.

Note that, although dimensionless, the actual value of the H_i implicitly depends on the choice of the concentration units. Therefore caution must be exercised if Henry constants or related measures from different sources are compared.

Often Equation (1) is formulated for each particular gas in terms of its partial pressure p_i (atm, bar, ...) and corresponding equilibrium concentration $C_{i,eq}$ (cm^3 STP g^{-1}, mol l^{-1}, mol kg^{-1}, mol mol^{-1}, ...)

$$p_i = H_i \cdot C_{i,eq} \tag{2}$$

Often, instead of Henry constants, the equilibrium concentration $C_{i,eq}$ for p_i = 1 atm is reported.

Weiss and co-workers reported solubilities for ^3He, ^4He, Ne, Ar, Kr as well as for O_2 and N_2 as a function of temperature and salinity for fresh and ocean waters (Table 1; Weiss 1970, 1971; Weiss and Kyser 1978). As this fundamental piece of work was strongly motivated by practical oceanographic research, the noble gas solubilities were expressed in the form of equilibrium concentrations with moist atmospheric air. For the atmosphere, it is justified to assume that its major elemental composition remains constant over the relevant time scales controlling gas exchange. Hence the gas partial pressure p_i can be expressed by the total atmospheric pressure p_{tot} corrected for water vapor content, $e_w(T)$, and the volume or mole fraction z_i of the gas i in dry air (Ozima and Podosek 1983).

$$p_i = z_i \cdot \left[\sum_j p_j - e_w(T)\right] = z_i \cdot \left[p_{tot} - e_w(T)\right] \tag{3}$$

The decrease in atmospheric pressure with increasing altitude h can be described by a (local) barometric altitude formula.

$$p_{tot}(h) \approx p_{tot}^{sl} \cdot e^{-h/h_{atm}} \tag{4}$$

where $p_{tot}(h)$ and p_{tot}^{sl} are the local and the sea level pressure, and h_{atm} the typical local scale height (8000-8300 m). This conversion is not unique and the pressure dependence on altitude has to be adapted to local conditions (e.g., Gill 1982).

Benson and Krause (1976), Clever (1979a,b; 1980) and others (Top et al. 1987) re-evaluated the solubilities for noble gases in pure water, whereas Smith and Kennedy (1983) expanded the noble gas solubilities to the typical salinity range of natural brines. These later works had a more chemical focus and consequently solubilities were quoted

in terms of Henry constants or related measures. Comparing solubility data of different sources can cause serious pitfalls as the sets often hide principle experimental caveats. Whereas moist air equilibrium concentrations can be applied directly, other forms of solubility data have to be converted in manageable equilibrium concentrations including a salinity term (see Eqn. 11).

Table 1. Equilibrium concentrations of noble gases, nitrogen and oxygen for environmental conditions met in open water bodies.

Equilibrium concentrations *[cm^3 STP g^{-1}]*							
T [°C]	**He** [10^{-8}]	**Ne** [10^{-7}]	**Ar** [10^{-4}]	**Kr** [10^{-8}]	**Xe** [10^{-8}]	N_2 [10^{-2}]	O_2 [10^{-3}]
S = 0.1‰ *'Baikal' water*, p_{tot}= 1atm							
4	4.78	2.15	4.47	10.89	1.64	1.66	9.16
10	4.64	2.02	3.86	9.10	1.32	1.45	7.89
20	4.47	1.85	3.12	6.96	0.95	1.19	6.36
S = 6‰ *'Issyk-Kul' water*, p_{tot}= 1atm							
4	4.62	2.06	4.28	10.41	1.63	1.59	8.76
10	4.49	1.94	3.70	8.71	1.31	1.37	7.56
20	4.34	1.79	3.00	6.68	0.95	1.14	6.11
S = 12.6‰ *'Caspian Sea' water*, p_{tot}= 1atm							
4	4.45	1.98	4.07	9.89	1.63	1.51	8.35
10	4.33	1.87	3.53	8.29	1.30	1.32	7.22
20	4.19	1.72	2.87	6.38	0.94	1.09	5.85
S = 35‰, p_{tot}=1 atm ≡ 0 masl, **Ocean**							
4	3.90	1.71	3.44	8.32	1.60	1.26	7.07
10	3.82	1.63	3.00	7.01	1.28	1.11	6.15
20	3.73	1.52	2.47	5.45	0.93	0.93	5.04
S = 0.1‰, p_{tot}= 0.947 atm ≡ 458 masl, **Lake Baikal**							
4	4.53	2.03	4.23	10.31	1.55	1.57	8.67
10	4.39	1.91	3.65	8.60	1.25	1.37	7.47
20	4.23	1.75	2.95	6.58	0.90	1.13	6.01
S = 6‰, p_{tot} = 0.813 atm ≡ 1608 masl, **Lake Issyk-Kul**							
4	3.76	1.68	3.48	8.45	1.33	1.29	7.11
10	3.65	1.58	3.01	7.06	1.06	1.12	6.13
20	3.53	1.45	2.44	5.40	0.77	0.92	4.94

For additional information on the gas concentrations or the water bodies refer to:

- General aspects: Aeschbach-Hertig et al. 1999b; Peeters et al. 2002.
- Lake Baikal: Hohmann et al. 1998; Aeschbach-Hertig et al. 1999b.
- Caspian Sea: Aeschbach-Hertig et al. 1999b, Peeters et al. 2000a.
- Lake Issyk-Kul: Hofer et al. 2002.
-

Table 1 is continued on the next page.

Table 1B. Noble gas concentrations at equilibrium may be calculated using the following parameterizations: *Equilibrium concentration of* ***He, Ne, Ar, Kr,*** $(^3He/^4He)_{eq} = R_{eq}$ *and* ***Xe***:

$$C^i_{eq} = \exp\left(\begin{matrix} t_1 + t_2 \cdot (100/T) + t_3 \cdot \ln(T/100) + t_4 \cdot (T/100) + \\ S \cdot \left[s_1 + s_2 \cdot (T/100) + s_3 \cdot (T/100)^2\right] \end{matrix}\right) \cdot \frac{p_{tot} - e_w}{(p_{norm} - e_w) \cdot 1000}$$

$$R_{eq} = R_a / \exp\left((r_1 + r_2/T + r_3/T^2) \cdot (1 + r_4 \cdot S)\right)$$

$$X_{Xe} = \exp\left(x_1 + x_2 \cdot (100/T) + x_3 \cdot \ln(T/100)\right)$$

$$C^{Xe}_{eq} = X_{Xe} \cdot \frac{V_{Xe} \cdot z_{Xe}}{M_{H2O}} \cdot \exp\left(-NaCl \cdot \left[x_4 + x_5 \cdot (100/T) + x_6 \cdot \ln(T/100)\right]\right)$$

C^i_{eq}, C^{Xe}_{eq}:	Equilibrium concentration of He (= ^{4}He), Ne, Ar, Kr and Xe (cm^3 STP g^{-1})
p_{tot}, p_{norm}:	Total local atmospheric pressure (atm) and reference pressure (≡ 1 atm)
e_w:	Water vapor pressure (atm)
T, S:	Water temperature (K) and salinity (g kg^{-1})
t_i, s_i, r_i, x_i:	'Temperature', 'salinity', 'R_{eq}' and 'Xe' coefficient i (-)
R_a, R_{eq}:	Atmospheric ^{3}He/^{4}He ($1.384 \cdot 10^{-6}$, Clarke et al. 1976) and ^{3}He/^{4}He ratio at equilibrium
X_{Xe}, V_{Xe}:	Mole fraction solubility (-) and molar volume of Xe at STP (22280.4 cm^3 STP mol^{-1})
z_{Xe}:	Atmospheric (dry air) volume fraction of Xe ($8.7 \cdot 10^{-8}$)
NaCl:	NaCl concentration (mol l^{-1}), mass of salt being interpreted as the same mass of NaCl
M_{H2O}:	Molar weight of water (~18.016 g mol^{-1})
ρ(T,S):	Density of water as function of T and S [kg m^{-3}]

coefficient	***He***	***Ne***	***Ar***	***Kr***
t_1	-167.2178	-170.6018	-178.1725	-112.684
t_2	216.3442	225.1946	251.8139	153.5817
t_3	139. 2032	140.8863	145.2337	74.4690
t_4	-22.6202	-22.6290	-22.2046	-10.0189
s_1	-0.044781	-0.127113	-0.038729	-0.011213
s_2	0.023541	0.079277	0.017171	-0.001844
s_3	-0.0034266	-0.0129095	-0.0021281	0.0011201

	R_{eq}	*coefficient*	***XE***
r_1	-0.0299645	x_1	-74.7398
r_2	19.8715	x_2	105.21
r_3	-1833.92	x_3	27.4664
r_4	0.000464	x_4	-14.1338
		x_5	21.8772
		x_6	6.5527

To adapt $C_{i,eq}$ to local conditions, the local atmospheric pressure has to be translated into noble gas partial pressures. This transformation has to account for the facts that the ratio of water vapor pressure to total pressure p_{tot} is variable, and that noble gas volume fractions are only known in dry air (Ozima and Podosek 1983). Hence any adaptation of solubility data to the local altitude of the surface of an open water mass has to be corrected for atmospheric water vapor pressure (see Eqn. 12).

Beyerle et al. (2000a) and Aeschbach-Hertig et al. (1999b) compared the different sets of noble gas solubilities with noble gas concentrations measured in artificially equilibrated water and in samples from lakes that can be assumed to be in equilibrium with the atmosphere (Fig. 2). Although the different solubility data sets agree on the percent level there are some deviations, especially in case of He and Ne. As a conclusion of this comparison Aeschbach-Hertig et al. (1999b) suggested to use for common application in natural meteoric waters 'Weiss' solubilities and 'Clever' solubilities being generalised by a Setchenow equation to account for salinity-dependence (see Eqn. 11).

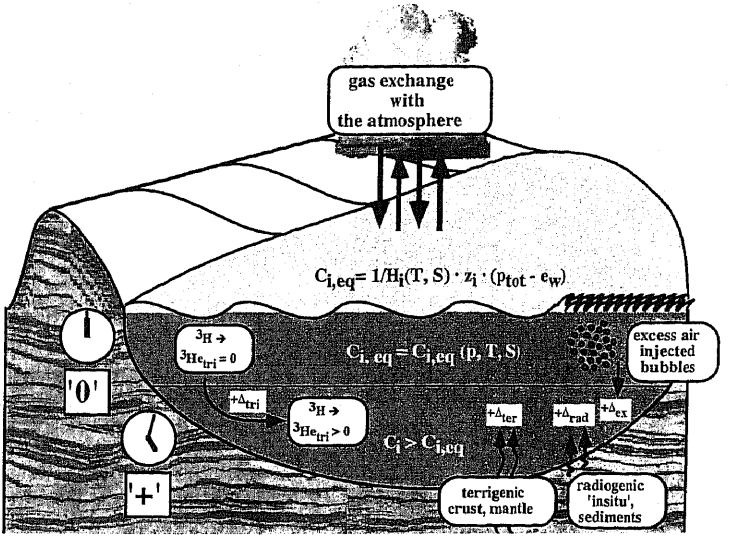

Figure 2. Origin of noble gases in lakes. Lakes have a large free surface in close contact with the atmosphere. Hence the concentrations of atmospheric (noble) gases are expected to coincide with equilibrium concentrations and to be large realtive to the radiogenic and terrigenic components. Wind-exposed lakes show small, but significant excesses of atmospheric noble gases, especially Ne is supersaturated by up to 5% ($+\Delta_{ex}$). This characteristic atmospheric excess that affects mainly light noble gas isotopes are attributed to the complete dissolution of air bubbles being submerged by wave activity. If a water parcel is transported away from the interface with the atmosphere gas exchange ceases and possible (noble) gas excesses are retained as the escape to the atmosphere is prevented. In particular non-atmospheric He ($+\Delta_{rad\ /\ tri,\ ter}$) accumulates in the deep water of lakes. $^3He_{tri}$ produced by ^3H decay in the water leads to an increase of ^3He concentration with time. The ratio $^3He_{tri}/^3H$ can be used for dating purposes. The deep water of lakes are only gently renewed during seasonal or even longer lasting stagnation periods and accumulate terrigenic and radiogenic He emanating from the sediments into the water body ($+\Delta_{rad,\ ter}$).

The noble gas equilibrium concentrations record changes in physical conditions during air / water partitioning, such as changes in (soil) temperature, altitude or pressure, and salinity. In the temperature range relevant for the environment, the noble gas solubilities in water—as for all other poorly soluble gases—generally decrease with increasing temperature (Fig. 1, Table 1). Interestingly, at temperatures higher than 60°C noble gas concentrations increase dramatically with increasing temperature (Crovetto et al. 1982). Generally noble gases become less soluble with increasing salinity (Fig. 1, Table 1, Smith and Kennedy 1983; Suckow and Sonntag 1993). The temperature and salinity dependence increases with the atomic mass of the noble gas and is most evident for Xe (Fig. 1, Table 1).

Both effects—the dependence on T and on S—can readily be explained by a conceptual model that describes poorly soluble substances in water (Schwarzenbach et al.

1993). The model conceptualises the solution of (noble) gases on the microscopic level as cavities built by water molecules that trap individual (noble) gas atoms. The attracting forces between water and host increase with the atomic radius and the dielectric constant of the (noble) gas. In consequence, the intermolecular forces increase with molecular mass. This explains why the ratios of elemental noble gas concentrations in water at atmospheric equilibrium are enriched with respect to the atmospheric abundance in favor of the heavier noble gases.

The general behavior of noble gases during solution and their dependence on T and S can be understood in a rudimentary fashion in thermodynamical terms. The increase in solubility with temperature can be qualitatively explained by entropy effects becoming the dominating control at higher temperatures, whereas enthalpy effects, that govern dissolution at low temperatures, weaken with growing temperatures and become less important (Schwarzenbach et al. 1993).

In conclusion, according to our experience noble gases behave as ideal gases during dissolution and partitioning processes in meteoric water (see also Ballentine et al. 2002, this volume).

Atmospheric noble gases 2: Excess Air

In contrast to surface waters, ground waters commonly contain significantly larger air-derived (noble) gas concentrations than the expected atmospheric equilibrium (Fig. 3). As the relative abundance of the noble gases in the excess is almost atmospheric, Heaton and Vogel (1979, 1981) called the gas surplus 'excess air'. In the case of Ar the phenomenon was described at least 20 years earlier (Oana 1957).

Although the occurrence of excess air is ubiquitous in ground waters, the excess air phenomenon only recently became subject of a detailed scientific discussion (Fig. 4). Although the relative elemental abundance of the observed gas excess of ground waters is often atmospheric, some ground waters show noble gas excesses that are not simply caused by injection and complete dissolution of pure air (Stute et al. 1995b; Aeschbach-Hertig et al. 1999b, 2000; Ballentine and Hall 1999; Weyhenmeyer et al. 2000; Holocher et al. 2001). All these waters have atmospheric noble gases in excess, but the heavier noble gases are more enriched than the light noble gases, i.e., the excess is fractionated relative to pure air (Figs. 4 and 5).

Until now, two models have been proposed to conceptualisze the fractionation of excess air in ground waters (Fig. 5). Although both models describe only the bulk behavior of atmospheric gas dissolution, the two concepts are able to describe the observed noble gas abundances, including the possible fractionation of the excess in favor of the heavy noble gases.

In the first model Stute (1989; 1995b) interpreted the fractionation in terms of a two-step concept. In a first step, ground water inherits pure excess air during ground-water recharge (unfractionated excess, UA-model). In the second step the initial pure air excess is partly lost by diffusively controlled gas exchange through the water / soil air interface which results in the partial re-equilibration of the ground water with respect to free atmospheric conditions (PR-model). Although there is no direct experimental evidence to support the PR-model, the development of a correction scheme to separate the fractionated excess component from the equilibrium concentrations allowed Stute et al. (1995b) to reconstruct successfully the temperature shift during the Pleistocene / Holocene transition in tropical Brazil.

In many cases the PR-model requires large amounts of initially dissolved excess air which can be several hundred percent of the equilibrium Ne concentration. In contrast,

the observed supersaturation of ground waters due to the presence of excess air is typically in the range of 10-50%. Hence the PR-model implies that the diffusive processes expel most of the initially dissolved excess air. Except for some rare Pleistocene ground waters, being recharged possibly in close vicinity of large inland ice masses of northern Europe (Juillard-Tardent 1999), the extreme amounts of initial excess air required by the PR-model appear to be unrealistic. The dissolution of enormous amounts of air would either force degassing or would demand that hydrostatic pressure in response to ground-water recharge increase by several atmospheres to keep the excess air in solution.

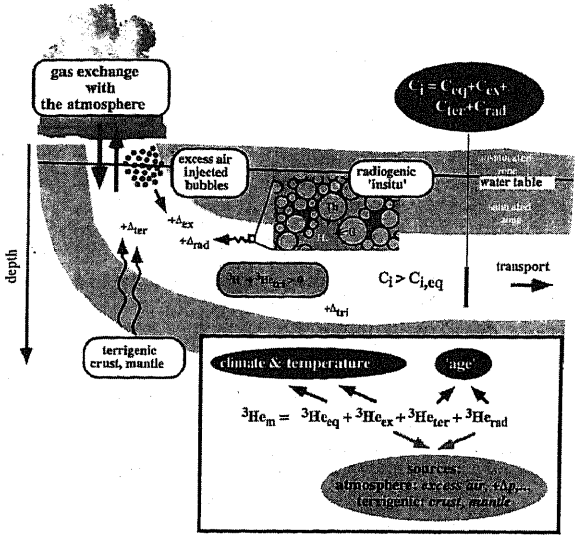

Figure 3. Origin of noble gas components in ground waters. Atmospheric gases are dissolved in ground waters near the water table by gas exchange between water and soil air. However during soil air / water partitioning ground waters dissolve atmospheric (noble) gases in significant excess ($+\Delta_{ex}$) compared to the equilibrium concentrations. This excess air component is most probably generated by re-equilibration between water with entrapped air that can cover up to 10% of the available pore space in the quasi-saturated zone. The slightly enhanced pressure prevailing in this soil zone leads to a new secular equilibrium between entrapped air and the super saturated water that is enriched relative to air in favor of heavy noble gases (note, hydrostatic overload prevents the supersaturated gases from degassing). During the water flow through the aquifer the ground water continuously accumulates non-atmospheric noble gases, in particular He of terrigenic ($+\Delta_{ter}$) and radiogenic ($+\Delta_{rad\ /\ tri}$) origin. The measured noble gas concentrations exceed commonly the expected equilibrium concentrations because the noble gas abundance represents a mixture of various components in varying proportions. Thereby air-derived noble gases can be interpreted in terms of the physical and climatic conditions prevailing ground-water recharge, radiogenic and terrigenic noble gases carry information on water residence time and on the origin of terrigenic fluids.

The conceptual problem of the PR-model can be overcome if it is assumed that theexcess gas does not enter ground water in a large single event of injection and degassing, but in a cycle of various injection and degassing steps (multi-step re-equilibration, MR-model, Fig. 5). Each step injects a much smaller amount of excess air and hence remains physically more acceptable. It can be shown that a multiple stepwise build-up of excess air leads in the limiting case to a similar fractionation pattern as single step formation (Eqn. 26). Aquifers that undergo ground-water table fluctuations in response to intermittent recharge events might conceptually experience such step-wise formation of excess air.

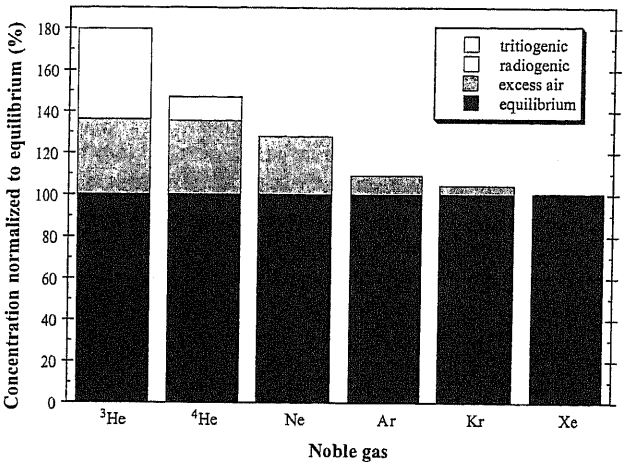

Figure 4. Noble gas components in a shallow ground-water sample. All concentrations are normalized to the respective atmospheric equilibrium concentration (given as 100 %). Note that the excess air component for Xe and the radiogenic component for ^{3}He are too small to be clearly visible on this scale. The data represent an actual sample from southern France, which was interpreted assuming unfractionated excess air. It has an infiltration temperature of 10.8°C, an excess air component of 3×10^{-3} cm^{3}STP g^{-1} (ΔNe = 29 %), and a ^{3}H-^{3}He age of 21 yr (^{3}H = 5 TU).

Being aware of the physical limitation of the PR-model, Aeschbach-Hertig et al. (2000) suggested a second model of the formation and elemental fractionation of excess air. The concept assumes (noble) gas equilibration in a closed system between ground water and small air bubbles being trapped in the quasi-saturated zone (CE-model, Fig. 5). The unsaturated and saturated zones of soils are not separated by a sharp interface. Rather the wetting conditions change over the transition of the quasi-saturated zone, where water saturation widely prevails, but where up to 10-20% of the pore space is still occupied by immobile entrapped soil air bubbles. This 'entrapped air' is a major control of ground-water recharge. It builds a rigid, but transient barrier against water infiltration into soils (Christiansen 1944; Faybishenko 1995).

Such entrapped air is conceptually thought to be a gas reservoir of restricted volume that does not exchange with the free soil air. In the quasi-saturated zone, water velocities are small (<0.5 m d^{-1}, Faybishenko 1995) and the pressure is slightly enhanced relative to the free atmospheric pressure due to the hydrostatic loading. Under these conditions it can be assumed that the (noble) gases re-partition by establishing a new equilibrium between the entrapped air and the water. As the soil gas volume is limited and the total amount of gas has to be conserved, the volume ratios of the atmospheric gases in the bubbles as well as the gas concentrations in the water have to change according to the different physical condition of the quasi-saturated zone. Because partitioning of individual gas species is controlled by the specific Henry coefficient, the more soluble gases are enriched in the water phase with respect to pure air. The relative elemental (noble) gas abundance in the gas phase is fractionated in favor of the less soluble (larger Henry coefficient) gases. In consequence the CE-model predicts the typical fractionation pattern of excess air in ground water with its characteristic enrichment of the heavier noble gases.

Although both concepts on the formation of excess air can produce the 'ground-water-like' enrichment of heavy noble gases, it has to be realised that the underlying

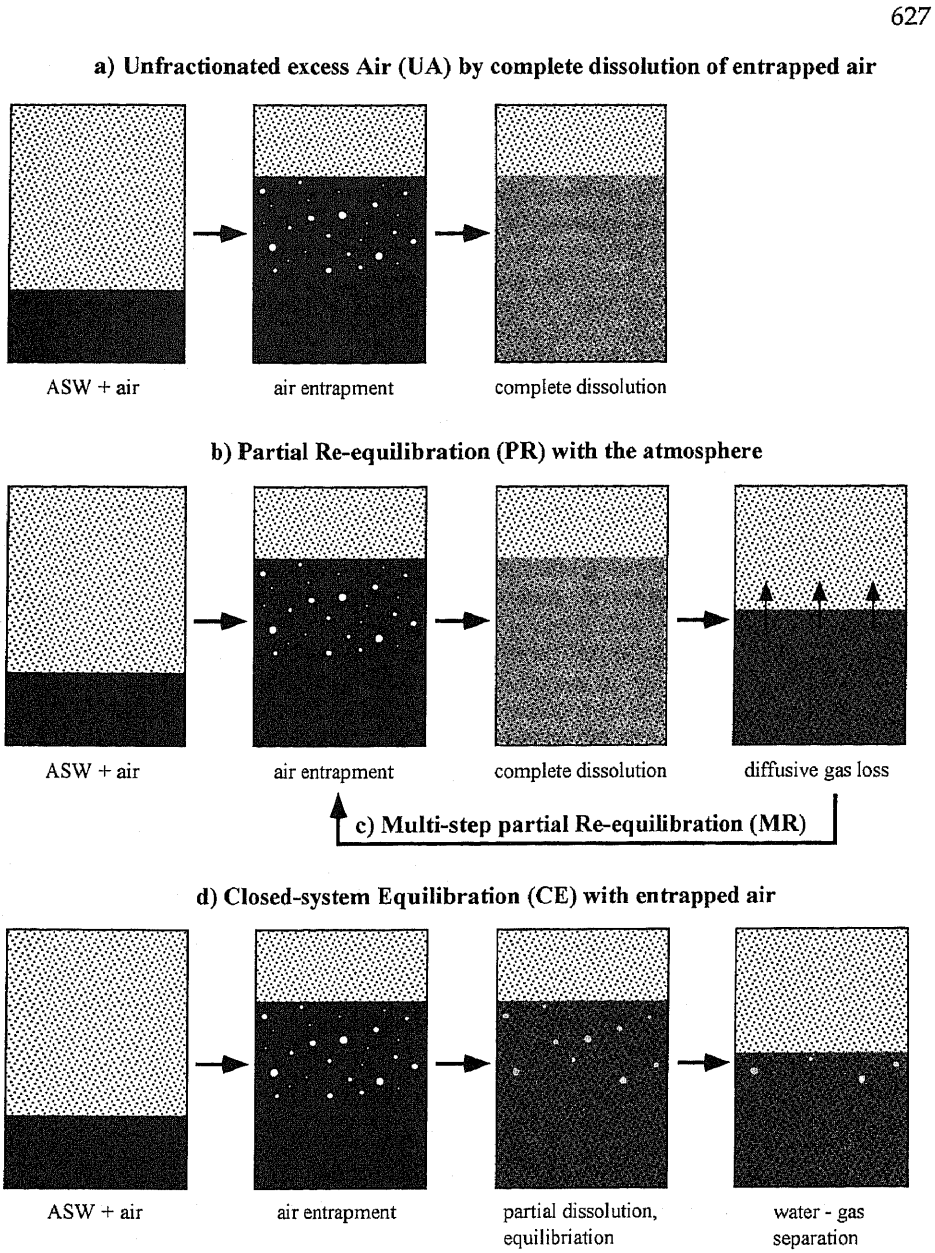

Figure 5. Schematic representation of the different model concepts for the formation of excess air in ground water. Note that different greyscales indicate changes in the noble gas composition of the respective reservoir.

physical processes are completely different. Whereas the PR / MR-model assumes that noble gas fractionation is controlled by molecular diffusion, the CE-model explains fractionation as the result of a new equilibrium between the dissolved gases in the water and the gas phase of the entrapped air. In case of moderate amounts of excess air and small fractionation both concepts lead to similar predictions of elemental (noble) gas

fractionation. But in the case of intense fractionation the models significantly differ in their predictions of elemental and isotopic composition of atmospheric noble gases.

Recently, laboratory experiments improving first experimental work of Gröning (1989) and Osenbrück (1991) have been able to generate 'ground-water-like' excess air in simple soil columns in a reliable and reproducible manner (Holocher et al. (2000). The results from the column experiments put the conclusion drawn from studies on natural systems in a new perspective. A numerical model describing the physics of the dissolution of gas bubbles in porous media reveals that the PR / MR and CE-concepts, that capture only the bulk behavior of water and excess air, represent extreme and limiting cases of gas dissolution in ground water. PR / MR or CE-type fractionation is reproduced depending on the applied external boundary conditions, such as water discharge, water table fluctuations, pore / bubble size distribution and preconditioning of the entrapped air reservoir (Holocher et al. 2000).

To our knowledge, in all ground waters that contain fractionated noble gases in excess and in which isotopic ratios have been determined, fractionation seems to take place according to the CE-concept (e.g., Aeschbach-Hertig et al. 2000; Holocher et al. 2001; Peeters et al. 2002). The reasons why natural ground waters apparently only show CE-type fractionation are the subject of ongoing research. The CE-model connects the amount and the fractionation of excess air directly with observable physical parameters that control air / water partitioning, e.g., ground-water table fluctuations resulting in pressure changes in the quasi-saturated zone. Hence the CE-model allows the interpretation of excess air in terms of the physical conditions prevailing during gas exchange. It opens perspectives to use excess air as an additional proxy to reconstruct soil and climate conditions at ground-water recharge (Aeschbach-Hertig et al. 2001).

Conclusions drawn from the excess of noble gases in ground water are also applicable to other gases that enter the water by atmospheric gas exchange, in particular N_2 and O_2. As the same physical processes control the dissolution of all atmospheric gases in ground water an excess of oxygen has to be expected at ground-water recharge assuming that oxygen partial pressure of the soil air is not already reduced by mineralization (Beyerle et al. 1999a). Since the Henry coefficient of O_2 lies between those of Ne and Ar, the anticipated oxygen excess should range between the excesses of Ne and Ar. Excess oxygen introduced during ground-water infiltration may be relevant for bio-geochemical transformations and thus for the ecological conditions in the aquifer.

Nitrogen concentrations in ground waters are also affected by excess air. Vogel, Heaton and colleagues provide convincing evidence for N_2 excess (ΔN_2) due to NO_3 reduction in old anoxic ground waters in Southern Africa (Vogel et al. 1981; Heaton et al. 1983). The authors show that the observed excess of molecular nitrogen consists of at least two components similar in magnitude: (1) ΔN_2 due to excess air formation, and (2) excess N_2 as the product of nitrate reduction. The amount of N_2 attributed to denitrification, i.e., excess N_2 after the correction for atmospheric N_2 (equilibrium plus excess air), depends on the model of excess air formation. The occurrence of excess N_2 in anoxic meteoric waters does not necessarily indicate denitrification and may be related to excess air. ΔN_2 is only an indicator for denitrification, if excess air and possible fractionation processes are accounted for.

Excess air is a ubiquitous and important constituent of atmospheric (noble) gases in ground waters, whereas atmospheric (noble) gas excesses in the open waters of lakes are of far less importance. Nevertheless large wind exposed lakes show sometimes small air excess amounts ranging up to few percent in case of Ne (Fig. 2, Aeschbach-Hertig et al. 1999b; Kipfer et al. 2000; Peeters et al. 2000a).

Radiogenic He (and Ar)

Radiogenic noble gases are produced either directly by radioactive decay or indirectly by subsequent nuclear reactions triggered by the initial radioactive disintegration. ^{3}He, ^{4}He, and to a lesser extent also ^{40}Ar, are the most prominent noble gas isotopes that are produced by the decay of their radioactive precursors ^{3}H, U, Th, other α emitting isotopes, and ^{40}K. α decay induces secondary nuclear reactions in rock and minerals that produce several noble gas isotopes (Ozima and Podosek 1983; Mamyrin and Tolstikhin 1984; Andrews et al. 1989; Lehmann and Loosli 1991; Ballentine and Burnard 2002 in this volume). But only ^{3}He is generated by these secondary reactions in sufficient amounts that it can be observed routinely in natural waters. All other noble gas isotopes have such low production yields that they are hardly detectable against their atmospheric background. The only exception may be $^{21}Ne_{rad}$ in very old ground waters (e.g., Bottomley et al. 1984).

Due to its unique chemical properties that are also for noble gases exceptional—low atmospheric abundance in combination with low solubility, high diffusivity and high mobility—He tends to accumulate in fluid phases if they are not in direct contact with the atmosphere. Hence, both He isotopes of radiogenic origin convey information about the time elapsed since gas exchange with the atmosphere. This so called 'water age' is a measure of the water residence time. ^{4}He concentrations are commonly interpreted in qualitative terms as residence time of old (ground) waters that recharged on times scales of thousands of years. ^{3}He generated by the decay of atmospheric ^{3}H (tritiogenic $^{3}He_{tri}$) is successfully used in quantitative terms ...

i. ...to date young ground waters having residence times up to 50 years (e.g., Tolstikhin and Kamenskiy 1969; Schlosser et al. 1988, 1989; Solomon et al. 1993; Szabo et al. 1996; Cook and Solomon 1997; Stute et al. 1997; Aeschbach-Hertig et al. 1998; Dunkle Shapiro et al. 1998, 1999; Beyerle et al. 1999a; Holocher et al. 2001), and

ii. ...to analyze deep water exchange and determine mixing rates in lakes (Torgersen et al. 1977; Aeschbach-Hertig et al. 1996a; Hohmann et al. 1998) and oceans (Peeters et al. 2000a; Schlosser and Winckler 2002, this volume).

Terrigenic He

The term 'terrigenic noble gases' describes noble gas components originating from different geochemical reservoirs of the solid Earth, such as the Earth's mantle or rocks of the continental crust. Noble gases are among the most prominent defining features of fluids from these large geochemical regions that are characterized by their particular isotope geochemistry.

Part of the radiogenic ^{3}He production is causally linked to α decay, i.e., the production of ^{4}He (e.g., Mamyrin and Tolstikhin 1984; Ballentine and Burnard 2002 in this volume). Such type of He is defined by a uniform $^{3}He/^{4}He$ ratio that intrinsically characterizes the geochemical environment.

As He is the most mobile noble gas, it emanates and ascends from deeper strata towards the Earth surface. This general He degassing from the Earth is often assessed in terms of pseudo-diffusive He fluxes from different geochemical reservoirs (e.g., O'Nions and Oxburgh 1983; Oxburgh and O'Nions 1987; O'Nions and Oxburgh 1988; Torgersen 1989). Deep circulating ground waters trap the ascending He. Hence He accumulates continuously in ground waters. Independent of its geochemical classification the accumulating He is a qualitative measure for the ground-water residence time (Fig. 3). Radiogenic and / or terrigenic He concentrations can even be interpreted quantitatively if the respective (terrigenic) He fluxes and / or the (radiogenic) He production rates are known.

Similarly He from the geological basin enters a lake where He is transported passively by the general mixing processes that control water exchange within the water body (Fig. 2). If the mixing dynamics of a specific lake is known, the continental terrigenic noble gas fluxes can be determined, i.e., noble gas fluxes from the continental crust and / or the Earth's mantle can be quantified (Torgersen et al. 1981; Igarashi et al. 1992; Kipfer et al. 1994; Hohmann et al. 1998).

Radioactive noble gas isotopes

Nuclear reactions produce not only stable, but also some radioactive noble gas isotopes. Due to their radioactivity the natural background of these isotopes is small and the nuclei are easily detected by their radioactive decay. Although radioactive, these isotopes are noble gases and thus behave chemically inert. As a result, any change in concentration is controlled solely by physical processes, such as radioactive production / decay and mixing of different components. The concentrations of radioactive noble gas isotopes therefore can most directly be employed to calculate the time elapsed since the system was isotopically closed, i.e., the time since radioactive decay alone determined the change of the concentrations of the radioactive isotopes. Some radioactive noble gas isotopes have half-lives similar to renewal times of natural water resources and hence can be used to determine water residence times.

The most prominent noble gas isotopes used in hydrology are ^{222}Rn, ^{85}Kr, ^{39}Ar and ^{81}Kr with half-lives of 3.82 d, 10.76 yr, 269 yr, and 230,000 yr (Fig. 6, Loosli et al. 2000). Due to its short half-life ^{222}Rn is suitable to trace processes in the aquatic environment that have short time constants. ^{39}Ar fills the time gap between ^{14}C and tracers used to date young ground water (e.g., ^{3}H-^{3}He, ^{85}Kr, and man made trace gases). ^{81}Kr is the isotope of choice to determine water residence times in ground waters that recharge on times scales of 10^5 years (Collon et al. 2000; Loosli et al. 2000).

With the exception of ^{222}Rn that can be continuously measured by α counting, detection and quantitative measurement of the other isotopes are experimental challenges as the particular noble gas abundances / activities are very small. Whereas the atomic abundance of ^{85}Kr, i.e., the ^{85}Kr/Kr ratio, is on the order of $1{:}10^{11}$, which is still relatively high for radioactive noble gases, ^{39}Ar and ^{81}Kr have extremely low atomic abundances on the order of $1{:}10^{15}$. Detection of these radioactive noble gases requires sample sizes of 500 l of water in case of ^{39}Ar, and about 15'000 l in case of ^{81}Kr. The water is usually degassed during field operations to avoid the transport of huge amounts of water (Loosli 1983; Collon et al. 2000; Loosli et al. 2000).

Because the half-lives of ^{85}Kr and ^{39}Ar are comparatively short, the radioactive activity and hence the concentration of the nuclides can be measured by ultra-low level counting techniques. The proportional counters need to be installed in shielded underground laboratories constructed by materials with very low natural activity (Loosli 1983; Loosli et al. 2000). The ^{81}Kr analysis is even more ambitious because it requires access either to synchrotron accelerators (Collon et al. 2000) or ultra sensitive laser techniques that are able of ionising a single isotope of an element (Ludin and Lehmann 1995). Because of the extreme requirements on sampling and detection, only few groups world wide, including the Institute of Environmental Physics of the University of Bern, have the experimental experience to extract and determine noble gas radioisotopes in natural waters. Comprehensive reviews on the use of radioisotopes in water are given in Loosli (1983), Lehmann et al. (1993), and Loosli et al. (2000).

In spite of the experimental difficulties there are at least two convincing reasons why radioactive noble gases are measured and applied to study transport in aquatic environments.

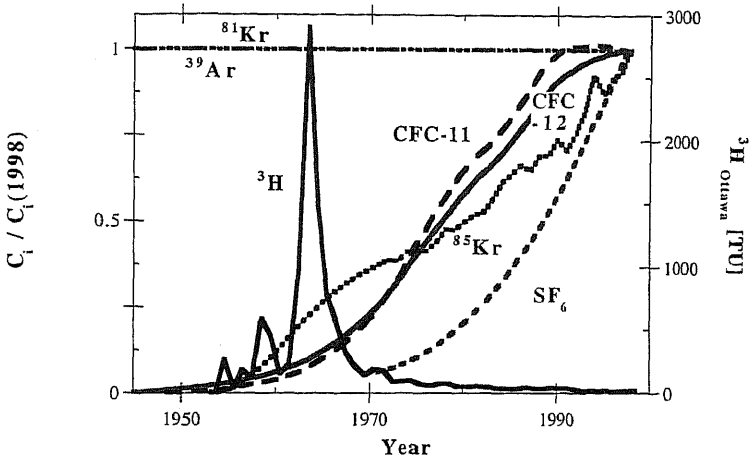

Figure 6. Atmospheric concentrations as functions of the radiogenic noble gases ^{39}Ar, ^{81}Kr, and ^{85}Kr and of the man made traces gases CFC-11, CFC-12, and SF_6. Concentrations are normalized to the respective atmospheric abundances in 1998. In addition a typical (input) curve of ^{3}H in precipitation is shown. Note, nuclear bomb tests in the atmosphere increased the global tritium inventory by up a factor of 1000. Since then ^{3}H concentrations steadily decreased, but still today tritium activity in young meteoric waters is commonly one order of magnitude larger than the natural background due to cosmic rays production.

i. The natural time scales of the dynamics of oceans and ground waters agree with the time-range assessable by radioactive noble gases and which hardly can be approached by any other tracer.
ii. The time information is recorded by the ratio of the radioactive and the stable isotope (NG_{ra}/NG_{st}) and thus does not depend on absolute concentrations.

^{39}Ar, ^{81}Kr and ^{222}Rn are of natural origin and are produced by nuclear reactions. The two lighter isotopes are generated predominantly in the atmosphere by cosmic ray / air interaction, e.g., spallation of ^{40}Ar yields ^{39}Ar, whereas ^{81}Kr originates from nuclear reactions with stable Kr isotopes (Loosli 1983; Lehmann et al. 1993; Loosli et al. 2000). As the typical mixing time of the atmosphere of only a few years is much shorter than the half-lives of the two isotopes, the atmospheric abundances of ^{39}Ar and ^{81}Kr are in first approximation at steady state and reflect the equilibrium between production due to cosmic ray interaction and radioactive decay (Fig. 6). Together with the stable isotopes of the respective element the 'atmospheric' radioactive noble gases, ^{39}Ar, ^{81}Kr (as well as ^{85}Kr) enter the meteoric water cycle via gas exchange with the atmosphere. Air / water partitioning determines the NG_{ra}/NG_{st} ratio in the water, whereby the inherited ratio coincides with the atmospheric ratio. After the water has been moved away from the air / water interface, radioactive decay remains the only process affecting the radioisotope concentrations. As a result, the ratio NG_{ra}/NG_{st} decreases with time and can be used as a measure of the time that elapsed since the water was last in contact with the atmosphere or soil air.

Besides atmospheric sources radioactive noble gases, in particular ^{37}Ar and ^{39}Ar, are produced in rocks an minerals (Loosli 1983, Loosli et al. 2000). The Ar isotopes are produced by natural nuclear reactions in the solids of the aquifer matrix, from where the generated nuclei tend to emanate and to accumulate in the surrounding ground waters. The subsurface production sets a natural limit down to which the radioisotope can be

used for dating of ground water. The terrigenic ^{39}Ar production can be quantified by the analysis of ^{37}Ar. ^{37}Ar stems from the atmosphere as well as from rocks, but due to its short half-life of 35 days ^{37}Ar in ground water can be expected to be of purely subsurface origin. Because nuclear reactions producing ^{37}Ar are similar to those generating ^{39}Ar, the ^{37}Ar abundance allows the correction of the terrigenic ^{39}Ar contribution and hence enables the ^{39}Ar method to be applied for ground-water dating (Loosli 1983; Loosli et al. 2000).

In contrast to other natural radioactive noble gases, radon is not of atmospheric origin. ^{222}Rn is produced within the α decay series of ^{238}U by disintegration of ^{226}Ra. ^{219}Rn and ^{220}Rn are produced in the other two α decay series of ^{235}U and ^{232}Th. But their half-lives of 4 and 56 s respectively are far too short to make them applicable in environmental research. Due to its chemical inertness and its large enough half-life ^{222}Rn emanates from the solids of the aquifer matrix and accumulates in the ground water.

In lakes, radon release from the sediment / water interface into the bottom water was used to determine transport rates in the turbulent boundary of the water column (Imboden 1977; Imboden and Emerson 1978).

Opposite to meteoric waters at recharge, that have Rn concentrations near zero reflecting the virtual absence of Rn in the atmosphere, ground waters show Rn concentrations near the expected production equilibrium characterizing the surrounding aquifer matrix. Hence all deviation of the Rn concentration towards smaller values can be interpreted in terms of admixture of very recent recharge into 'older' ground water or in terms of the travel time of the recent recharge, for example the transgression of riverine water through the transition of hyporeic zone, i.e., the water just below the river bed, into the near by ground water (Hoehn and von Gunten 1989).

^{85}Kr is not of natural origin but man made. The isotope is released from re-processing plants during recycling of spent nuclear fuel (Lehmann et al. 1993; Lehmann and Purtschert 1997; Loosli et al. 2000). As a consequence of the increased re-processing demands the ^{85}Kr activity in the atmosphere continuously and steadily increased since the 1950s reaching an activity of 1.4 Bq m^{-3} in 2000.

As long as water is in contact with the atmosphere, the $^{85}Kr/Kr$ ratio in the water reflects the atmospheric input function (Fig. 6). After the water is moved away from the air / water interface, gas exchange is interrupted and the $^{85}Kr/Kr$ ratio decreases due to radioactive decay. In order to date a young ground water that recharged on time scales similar to the half-life of ^{85}Kr, the measured $^{85}Kr/Kr$ ratio is calculated back in time to compensate for radioactive decay. The back-extrapolated $^{85}Kr/Kr$ ratio is compared with the known atmospheric input function. It can be shown that, as long as the atmospheric ^{85}Kr activity monotonously increases in time, the two functions only have one single intersection. The intersection marks the time of the last gas exchange between the water and the atmosphere.

The application of ^{39}Ar, ^{81}Kr, and ^{85}Kr for dating purposes requires only the measurement of a single isotopic ratio NG_{ra}/NG_{st}. In contrast to any individual gas concentration, the ratio NG_{ra}/NG_{st} is hardly affected by fractionation processes. Therefore dating based on radioactive noble gases can be employed even if the water is affected by strong elemental fractionation or by phase separation, e.g., during degassing upon sampling. Hence especially the use of ^{85}Kr is expected to have a large potential to date young ground water being affected by organic contamination. Such contaminated ground waters produce large amounts of CH_4 and CO_2 during organic degradation. The generated gases may trigger water / gas partitioning that alters the absolute gas concentrations, but cannot significantly bias isotopic ratios.

Man-made pseudo-conservative trace gases

Certain man-made compounds, such as chloro-fluoro-carbons, CFCs, and sulphur-hexafluoride, SF_6, are chemically non-reactive and behave almost as inert gases. SF_6 and the CFCs, particularly CFC-11 (CCl_3F) and CFC-12 (CCl_2F_2), stem from industrial production and are released to the atmosphere. There, these trace components accumulate due to their long atmospheric residence time of up to hundreds of years (Cunnold et al. 1994).

In response to increasing industrial use, atmospheric CFC concentrations continuously and rapidly rose between the 1930s and 1995 (Fig. 6, Busenberg and Plummer 1992). Then the international environmental regulations banning production of CFCs showed first impacts. The atmospheric SF_6 concentration increases exponentially since 1970 (Fig. 6). With regard to the changing atmospheric partial pressure of the conservative anthropogenic trace gases, their particular concentrations in a water parcel can be interpreted in terms of the time elapsed since the last gas exchange. Hence CFCs and SF_6 concentrations yield information on water renewal and recharge rates in lakes (Hofer et al. 2002; Vollmer et al. 2002) and ground waters (Busenberg and Plummer 2000) and thus complement the information on water dynamics obtained from noble gas dating techniques.

The combination of dating methods restricts the estimation of the mean residence time of aquatic systems much more than the use of only one technique (e.g., Hofer et al. 2002; Vollmer et al. 2002; Zeollmann et al. 2001). Because these trace gases are mostly chemically and biologically inert, they are mainly subject of physical processes in the water cycle. Thus in principle the chemical and biological alterations in the water body can be separated from the common physical transport.

Gas exchange at the air–water interface and mixing processes have different effects on different transient tracers, e.g., CFCs and rare gases are much more influenced by gas exchange with the free atmosphere and/or soil air than tritium being bound in water molecules ($^1H^3HO$). Hence the combination of tracer techniques enables not only the dating of water masses (e.g., Busenberg et al. 1993; Busenberg and Plummer 2000, Schlosser and Winckler 2002), but also the study of the dynamics of the gas–water interaction in the unsaturated zone (Cook and Solomon 1995; Brennwald et al. 2001).

DATA EVALUATION AND INTERPRETATION

Several different noble gas (particularly He) components can be present in natural waters. The information that we hope to obtain from the study of dissolved noble gases is related to the individual components. For instance, the radiogenic and tritiogenic He components contain age information, whereas the solubility equilibrium components of all noble gases may be used to derive the equilibration temperature. For the interpretation and use of dissolved noble gases, it is therefore necessary to evaluate the data in terms of individual components. In this section, we discuss techniques to separate the components contributing to the measured total noble gas concentrations and isotope ratios.

The component separation approach is based on the assumption that each source of noble gases contributes a single, well-defined portion to the total noble gas concentrations in a sample. This assumption can only be strictly valid if the water parcels retain their unique identity, i.e., if mixing and diffusion are negligible. The effect of mixing or diffusion depends on concentration gradients, which may differ between elements and even isotopes, thus resulting in noble gas compositions that cannot be interpreted as a sum of single components. For instance, mixing of two water parcels that equilibrated with air at different temperatures creates a composition that does not exactly correspond

to equilibrated water of any temperature. Of course, mixing, diffusion, and dispersion are always present in lakes and ground waters. Thus, in principle, the correct approach to interpret the data is to model the evolution of noble gases in the complete aquatic system under investigation and to use only the measured total noble gas concentrations to constrain model parameters. However, in practice this approach is often not feasible, whereas the component separation provides a direct way to derive valuable information about the studied system. In many cases, the approximation underlying the component separation appears to be reasonably well justified and to lead to reliable and useful results.

Any attempt to calculate individual noble gas components present in a sample must be based on a conceptual model, specifying which components are assumed to be present and what their composition is. In the first part of this section, we will discuss the models that up to the present have been developed. In the second part, actual techniques to perform the component separation are discussed. Finally, we introduce the basic concepts that are needed to interpret the inferred components in terms of age, temperature, or other quantities.

Conceptual models for noble gases in water

All conceptual models that have been applied to interpret dissolved noble gases in lakes and ground waters suppose that the measured concentrations are a sum of (some of) the components introduced in the previous section. In a general way, the basic model equation may be written as (compare Figs. 2, 3 and4):

$$C_{i,m} = C_{i,eq} + C_{i,ex} + C_{i,rad} + C_{i,ter} \tag{5}$$

where C_i stands for the concentration of the noble gas isotope i, and the subscripts indicate the components (m: measured (total), eq: atmospheric solubility equilibrium, ex: excess air, rad: radiogenic, ter: terrigenic). Obviously, a separation of the components in Equation (5) requires measurement of several noble gas isotopes and some knowledge of the elemental and / or isotopic composition of the individual components.

An important simplification results from the fact that the components of non-atmospheric origin (radiogenic and terrigenic) play a role only for certain isotopes. With the exception of He, all stable noble gases have at least one isotope that usually is only of atmospheric origin (e.g., ^{20}Ne, ^{36}Ar, and virtually all Kr and Xe isotopes). Therefore, it is usually sufficient to have a model for the noble gas components of atmospheric origin (equilibrium and excess air), and to calculate the non-atmospheric contributions to certain isotopes from the difference between their measured concentrations and the model predictions for their atmospheric components. Hence, we focus on models of the dissolved noble gases of atmospheric origin in ground water. We first address the atmospheric equilibrium component, and then discuss several descriptions for the excess air component.

Atmospheric solubility equilibrium. The dissolved concentrations of the noble gases in equilibrium with the atmosphere can easily be calculated from Henry's law (Eqn. 2), using the noble gas partial pressures in moist air given by Equation (3). The practical problem is to calculate the Henry coefficients $H_i(T,S)$ in appropriate units. Several different expressions for gas solubilities are common in the literature and a variety of units for the concentrations in the two phases are used. In Equation (2), the units atm for p_i and cm^3 STP g^{-1} for C_i are widely used in noble gas studies. For some calculations it is convenient to use the same concentration units (e.g., mol m^{-3}) for both phases, resulting in the 'dimensionless' Henry coefficient H_i', as in Equation (1). The conversion from H_i in volumetric units (e.g., $(mol/l_{gas})(mol/l_{water})^{-1}$) to H_i in units atm $(cm^3$ STP $g^{-1})^{-1}$ is a

simple application of the ideal gas law yielding

$$H_i = H_i' \cdot \frac{T}{T_0} \cdot P_0 \cdot \rho_w \tag{6}$$

where T_0 and P_0 are standard temperature and pressure, and ρ_w is the density of water. In these units, the coefficients H_i and H_i' have almost the same numerical values, because P_0 = 1 atm, $\rho_w \approx 1$ g cm^{-3}, and $T/T_0 \approx 1$ for temperatures not too far from $T_0 = 273.15$ K.

Yet, none of these units is common in the literature on gas solubilites. For the determination of gas solubilities in controlled lab experiments, often a pure gas phase at known pressure (usually 1 atm) is brought into contact with a known mass or volume of the solvent (e.g., pure water). A convenient way to express gas solubilities is then the Bunsen coefficient β_i, which is the volume of gas i at STP adsorbed per volume of solvent if the gas pressure p_i is 1 atm. Alternatively, the so-called mole fraction solubility X_i states the mole fraction of gas i in the solution at equilibrium with the pure gas at 1 atm. In field samples one usually determines the amount of dissolved gases per mass of solution.

Strictly speaking, the concentration measures 'per volume of solvent' (Bunsen), 'per number of moles in the solution' (mole fraction), and 'per mass of solution' (samples) are not linearly related, and hence Henry's law cannot simultaneously be valid for all forms. To illustrate the problem, consider the conversion from mole fraction concentrations x_i to per weight concentrations C_i:

$$x_i\left[\frac{\text{mol}_i}{\text{mol}_{\text{solution}}}\right] = \frac{n_i}{n_s + n_i} \tag{7}$$

$$C_i\left[\frac{\text{mol}_i}{\text{g}_{\text{solution}}}\right] = \frac{n_i}{M_s n_s + M_i n_i} \tag{8}$$

where n is the number of moles and M the molar mass (g mol^{-1}) and the subscripts refer to the dissolved gas i and the solvent s. The conversion from x_i to C_i is:

$$C_i = \frac{1}{M_s} \frac{1}{1/x_i - 1 + M_i/M_s} \tag{9}$$

which obviously is non-linear. If C_i were defined as 'per mass of solvent', then the term M_i/M_s in the denominator of Equation (9) would disappear. This expression is sometimes found in the literature. However, since actual measured concentrations of dissolved gases in field samples are per mass of solution, it is hardly appropriate in practice.

For low soluble gases such as noble gases and at low pressures, the contribution of the dissolved gases to the mass or number of moles of the solution is for all practical purposes negligible ($n_i << n_s$). Hence all terms with n_i can be neglected in the denominators of Equations (7) and (8), and the conversion reduces to the simple linear relationship

$$C_i = \frac{x_i}{M_s} \tag{10}$$

We recommend using this approximation, which is usually extremely good. The conversion of units for the Henry coefficients is then straightforward.

Another problem that is encountered in the calculation of atmospheric equilibrium concentrations is the dependence of the Henry coefficient on the concentration of dissolved ions, the so-called salting out effect. Difficulties are that (1) sometimes fresh-

water solubilities from one source have to be combined with salting-out coefficients from another source, (2) one should know the effect of each ion species, and (3) salt concentrations are also expressed in different units that may not be strictly convertible. In this problem, some approximations are inevitable. Aeschbach-Hertig et al. (1999b) gave an equation to calculate equilibrium concentrations from mole fraction solubilities X_i as given by Clever (1979a,b; 1980) and the salting coefficients K_i determined by Smith and Kennedy (1983). According to the above discussion, we rewrite this equation (Eqn. 5 of Aeschbach-Hertig et al. 1999b) as follows:

$$C_{i,eq} = \frac{X_i(T)}{M_s} \cdot \frac{(P - e_w(T))z_i}{P_0} \cdot \frac{\rho(T,S=0)}{\rho(T,S)} \cdot V_i \cdot e^{-K_i(T)c} \tag{11}$$

where $\rho(T,S)$ is the density of water (Gill 1982), V_i is the molar volume of gas i, and c is the molar concentration of NaCl. An approximative conversion between c [mol L^{-1}] and salinity S [g kg^{-1}] can be made by equating the two measures expressed in terms of total mass of salt per volume of solution (Aeschbach-Hertig et al. 1999b).

For He, Ne, Ar, and Kr, Weiss (1970, 1971) and Weiss and Kyser (1978) gave empirical equations that directly yield the atmospheric solublity equilibrium concentrations $C_{i,eq}$ at a total pressure of 1 atm. While this form of gas solubilities is very convenient in practice, it should be noted that such equilibrium concentrations are—as shown by Equations (2) and (3)—not directly proportional to P. The correct way to calculate the equilibrium concentrations at any pressure from those at P_0 = 1 atm is:

$$C_{i,eq}(T,S,P) = C_{i,eq}(T,S,P_0)\frac{P - e_w(T)}{P_0 - e_w(T)} \tag{12}$$

Unfractionated excess air. The most straightforward explanation of the phenomenon of a gas excess above atmospheric equilibrium in ground waters is complete dissolution of small air bubbles trapped in soil pores (Fig. 5a, Heaton and Vogel 1979, 1981; Rudolph et al. 1984). This traditional—but experimentally never directly verified—concept implies that the excess has the same composition as the entrapped gas, which is assumed to be atmospheric air, hence the name 'excess air'. We refer to this concept as the 'unfractionated air' (UA) model. Because the composition of air is given by the volume fractions z_i, the UA-model needs only one parameter to describe the excess air component, namely the amount of trapped and completely dissolved air per mass of water (A_d). The excess air term in Equation (5) is written as:

$$C_{i,ex}^{UA} = A_d \cdot z_i \tag{13}$$

It is important to address the physical interpretation of the UA-model. The parameter A_d is the concentration of dissolved excess air, but because the model assumes complete dissolution, it should also reflect the concentration of entrapped air in the soil of the recharge area. Values of A_d in units of cm^3 STP air per g of water may therefore approximately be interpreted as volume ratios of entrapped air to water. Typical values are on the order of a few times 10^{-3} cm^3 STP g^{-1}. Assuming that such excesses originate from complete dissolution of entrapped air, they indicate that entrapped air initially occupies only a few per mil of the available pore space volume. This is in contrast to the literature about air entrapment in soils (Christiansen 1944; Fayer and Hillel 1986; Stonestrom and Rubin 1989; Faybishenko 1995), in which entrapped air volume ratios ranging from a few percent up to several 10s of percent in extreme cases are reported.

The driving force for dissolution of trapped air bubbles is pressure. In order to keep gases permanently in solution, the total pressure must at least equal the sum of the partial pressures corresponding to equilibrium with the dissolved gas concentrations. Because the water is assumed to have been at atmospheric equilibrium before the dissolution of

the excess air, the sum of the partial pressures corresponding to the equilibrium components $C_{i,eq}$ is exactly balanced by the atmospheric pressure P. Thus, we can write the dissolution condition for the excess pressure and excess air only:

$$P_{ex} = P_{tot} - P \geq \sum_i p_{i,ex} = \sum_i H_i C_{i,ex} = A_d \sum_i H_i z_i \qquad (14)$$

The sum on the right hand side of Equation (14) is dominated by the most abundant atmospheric gases nitrogen and oxygen. According to Equation (14) an excess pressure of 0.1 atm is needed (at 13°C) to keep a typical amount of excess air of 2×10^{-3} cm^3 STP g^{-1} of air permanently in solution.

There are two sources of excess pressure on entrapped air in ground water: hydrostatic head and surface tension. In addition, the noble gas partial pressures may be increased in the soil air due to oxygen consumption. Surface tension is inversely related to the size of the trapped bubbles. For spherical bubbles, it reaches the magnitude of 0.1 atm at a diameter of ~30 μm. Thus, surface tension plays an important role in very fine-grained sediments, but may not be the dominant force in productive (e.g., sandy) aquifers. In the case of hydrostatic head, an excess pressure of 0.1 atm corresponds to a column height of the water overload of about 1 m. Water table fluctuations of the order of 1 m probably occur in most recharge areas, thus hydrostatic pressure has the potential to contribute significantly to the dissolution of entrapped air. Complete removal of oxygen from the soil air would increase the partial pressures of the conservative gases by about 25%. However, the oxygen in the soil air may not be completely consumed and at least part of it is replaced by CO_2 (Frei 1999). Therefore, it is questionable whether the effect of oxygen consumption can reach the magnitude of 0.1 atm.

Despite the initial success of the UA-model, there is increasing evidence that excess air tends to be fractionated relative to atmospheric air, with an enrichment of the heavy gases compared to the light gases (e.g., Stute et al. 1995b; Clark et al. 1997; Aeschbach-Hertig et al. 2000). Thus, strictly speaking the traditional name 'excess air' is somewhat misleading.

If excess air is fractionated, it can no longer be expressed by a single parameter such as A_d. A convenient and widely used measure for the size of the gas excess, which is independent of its composition, is the relative Ne excess ΔNe:

$$\Delta Ne(\%) = \left(\frac{C_{Ne,m}}{C_{Ne,eq}} - 1 \right) \cdot 100\% \qquad (15)$$

Ne is best suited to quantify excess air because it has almost only atmospheric components and a low solubility, resulting in a relatively large excess. Moreover, because the equilibrium concentration $C_{Ne,eq}$ does not strongly depend on temperature, an approximative value for ΔNe can be calculated even if the exact equilibration temperature is not known. Thus, ΔNe is practically an observable quantity. As a rule of thumb, in the case of unfractionated excess air 10% ΔNe correspond approximately to 10^{-3} cm^3 STP g^{-1} of dissolved air, requiring at least 0.05 atm overpressure.

Partial re-equillibration. The conceptual idea of the partial re-equilibration (PR) model introduced by Stute et al. (1995b) is that entrapped air bubbles are initially completely dissolved as in the UA-model, but later a part of the resulting excess is lost by molecular diffusion across the water table (Fig. 5b). Due to the different molecular diffusivities D_i, this process leads to a fractionation of the excess air with respect to atmospheric air. Stute et al. (1995b) parameterized the degree of re-equilibration by the remaining fraction of the initial Ne excess and wrote the model equation for the excess components as:

$$C_{i,ex}^{PR} = C_{i,ex}(0) \cdot \left(\frac{C_{Ne,ex}}{C_{Ne,ex}(0)} \right)^{D_i / D_{Ne}} \quad (16)$$

By using $A_d \cdot z_i$ instead of $C_{i,ex}(0)$ and introducing the re-equilibration parameter $R = -\ln[C_{Ne,ex}/C_{Ne,ex}(0)]$, the PR-model may be rewritten as (Aeschbach-Hertig et al. 2000):

$$C_{i,ex}^{PR} = A_d \cdot z_i \cdot e^{-R \frac{D_i}{D_{Ne}}} \quad (17)$$

This formulation highlights the physical interpretation of the PR-model: The exponential term describes the result of gas exchange between water and soil air. The PR-model is based on the assumption that the gas exchange rate is proportional to the molecular diffusivity. This is the case in the stagnant boundary layer model of gas exchange, in which the exchange rate r_i is given by (Schwarzenbach et al. 1993):

$$r_i = \frac{D_i}{\delta \cdot h} \quad (18)$$

where δ is the thickness of the boundary layer and $h = V/A$ is the (mean) depth of the water body (with surface area A and volume V) affected by the exchange.

The dynamic development of dissolved gas concentrations under the influence of gas exchange is given by:

$$C_i(t) = C_{i,eq} + C_{i,ex}(0) \cdot e^{-r_i t} \quad (19)$$

Comparison with the PR-model Equation (17) yields the following interpretation:

$$C_{i,ex}(0) = A_d z_i \text{ and } r_i t = R \frac{D_i}{D_{Ne}} \quad (20)$$

Thus, the parameter $R = r_{Ne} t$ describes the degree of re-equilibration for Ne. By defining

$$R_i = R \frac{D_i}{D_{Ne}} = r_i t = \frac{D_i}{\delta \cdot h} t \quad (21)$$

we can re-write the PR-model equation as:

$$C_{i,ex}^{PR} = A_d \cdot z_i \cdot e^{-R_i} \quad (22)$$

The physical quantities determining the degree of re-equlibration are the thickness of the boundary layer (δ), the depth of the exchanging water body (h), and the duration of gas exchange (t). The differences between the individual gases originate from their different molecular diffusivities (D_i).

Because the molecular diffusivity decreases with the mass of the isotopes, the PR-model predicts that the depletion of the initially unfractionated excess air is largest for the light noble gases, whereas the heavy gases are enriched relative to air in the remaining excess. In particular, He should be strongly depleted in the excess air component, because of its extraordinarily high diffusion coefficient. However, due to the presence of non-atmospheric He components, it is difficult to verify this prediction.

Another consequence of the diffusion controlled fractionation process is that significant isotopic fractionations should occur. Peeters et al. (2002) suggested the use of $^{20}Ne/^{22}Ne$ ratios to test the validity of PR-model to describe gas partitioning in ground waters. In the few aquifers where Ne isotopes have been analyzed, no significant diffusive isotopic fractionation has been found so far (Peeters et al. 2002).

Multi-step partial re-equilibration. The PR-model frequently predicts rather high

values for the initial concentration of dissolved air (A_d). For instance, in the study of a Brazilian aquifer, in which the model was introduced Stute et al. (1995b) found initial Ne excesses up to about 300%, corresponding to A_d-values of up to 3×10^{-2} cm^3 STP g^{-1}. Complete dissolution of such amounts of air would require excess pressures of more than 1.5 atm, or—if hydrostatic pressure dominates—water table fluctuations of more than 15 m, which seem rather unrealistic. Moreover, if air bubbles would be trapped and dissolved at such large depths, it appears unlikely that a diffusive flux to the water table would still occur. Such findings render the physical interpretation of the PR-model concept problematic.

To circumvent the problem of high initial excess air, while retaining the concept of diffusive re-equilibration, we propose a model of multi-step partial re-equilibration (MR). The conceptual idea of this new model is that the water table periodically fluctuates, thereby repeating cycles of trapping, dissolution and diffusive loss of air (Fig. 5c). Starting as usual with equilibrated water, the excess air component after the first dissolution-degassing step is given by Equation (22). After the second step, we have

$$C_{i,ex}^{MR,2} = \left(A_d \cdot z_i \cdot e^{-R_i} + A_d \cdot z_i\right) \cdot e^{-R_i} = A_d \cdot z_i \left(e^{-R_i} + e^{-2R_i}\right) \tag{23}$$

and after n steps, the general equation is:

$$C_{i,ex}^{MR,n} = A_d \cdot z_i \cdot \sum_{k=1}^{n} e^{-kR_i} = A_d \cdot z_i \cdot \sum_{k=1}^{n} \left(e^{-R_i}\right)^k \tag{24}$$

The sum in Equation (24) is the sum of a finite geometric series, and from the respective theory we finally find the MR-model equation:

$$C_{i,ex}^{MR,n} = A_d \cdot z_i \cdot e^{-R_i} \frac{1-e^{-nR_i}}{1-e^{-R_i}} \tag{25}$$

Note that the MR-model has three parameters: the number of steps (n) and the parameters A_d and R as in the PR-model. The quantities R_i in Equation (25) are related to the universal parameter R by Equation (21).

To discuss the predictions of the MR-model, we consider four limiting cases:

(1) $R_i \rightarrow \infty$: This case of complete re-equilibration is trivial ($C_{i,ex} = 0$).

(2) $R_i = 0$: No degassing at all, the model reduces to the UA-model ($C_{i,ex} = n \cdot Ad \cdot zi$).

(3) $n = 1$: This case is equivalent to the PR-model ($C_{i,ex} = A_d \cdot z_i \cdot e^{-R_i}$).

(4) $n \rightarrow \infty$ This is the most interesting case. Provided that $R_i > 0$, the term e^{-nR_i} approaches zero and Equation (25) becomes (proceeding from the finite to the infinite geometric series):

$$C_{i,ex}^{MR,\infty} = A_d \cdot z_i \cdot \sum_{k=1}^{\infty} \left(e^{-R_i}\right)^k = A_d \cdot z_i \cdot \frac{e^{-R_i}}{1-e^{-R_i}} \tag{26}$$

This case differs from the PR-model only by the correction factor $\left(1-e^{-R_i}\right)^{-1}$. For $R_i >> 1$ (strong degassing), the correction factor tends to unity and the MR-model approaches the PR-model. In reality, neither n nor R_i need to be particularly large to approach the PR-model rather closely. Thus, the MR concept may be seen as a more realistic description of excess air formation for samples with a strong diffusive fractionation pattern, that according to the PR-model would require unrealistically large initial dissolution of entrapped air.

However, as the MR-model approaches the PR-model, it also predicts diffusive isotopic fractionation, i.e., the $^{20}Ne/^{22}Ne$ should be significantly lower than the atmospheric ratio (Peeters et al. 2002). Since such a depletion of air-derived light noble

gas isotopes has not been observed in field studies, a concept is needed that explains the enrichment of heavy noble gases in the excess air component without diffusive fractionation of noble gas elements *and* isotopes.

Closed-system equilibration. Such a concept is provided by the closed-system equilibration (CE) model (Aeschbach-Hertig et al. 2000). The idea of this model is that the entrapped air dissolves only partially, and a new solubility equilibrium is attained in a closed system consisting initially of air-saturated water and a finite volume of entrapped air under elevated total pressure P_{tot} (Fig. 5d). The CE-model equation is (Aeschbach-Hertig et al. 2000):

$$C_{i,ex}^{CE} = \frac{(1-F)A_e z_i}{1+FA_e z_i/C_{i,eq}} \tag{27}$$

where A_e is the initial amount of entrapped air per unit mass of water and F is a fractionation parameter. Note that A_e (entrapped air) is the same as A_d (dissolved air) only in the case of total dissolution.

The model parameters A_e and F in the CE-model have a clear physical interpretation (Aeschbach-Hertig et al. 2000, 2001). A_e given in cm^3 STP g^{-1} approximately equals the initial volume ratio between entrapped air and water, whereas F describes the reduction of the gas volume by partial dissolution and compression. Correspondingly, F can be expressed as the ratio of two parameters v and q, where v is the ratio of the entrapped gas volumes in the final (V_g) and initial state (V_g^v), and q is the ratio of the dry gas pressure in the trapped gas to that in the free atmosphere (P):

$$F = \frac{v}{q} \quad \text{with} \quad v \equiv \frac{V_g}{V_g^0} \quad \text{and} \quad q \equiv \frac{P_{tot} - e_w}{P - e_w} \tag{28}$$

Provided that $P_{tot} \geq P$, the following inequalities hold: $q \geq 1$ and $0 \leq v, F \leq 1$. Note that only the combined parameter $F = v/q$ is needed to define the excess air component, not v and q individually. The parameters q, v, and A_e are coupled by the physical requirement that the sum of the partial pressures of all gases in the trapped volume equals P_{tot}. Any pair of the parameters A_e, F, q, and v fully determines the amount and composition of excess air, the most intuitive choice being A_e ($\approx$ air / water volume ratio) and q ($\approx$ pressure exerted on the entrapped air). The CE-model thus allows a direct physical interpretation of the excess air component.

Typical values for the CE-model parameters A_e and q found in several aquifers support the notion that these parameters reflect actual physical conditions during infiltration. Aeschbach-Hertig et al. (2001) found that typical values of A_e in six aquifers ranged from 0.02 to 0.04 cm^3 STP g^{-1}, indicating that a few percent of the pore space were occupied by entrapped air during infiltration, in full agreement with expectations (Fayer and Hillel 1986; Holocher et al. 2002). Typical q-values were ~1.2 for three temperate zone aquifers and ~1.5 for three semi-arid sites. Explaining these values by hydrostatic pressure due to water table fluctuations implies typical amplitudes of 2 and 5 m, respectively. Such amplitudes of water table fluctuations are probably at the upper limit of what can be expected.

These results provide a natural solution to the apparent discrepancy between typical concentrations of entrapped air (several percent of the pore space, corresponding to A_e-values of the order of 10^{-2} cm^3 STP g^{-1}) and those of actually dissolved excess air (A_d-values of the order of 10^{-3} cm^3 STP g^{-1} in the UA-model). It seems that typically more air is entrapped than can be dissolved at the prevailing pressure. In this situation, the resulting excess air component is fractionated according to the CE-model and its size

(expressed, e.g., by ΔNe) is limited not by the available air reservoir A_e, but by the pressure acting on that reservoir (q). As a result, the observable quantity ΔNe is strongly correlated with q (Aeschbach-Hertig et al. 2001) and obtains a direct physical interpretation: it is essentially a measure of the pressure on the entrapped air.

If the excess pressure is ascribed to the hydrostatic load of infiltrating water, then ΔNe should be a measure of the amplitude of water table fluctuations. A verification of a direct link between water table fluctuations and ΔNe or q under field conditions is still missing. Experiments with sand columns (Holocher et al. 2002) support the correlation of q with the amplitude of water level changes.

When comparing the different excess air models, which are summarized in Table 2, we may first note that the UA-model is contained as a special case (R or F = 0) in the more advanced models. There is growing evidence that this special case is not generally realized in natural systems (Stute et al. 1995b; Ballentine and Hall 1999; Aeschbach-Hertig et al. 2000, 2001). Thus, the problem of model choice essentially reduces to the PR / MR and CE models. Although the experience with the comparison of these models is still limited at present, it seems that in many cases all of them provide a reasonable fit to the measured concentrations of Ne, Ar, Kr, and Xe. The models differ strongly in their predictions for He and the He, Ne, and Ar isotope ratios (Aeschbach-Hertig et al. 2000; Peeters et al. 2002). Because of the non-atmospheric components, He can rarely be used to test the models, and $^{40}Ar/^{36}Ar$ may also be equivocal for the same reason. Thus, analysis of the $^{20}Ne/^{22}Ne$ ratio provides the best option to distinguish between the models and so far appears to favor the CE-model (Peeters et al. 2002). Field and laboratory studies under various conditions are needed to understand which model provides the best approximation of reality under which conditions.

Table 2. Excess air models.

Model	*Equation*	*Parameters*	*Reference*
Unfractionated excess Air (UA)	$C_{i,ex}^{UA} = A_d \cdot z_i$	A_d: Conc. dissolved excess air	Heaton and Vogel (1981)
Partial Re-equilibration (PR)	$C_{i,ex}^{PR} = A_d \cdot z_i \cdot e^{-R \cdot D_i/D_{Ne}}$	A_d: Initial conc. of dissolved excess air R: Degree of re-equilibration	Stute et al. (1995b)
Multi-step partial Re-equilibration (MR)	$C_{i,ex}^{MR,n} = A_d \cdot z_i \cdot e^{-R_i} \cdot \frac{1-e^{-nR_i}}{1-e^{-R_i}}$	$R_i = R \cdot D_i/D_{Ne}$ A_d, R: as in PR, for each step n: Number of dissolution–degassing steps	This work
Closed-system Equilibration (CE)	$C_{i,ex}^{CE} = \frac{(1-F)A_e z_i}{1+FA_e z_i/C_{i,eq}}$	A_e: Initial conc. entrapped air F: Reduction of entrapped volume by dissolution and compression	Aeschbach-Hertig et al. (2000)

Separation of the components

Separation of He components using Ne. In applications of the He isotopes, particularly the tritiogenic $^3He_{tri}$, for dating purposes, usually only He and Ne are analyzed. The Ne concentration is used to estimate the atmospheric He components in order to calculate the non-atmospheric He components that carry the time information. This approach is based on the fact that in Equation (5) Ne usually has only two

components (equilibrium and excess air), whereas ^{4}He has one additional component (terrigenic), and ^{3}He has two non-atmospheric components (terrigenic and radiogenic / tritiogenic). The equations for Ne, ^{4}He, and ^{3}He are linked by the elemental composition $L_{ex} = (He/Ne)_{ex}$ of the excess air component as well as the isotopic compositions $R_{ex} = (^3He/^4He)_{ex}$ and $R_{ter} = (^3He/^4He)_{ter}$ of both the excess air and terrigenic He components. Further introducing $R_{eq} = (^3He/^4He)_{eq}$, we can write Equation (5) explicitly as:

$$Ne_m = Ne_{eq} + Ne_{ex} \tag{29a}$$

$$^4He_m = {}^4He_{eq} + L_{ex} \cdot Ne_{ex} + {}^4He_{ter} \tag{29b}$$

$$^3He_m = R_{eq} \cdot {}^4He_{eq} + R_{ex} \cdot L_{ex} \cdot Ne_{ex} + R_{ter} \cdot {}^4He_{ter} + {}^3He_{tri} \tag{29c}$$

This equation system can easily be solved for the non-atmospheric He components. From Equation (29a) we determine Ne_{ex}, insert the result into Equation (29b) to obtain $^4He_{ter}$, and finally solve Equation (29c) for the sought-after $^3He_{tri}$:

$$\begin{aligned} {}^3He_{tri} = {} & {}^4He_m \cdot (R_m - R_{ter}) - {}^4He_{eq} \cdot (R_{eq} - R_{ter}) \\ & - L_{ex} \cdot (Ne_m - Ne_{eq}) \cdot (R_{ex} - R_{ter}) \end{aligned} \tag{30}$$

Of course, the applicability of Equation (30) depends crucially on our knowledge of the quantities on the right hand side. If the infiltration conditions – in particular the recharge temperature – are known, the equilibrium components can be calculated. The elemental and isotopic compositions of the excess air component (L_{ex} and R_{ex}) are usually assumed to be atmospheric. Finally, the terrigenic He component usually originates from the crust and a typical value of 2×10^{-8} is assigned for R_{ter}. These traditional assumptions should be critically assessed in each particular case (Holocher et al. 2001). Some general features are discussed in the following.

In lakes, often even further simplifications can be made. Ne concentrations are usually close to atmospheric equilibrium, and also the terrigenic He component is usually small, although it can be important in lakes with high water residence times or high terrigenic fluxes. In the simplest case, both Ne and ^{4}He concentrations are at equilibrium at the water temperature. The concentration of tritiogenic $^3He_{tri}$ can then be calculated as follows:

$$^3He_{tri} = {}^4He_m \cdot (R_m - R_{eq}) \tag{31}$$

Note that the difference is taken between isotope ratios rather than between ^{3}He concentrations, because the ratios are usually measured with higher precision than the concentrations. The analytical precision of the $^3He/^4He$ ratio measurement usually ranges between 0.2 and 1%. This uncertainty essentially determines the precision and detection limit for $^3He_{tri}$ and hence for the derived ^{3}H-^{3}He age. It should also be noted that $^3He_{tri}$ and thus the age becomes zero if R_m equals the $^3He/^4He$ ratio at solubility equilibrium ($R_{eq} \approx 1.36\times10^{-6}$, Benson and Krause 1980), not the atmospheric $^3He/^4He$ ratio ($R_a = 1.384\times10^{-6}$, Clarke et al. 1976).

In many lakes, significant ^{4}He excesses are found while ΔNe is close to zero, indicating the presence of terrigenic helium. In such cases, the correction for excess air based on Ne only adds noise, and $^3He_{tri}$ may be calculated from a simplified version of Equation (30) without the Ne-term. However, a value for R_{ter} is needed. Usually the excess ^{4}He is radiogenic, originating from crustal rocks. Because typical values for R_{ter} are then much smaller than R_m and R_{eq}, the correction for terrigenic $^3He_{ter}$ is small, and the uncertainty of the assumed value of R_{ter} does not strongly increase the error of $^3He_{tri}$. However, in several lakes in volcanic areas, terrigenic He of mantle origin has been

found (Sano and Wakita 1987; Igarashi et al. 1992; Kipfer et al. 1994; Aeschbach-Hertig et al. 1996b, 1999a; Clark and Hudson 2001). Because typical mantle helium isotope ratios (about 10^{-5}, e.g., Mamyrin and Tolstikhin 1984) are much larger than R_m and R_{eq}, the mantle-derived ^3He may become the dominant ^3He-component, rendering it difficult or even impossible to calculate $^3He_{tri}$.

The best way to reduce the uncertainty about the terrigenic He isotope ratio R_{ter} is to look for samples that contain large concentrations of terrigenic He from the local or regional source, from which R_{ter} can be derived. Such samples may be found in thermal or mineral springs, or in deep ground waters. For example, hydrothermal water entering the northern basin of Lake Baikal was found to have a similar He isotopic composition as nearby hot springs on land (Kipfer et al. 1996). In studies of shallow aquifers, samples of deeper, He rich ground water have proven to be very valuable (Aeschbach-Hertig et al. 1998; Dunkle Shapiro et al. 1998; Holocher et al. 2001).

The most general case, when both excess air and terrigenic He are present, is rather unusual for lakes but typical for ground waters. The decisive parameter is then the He/Ne ratio of the excess air component, L_{ex}. In view of the different excess air models discussed above, it appears questionable whether the traditional assumption that L_{ex} equals the atmospheric He/Ne ratio ($L_{air} = 0.288$) is valid in general. If the excess air is fractionated, L_{ex} is always lower than L_{air} (Fig. 7). The important point to note in Figure 7 is that in the case of the CE-model, L_{ex} is restricted to the range between L_{air} and the He/Ne ratio of air-saturated water (L_{eq}). Depending on temperature, L_{eq} varies between 0.22 and 0.25. L_{ex} is thus restricted to the range between 0.22 and 0.288. In contrast, if the PR-model applies, L_{ex} decreases exponentially with R. Because R is not restricted, L_{ex} can in principle approach zero. R-values of the order of 1 (corresponding to a decrease of the Ne excess by a factor of 1/e) are not unusual, implying significantly lower values for L_{ex} than in the case of the CE-model.

Based only on He and Ne data, the appropriate value of L_{ex} cannot be determined. Additional information from other noble gas concentrations or isotope ratios is needed to distinguish between the different models and to determine the model parameters (Peeters et al. 2002). However, up to now only very few ^3H-^3He studies of shallow ground waters provide such additional information (Beyerle et al. 1999a; Holocher et al. 2001). In all previous studies, only He and Ne were measured and the assumption $L_{ex} = L_{air}$ was applied. Because L_{air} is actually only the upper limit of L_{ex}, this approach tends to overestimate the atmospheric and thus to underestimate the non-atmospheric He components. A clear sign that this approach is not always appropriate is the common occurrence of negative values for $^4He_{ter}$ or even $^3He_{tri}$.

For example, in the large ^3H-^3He study of a shallow sandy aquifer on Cape Cod of Dunkle Shapiro et al. (1999), 55 out of a total of 91 samples yielded negative $^4He_{ter}$ concentrations, clearly indicating that L_{ex} was overestimated. For each sample, the upper limit for L_{ex} is defined by the physical requirement $^4He_{ter} \geq 0$. Most of these upper limits are higher than 0.25, thus well within the range predicted by the CE-model. Only two samples require values of L_{ex} that are significantly below the range of the CE-model and can only be explained by the PR-model. We conclude that for the majority of the samples the CE-model would be sufficient to remove the inconsistency of negative $^4He_{ter}$ concentrations.

Using L_{ex}-values lower than L_{air} yields higher results for $^4He_{ter}$, $^3He_{tri}$, and the ^3H-^3He ages. Yet, as long as the value of L_{ex} is restricted to the range allowed by the CE-model, the differences in the calculated quantities are usually small. In the study of Dunkle Shapiro et al. (1999) practically no changes result, because $^4He_{ter} = 0$ was assumed in the calculation of most ages. In principle, however, for samples with a large

and strongly fractionated excess air component the usual atmospheric excess air correction can result in significantly underestimated ages.

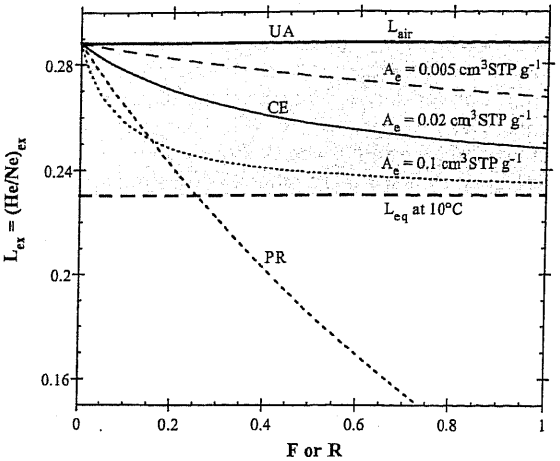

Figure 7. He/Ne ratios of the excess air component (L_{ex}) for different excess air models as functions of the fractionation parameters F or R. The atmospheric He/Ne ratio L_{air} = 0.288 defines the upper limit for L_{ex}. In the CE-model, the He/Ne ratio of air saturated water (L_{eq}) defines a lower limit for L_{ex}, which depends on both A_e and F (curves for three A_e values are shown). In the PR-model, L_{ex} is independent of A_d and decreases exponentially with R towards zero. For R > 0.25, the PR-model predicts L_{ex}-values below the range allowed by the CE-model.

Separation using all noble gases: Iterative approaches. If the equilibrium component is unknown (e.g., because of unknown equilibration temperature) and excess air is present, we have for each noble gas at least two unknown components (equilibrium and excess air) in Equation (5). However, because both components have defined (although in general unknown) elemental compositions, the equations are linked and can be solved. This is the typical situation in applications of the 'noble gas thermometer', where the equilibration temperature is to be derived from the concentrations of dissolved noble gases in ground water.

In principle, the measurement of two noble gases of purely atmospheric origin (usually all except He) and the assumption of atmospheric excess air enables the calculation of the two unknown components. The solution can be found by a graphical method, which has been used in some early studies involving the measurement of Ar and N_2 (e.g., Heaton and Vogel 1981; Heaton et al. 1986). Of course, N_2 is not a noble gas and can be affected by biogeochemical processes (e.g., denitrification, Heaton et al. 1983). A better choice of gases would be Ne and Xe, because their solubilities differ strongly (compare Fig. 1). Ne is strongly affected by excess air, whereas Xe reacts most sensitive to temperature. In a plot of Ne versus Xe concentrations (Fig. 8), the data align along straight lines representing addition of excess air to air saturated water (ASW). The intersection of these lines with the ASW-curve yields the equilibrium component (and the temperature), whereas the excess air component is given by the offset along the lines. The disadvantage of this approach is that an explicit assumption about the elemental composition of excess air (slope of the lines) has to be made in order to obtain unequivocal results.

However, if the effort is made to measure Ne and Xe, it is natural to measure Ar and

Kr as well. The traditional approach to determine recharge temperatures from full noble gas data sets involves an iterative correction for excess air (Andrews and Lee 1979; Rudolph 1981; Rudolph et al. 1984; Stute and Deák 1989; Pinti and Van Drom 1998). The measured concentrations of Ne, Ar, Kr, and Xe are corrected for excess air—assumed to be of atmospheric composition—and the equilibration temperature is calculated from the corrected concentration of each noble gas. This process is iteratively repeated with varying amounts of excess air until optimum agreement between the four temperatures is reached.

The extra information gained by analysing all noble gases can be used to estimate the uncertainty of the derived temperature from the standard deviation of the individual temperatures. Systematic trends in the temperatures derived from the individual noble gases indicate that the composition of the gas excess differs from atmospheric air. The iterative approach to correct for excess air is still applicable in such cases, as long as the composition of the gas excess can be described by one additional parameter. Stute et al. (1995b) used this approach in connection with the PR-model.

Separation using all noble gases: Inverse techniques. Although the iterative method works well in most cases, there is a more fundamental way to solve the problem, which has a number of advantages. The problem is to solve Equation (5), which can be written as an explicit equation system by inserting Equations (2) and (3) for the equilibrium component and one of the model Equations (13), (17), (25), or (27) for the excess air component. Restricting the problem to atmospheric gases, we are left with equations for the equilibrium and excess air components of Ne, Ar, Kr, and Xe. In this form, we recognize that the actual unknowns are no longer the individual components, but their defining parameters T, S, P, A_d or A_e, and R or F.

Thus, in general we have 4 measured atmospheric noble gas concentrations but 5 unknown parameters. Obviously, this general problem cannot be solved. Yet, in most practical cases, some of the 5 parameters are well constrained. We can usually set $S \approx 0$, because infiltrating ground water is fresh, and we can estimate P from the altitude of the recharge area (Eqn. 4). We are then left with 3 unknown parameters and 4 measured concentrations, thus the system is over-determined. It can be solved for the model parameters by inverse modeling techniques based on error weighted least squares fitting (Aeschbach-Hertig et al. 1999b; Ballentine and Hall 1999).

The inverse approach determines those parameter values that within the framework of each conceptual model yield the best fit to the observed concentrations. The best fit is the one that minimizes χ^2, which is the sum of the weighted squared deviations between the modeled and measured concentrations:

$$\chi^2 = \sum_i \frac{\left(C_i^{meas} - C_i^{mod}\right)^2}{\sigma_i^2} \tag{32}$$

where C_i^{mod} are the modeled concentrations, and $C_i^{meas} \pm \sigma_i$ are the measured concentrations with their experimental 1σ-errors. This solution approach is very flexible with regard to the choice of the parameters to be varied, the constraints (measured concentrations) to be used, as well as the incorporation of different conceptual models for excess air.

An essential feature of the inverse approach is the use of the experimental errors as weights in Equation (32). This assures that the influence of each individual measurement on the final parameter values is properly weighted. Moreover, the use of the experimental errors allows the derivation of objective error estimates for the obtained parameter values. In the theory of least squares fitting, uncertainties of the estimated parameters are

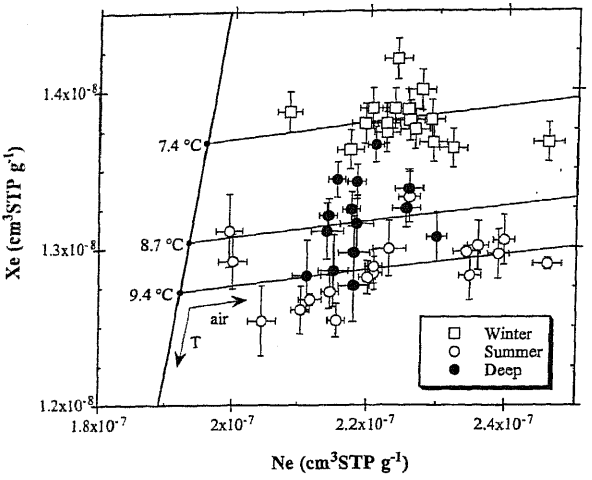

Figure 8. Ne vs. Xe concentrations from an alluvial aquifer (Beyerle et al. 1999). The data are explained by variations of the recharge temperature (solid line) and varying amounts of excess air (thin lines). The excess air lines were calculated by fitting straight lines with prescribed slope (atmospheric Xe/Ne ratio) to three groups of samples. Samples from shallow boreholes taken in winter (open squares) have the highest Xe concentrations, corresponding to the lowest temperatures (7.4°C). Shallow samples from summer and fall (open circles) indicate warmer recharge temperatures (9.4°C). The samples from deeper boreholes (full circles) lie in between (8.7°C). These mean temperatures calculated only from Ne and Xe data lie close to the mean temperatures calculated from all noble gases (7.4, 9.2, and 8.6°C, respectively).

derived from the covariance matrix. These errors correspond to a rigorous propagation of the experimental uncertainties. Besides the uncertainties of the parameters, also their mutual correlation can be obtained from the covariance matrix.

Most importantly, however, the use of the experimental errors allows an objective judgement of the agreement between model and data, i.e., the validity of the conceptual model that was adopted to describe the data. The model selection is based on the χ^2-test. The expected minimum value of χ^2 is the number of degrees of freedom $\nu = n - m$, where n is the number of data points and m is the number of free parameters. The probability p for χ^2 to be higher than a given value due to random analytical errors, although the model description is correct, can be obtained from the χ^2-distribution with ν degrees of freedom. If p is lower than some cut-off value p_c ($p_c = 0.01$ proved to be appropriate), the model is rejected.

The χ^2-test can be generalized to assess the applicability of a conceptual model to a whole data set consisting of N samples. Applying the same model to each sample of the data set may be interpreted as fitting one model with $N \cdot m$ free parameters to $N \cdot n$ data points. The χ^2-value for the whole data set is then the sum of the χ^2-values of the individual samples, and the number of degrees of freedom is $N \cdot \nu$. This data set χ^2-value also follows a χ^2-distribution, but with a much larger number of degrees of freedom than for each individual sample. Therefore, a conceptual model may not be consistent with a whole data set although it cannot be rejected based on any single sample.

The results of the inverse approach are not the individual components, but values for the parameters from which the equilibrium and excess air components for all species (including those that were not used in the inverse procedure, such as ^{3}He and ^{4}He) can be

calculated. The result of such calculations can then be used to determine possible non-atmospheric components using Equation (5). Alternatively, the non-atmospheric components may be treated as fit parameters in an inverse modeling approach based on an ensemble of samples, as demonstrated by Peeters et al. (2002).

Interpretation

The whole effort of component separation is undertaken to provide quantities that can be interpreted in terms of meaningful parameters such as water residence times ('ages'), recharge temperatures, or other environmental conditions at recharge. Here we discuss the basic steps that lead from the individual components to these interpreted quantities.

^{3}H-^{3}He age. As ^{3}H decays, $^3He_{tri}$ is produced. However, as long as the water is in contact with the atmosphere, the resulting excess $^3He_{tri}$ can continuously escape into the air. As soon as a water parcel is isolated from the gas exchange with the atmosphere, the ^{3}H decay is matched by a corresponding increase of $^3He_{tri}$ (Fig. 9). The ^{3}H-^{3}He clock starts ticking, and measures the isolation time of the water parcel.

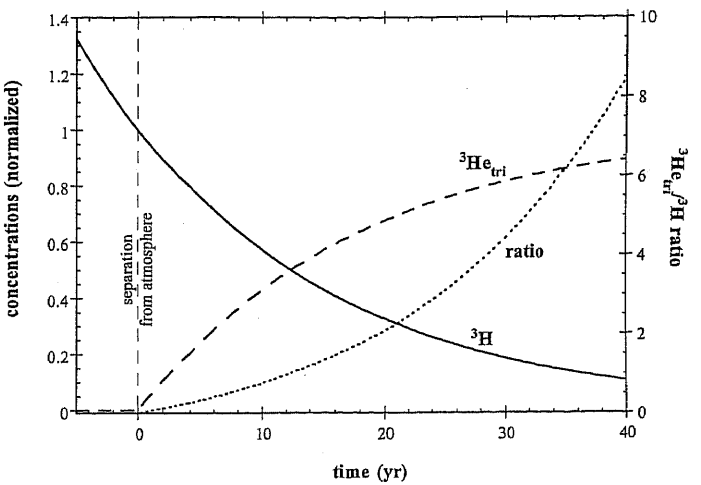

Figure 9. Temporal evolution of ^{3}H and $^3He_{tri}$ concentrations, normalized to ^{3}H(t = 0), and the $^3He_{tri}/^3$H ratio in a water parcel. As long as the water is in contact with the atmosphere, ^{3}H decays but $^3He_{tri}$ remains zero due to gas exchange. After isolation from the atmosphere, $^3He_{tri}$ increases as ^{3}H decreases. The $^3He_{tri}/^3$H-ratio is a unique function of the time elapsed since isolation, the so-called ^{3}H-^{3}He water age.

As shown in Figure 9, the $^3He_{tri}/^3$H ratio steadily increases with time, and thus the ^{3}H-^{3}He water age τ is a unique function of this ratio. The expression for τ is easily obtained from the law of radioactive decay (e.g., Tolstikhin and Kamenskiy 1969):

$$\tau = \frac{1}{\lambda} \cdot \ln\left(1 + \frac{^3He_{tri}}{^3H}\right) \qquad (33)$$

where λ is the decay constant of tritium (half-life 4500 days or 12.32 yr, $\lambda = 0.05626\ yr^{-1}$, Lucas and Unterweger 2000). ^{3}H is usually given in TU (tritium units, 1 TU is equivalent to a ^{3}H/^{1}H ratio of 10^{-18}), $^3He_{tri}$ in cm^3 STP g^{-1}. In order to evaluate Equation (33), these units have to be converted as follows (for fresh water): 1 cm^3 STP g^{-1} = $4.019 \cdot 10^{14}$ TU.

The water age τ depends in a non-linear way on the concentrations of $^3He_{tri}$ and ^3H. As a result, mixing of water parcels with different concentrations results in water ages that deviate from the true age of the mixture. For this reason, τ is sometimes referred to as the 'apparent water age'. In situations with strong mixing, e.g., in lakes, τ should be interpreted with some caution. The distortion of τ due to mixing is less important for small ages. If $^3He_{tri}/^3H \ll 1$ or equivalently $\tau \ll 1/\lambda$, Equation (33) can be linearised to give:

$$\tau = \frac{1}{\lambda} \cdot \frac{^3He_{tri}}{^3H} \tag{34}$$

In this case, τ is a linear function of the ratio $^3He_{tri}/^3H$, but not of ^3H. The age behaves only linearly if water parcels with equal ^3H concentrations are mixed. Otherwise, the apparent age of the mixture is always biased towards the component with the higher ^3H concentration (see also Schlosser and Winckler 2002, this volume).

^{4}He accumulation age. Radiogenic He produced by α-decay of U and Th series nuclides in crustal minerals accumulates both in ground water and deep water of lakes. Assuming a constant accumulation rate J_{He}, the water residence time τ follows directly from the concentration of radiogenic He:

$$\tau = \frac{^4He_{rad}}{J_{He}} \tag{35}$$

The problem is to determine the accumulation rate J_{He}. In ground water, there are three potential sources of radiogenic He: (1) *in situ* production within the aquifer matrix (e.g., Andrews and Lee 1979; Marine 1979; Torgersen 1989), (2) a flux from adjacent layers or even the whole underlying crust (Heaton and Vogel 1979; Torgersen and Clarke 1985), and (3) release of stored He from sediments by weathering (Torgersen 1980; Heaton 1984) or diffusion (Solomon et al. 1996). In lakes, *in situ* production from dissolved U and Th in the water column is negligible, but radiogenic He emanates from the sediments or deeper layers of the crust (Figs. 2 and 3). With the exception of *in situ* production in aquifers, the relative contribution of the He sources is difficult to estimate as it can vary by orders of magnitude depending on the geological setting.

Assuming that the He production in the entire crust is balanced by degassing, an average continental crustal He flux of 2.8×10^{10} atoms m^{-2} s^{-1} = 3.3×10^{-6} cm^3 STP cm^{-2} yr^{-1} can be derived (O'Nions and Oxburgh 1983). This flux may in some cases be useful to estimate the He accumulation rate, but it remains questionable whether the assumption of a uniform flux is justified (e.g., Castro et al. 1998b; Ballentine et al. 2002 in this volume; Ballentine and Burnard 2002 in this volume). Therefore, He accumulation usually provides only a qualitative timescale.

If it can be demonstrated that *in situ* production is the dominant ^4He source, quantitative dating is possible *in situ* ^4He production rate and the resulting accumulation rate J_{He} can be calculated from the U and Th concentrations of the aquifer material (Andrews and Lee 1979; Castro et al. 2000):

$$J_{He} = \Lambda_{He} \frac{\rho_r}{\rho_w} \left(C_U \cdot P_U + C_{Th} \cdot P_{Th}\right) \cdot \left(\frac{1-\Theta}{\Theta}\right) \tag{36}$$

The release factor Λ_{He} (fraction of produced ^4He which is released from minerals into the water) is usually taken to be 1 (e.g., Andrews and Lee 1979; Torgersen and Clarke 1985). ρ_r and ρ_w are the densities of the aquifer material and the water, respectively. The ^4He production rates from U and Th decay are P_U = 1.19×10^{-13} cm^3 STP μg_U^{-1} yr^{-1} and P_{Th} = 2.88×10^{-14} cm^3 STP μg_{Th}^{-1} yr^{-1} (Andrews and Lee 1979). The U and Th

concentrations (C_U, C_{Th}, in $\mu g\ g^{-1}$) and the porosity (Θ) of the aquifer matrix have to be measured.

Recharge temperature, salinity, and altitude. From the equilibrium concentrations $C_{i,eq}$ we can potentially learn something about the water temperature T and salinity S, as well as the atmospheric pressure P. The water temperature is related to the soil and eventually to the mean annual air temperature, whereas salinity may indicate evaporative enrichment, and pressure is closely related to altitude. Although the focus has, in most cases, been directed to temperature, the other options should not be neglected.

After the separation of components, each individual parameter T, S, or P can be calculated by inversion of the solubility equations $C_{i,eq}$ (T,S,P) if the other two parameters are known. The inverse techniques discussed above offer the possibility to determine all three parameters at once. However, these parameters are rather strongly correlated, in particular in the presence of excess air (Fig. 1; Aeschbach-Hertig et al. 1999b). The reason for this problem is that the dependence of noble gas concentrations on the parameters follows some systematic trends. The effects of changes of T and S on the concentrations increase with molar mass of the gas, whereas the effect of excess air (A_d) decreases, because the solubilities strongly increase with molar mass. P has a uniform effect relative to equilibrium concentrations, but in the presence of excess air it is relatively more important for the heavy noble gases. As a result, especially the effects of P and S are very similar, and both can be approximated by a combination of T and A_d (see Fig. 1).

Parameter combinations that have very different patterns of effects on the concentrations (e.g., T-A_d, Fig. 1) are readily identifiable. In contrast, parameter pairs that have similar effects (e.g., S-P, Fig. 1) are hard to separate. Attempts to simultaneously fit two or more correlated parameters result in large uncertainties. Table 3 lists the errors obtained for T, S, and P from fitting various parameter combinations to a synthetic data set calculated with T = 10°C, S = 0‰, P = 1 atm, and $A_d = 3\times10^{-3}$ cm^3 STP g^{-1}, assuming experimental errors of ±1% on all concentrations. Each parameter on its own can be determined quite precisely. The errors increase only slightly if in addition an unknown amount of excess air (A_d) is present. Fractionated excess air enlarges the errors by a factor of two to three. Combinations of two parameters among T, S, and P yield even larger errors, and if in addition excess air is present, the uncertainties increase strongly. Finally, it is practically impossible to simultaneously fit T, S, and P.

It should however be stressed that each individual parameter of the equilibrium component can be well determined even in the presence of fractionated excess air. This fact provides the basis for the application of noble gas concentrations in ground water as indicators of paleotemperature.

Excess air parameters. Separation of the components, in particular by the inverse technique, also provides the parameters that define the excess air components such as the concentrations of dissolved or entrapped air (A_d or A_e), and the fractionation parameters R or F. Even without a perfect description of excess air, ΔNe can be quantified. Although the potential of excess air as an indicator of past recharge conditions was discussed in the first studies that identified the excess air component (Heaton and Vogel 1981; Heaton et al. 1983), little further progress has been made in the interpretation of the excess air signal.

The recent development of different models for the formation of excess air, and the methods to distinguish between these models and to determine their parameters based on

Table 3. Uncertainties of the inverse parameter estimation for different sets of free parameters, using a synthetic data set corresponding to T = 10°C, S = 0 ‰, P = 1 atm, $A_d = 3\times10^{-3}$ cm^3 STP g^{-1}, with errors of 1% on all concentrations.

Parameters	*ΔT [°C]*	*ΔS [‰]*	*ΔP [atm]*
T or S or P	0.19	0.75	0.005
T, A_d	0.21	-	-
S, A_d	-	1.0	-
P, A_d	-	-	0.007
T, A_d, R	0.49	-	-
T, A_e, F	0.38	-	-
S, A_d, R	-	2.5	-
S, A_e, F	-	1.9	-
P, A_d, R	-	-	0.021
P, A_e, F	-	-	0.015
T, S	0.82	3.0	-
T, P	0.62	-	0.017
S, P	-	9.3	0.067
T, S, A_d	2.6	11	-
T, P, A_d	2.0	-	0.067
S, P, A_d	-	39	0.30
T, S, P	7.6	110	0.63

field data (inverse fitting, isotope ratios) provide the basis for further investigations of the information potentially available from the excess air (Aeschbach-Hertig et al. 2001). The models suggest that excess air is related to physical conditions in the quasi-saturated zone, where air is trapped during ground-water infiltration. Potentially important parameters are the air / water volume ratio, the pore size distribution, and the pressure in this zone. The pressure acting on the entrapped air may in turn be related to the amplitude of water table fluctuations and thus ultimately to the amount or variability of recharge.

APPLICATIONS IN LAKES

Applications of noble gases in lakes are mostly concerned with the identification of transport processes and the estimation of exchange rates between different regions within a lake. Torgersen et al. (1977) were the first to propose ^{3}H-^{3}He ages as a methodology in physical limnology and suggested that gas exchange rates and residence times can be determined from ^{3}H-^{3}He water ages. The time information provided by the combination of ^{3}H and ^{3}He is especially useful in estimating vertical water exchange in deep lakes, e.g., Lake Lucerne (Aeschbach-Hertig et al. 1996a), Lake Baikal (Peeters et al. 1997; Hohmann et al. 1998; Peeters et al. 2000b), Lake Issyk-Kul (Hofer et al. 2002; Vollmer et al. 2002), the Caspian Sea (Peeters et al. 2000a), the great lakes of North America (Torgersen et al. 1977), and in chemically stratified lakes, e.g., Green Lake (Torgersen et al. 1981), Lake Zug (Aeschbach-Hertig 1994) and Lake Lugano (Wüest et al. 1992). In addition to vertical mixing horizontal exchange between different lake basins can be studied (Zenger et al. 1990; Aeschbach-Hertig et al. 1996a). The ^{3}H-^{3}He ages may also be employed as time information required for the calculation of oxygen depletion and of

the terrigenic ^{4}He flux from the sediments (Top and Clarke 1981; Mamyrin and Tolstikhin 1984; Aeschbach-Hertig 1994; Aeschbach-Hertig et al. 1996a; Hohmann et al. 1998; Peeters et al. 2000a).

The atmospheric noble gases Ne, Ar, Kr and Xe that have been measured in Lake Baikal (Hohmann et al. 1998; Aeschbach-Hertig et al. 1999b), in the Caspian Sea (Peeters et al. 2000a), and in Lake Tanganyika (Kipfer et al. 2000) carry information on the conditions at the lake surface during gas exchange. This information has been used to study lake level fluctuation in Lake Tanganyika (Craig et al. 1973; Kipfer et al. 2000) but might also be exploitable with respect to paleoclimate if the noble gases can be measured in the pore water of lake sediments. The behavior of the noble gas ^{222}Rn differs from that of the other noble gases because it is lost rapidly by radioactive decay. ^{222}Rn has been employed to study horizontal and vertical mixing in the near sediment region of lakes (Imboden and Emerson 1978; Imboden and Joller 1984; Weiss et al. 1984; Colman and Armstrong 1987) and to trace river flow in Lake Constance (Weiss et al. 1984).

Mixing and the distribution of dissolved substances in lakes

In most lakes the distribution of dissolved substances is dominated by transport due to turbulent motions. Mixing in the horizontal direction is rapid, resulting in nearly homogeneous concentrations horizontally. In the vertical direction, density stratification suppresses turbulence, thus reducing vertical exchange of dissolved substances and heat. As a consequence vertical concentration and heat gradients can build up. Because density stratification varies seasonally, vertical mixing varies substantially over the year.

During spring and summer, warming of the surface waters due to the heat flux from the atmosphere leads to a warm surface layer that is mixed by wind forcing and convection during nighttime cooling. This layer is separated from the deep-water body by a strong thermocline (May and July profiles, Fig. 10). Associated with the thermocline is a strong density stratification preventing exchange of heat and dissolved substances between the surface layer and the cold deep water. In fall and winter, surface cooling causes convection that successively erodes the thermocline from the top thus increasing the depth of the homotherm surface layer (November profile, Fig. 10). This process leads

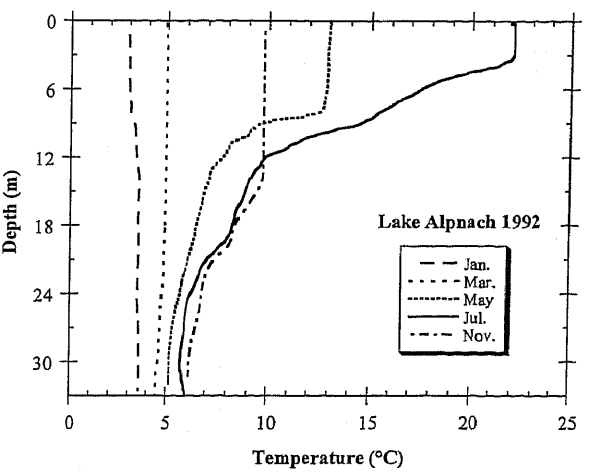

Figure 10. Seasonal variation of the vertical temperature distribution in temperate lakes exemplified by temperature profiles from Lake Alpnach (Switzerland).

to a vigorous redistribution of all dissolved substances. In quite a few lakes convective mixing by surface cooling continues until the entire water column becomes homotherm that is commonly termed 'full turnover'. Note however, that this does not necessarily imply a fully mixed water column. In freshwater lakes further winter cooling can lead to a cold surface layer and an associated density-stratification (January profile, Fig. 10), because below 4°C freshwater density decreases with decreasing temperature. Warming of the surface waters in early spring removes the cold surface layer leading again to homotherm conditions with vigorous mixing (March profile, Fig. 10). Then the seasonal mixing cycle with the development of a surface layer begins anew.

The pattern of seasonal mixing can vary substantially between lakes and depends on climatic and meteorological conditions. In addition it may be altered e.g., by density stratification due to gradients in the concentration of dissolved substances, a feature typical for lakes with anoxic deep water. In very deep lakes the deep-water body may not be affected by seasonal mixing at all (e.g., Lake Tanganyika). River inflows introduce dissolved substances to the lakes and may contribute to vertical transport if the river water is denser than the lake water and sinks to greater depths resulting in upwelling of lake water (e.g., in Lake Baikal). However, in most lakes turbulent motions are predominantly responsible for vertical transport of dissolved matter and thus central for the understanding of the lake ecosystem. Hence, the quantification of the vertical exchange is one of the central questions in lakes research to which noble gases and especially ^{3}H-^{3}He dating have been applied.

The vertical flux F of a dissolved substance resulting from turbulent motion is commonly described in analogy to transport by molecular diffusion:

$$F = -K_z \cdot \frac{\partial C}{\partial z} \tag{37}$$

where C is the concentration, z the depth (positive upwards) and K_z the vertical turbulent diffusivity. In contrast to molecular diffusivities, the turbulent diffusion coefficient is a characteristic property of the turbulent motion. Hence, K_z is independent of the specific properties of the dissolved substance and the same K_z applies to substance concentrations and heat. In most lakes the transport by turbulence is several orders of magnitude larger than the transport by molecular diffusion. As a consequence, estimations of the vertical flux of tracers can be employed to estimate K_z, from which the flux of ecologically relevant substances such as nutrients or dissolved oxygen can be derived.

The net flux of mass of dissolved substance or of heat by turbulent motion can be interpreted as being the result of the exchange of water volume per unit time between neighboring regions in the water body which have different substance concentrations or temperatures:

$$F_{12} = \frac{Q_{ex}}{A_{12}} \cdot (C_1 - C_2) \tag{38}$$

where F_{12} is the net flux from region 1 to region 2, Q_{ex} is the volume exchange rate, A_{12} is the area of the interface between region 1 and 2, and C is the concentration or temperature in regions 1 and 2, respectively. The interpretation of the turbulent flux as caused by exchange of water volume is the concept behind exchange rates and residence times commonly derived from ^{3}H and ^{3}He concentrations. The exchange rate is the volume exchange per unit time divided by the volume of the water body considered and the residence time is the inverse of the exchange rate. In lakes exchange rates are usually calculated for two-box models in which one box represents the surface mixed layer and the other the deep water layer, because the exchange of nutrient rich deep water with

surface water across the thermocline is a key question to understand biological production in surface waters.

Distribution of noble gases in lakes

Atmospheric noble gases Ne, Ar, Kr and Xe. The predominant source of atmospheric noble gases in lakes is gas exchange between atmosphere and water (Fig. 2). Usually the concentrations of the atmospheric noble gases Ne, Ar, Kr and Xe measured in the deep water of lakes are close to atmospheric equilibrium at the water temperature of the sample and atmospheric pressure at the lake surface. Profiles of ^{20}Ne concentrations in Lake Baikal are shown in Figure 11b. Assuming that concentrations in the water remain unchanged after the water is transported from the lake surface to greater depths, concentrations of Ne, Ar, Kr and Xe carry information on temperature, salinity and atmospheric pressure during gas exchange which can be inferred from the data using inverse fitting techniques (Aeschbach-Hertig et al. 1999b). In Lake Baikal and in the Caspian Sea temperatures derived from noble gas concentrations agree well with temperatures measured with temperature sensors (Fig. 12; Aeschbach-Hertig et al. 1999b; Peeters et al. 2000a) In large lakes, noble gas concentrations can be raised compared to atmospheric equilibrium by unfractionated excess air which probably stems from dissolution of air bubbles injected into the water by breaking waves (Fig. 2). Excess air expressed as Ne excess above atmospheric equilibrium, ΔNe, is on average 1% ΔNe in Lake Baikal (Aeschbach-Hertig et al. 1999b) but can be up to 5% ΔNe in Lake Tanganyika (Kipfer et al. 2000) and 4% ΔNe in the Caspian Sea (Peeters et al. 2000a). The latter values are on the same order as in the ocean (Bieri 1971). The information captured by the dissolved atmospheric noble gas concentrations is potentially stored in the pore water of lake sediments and thus could be an excellent tool in paleolimnology to study temperature changes in tropical lakes or variations of the salt content in closed-basin lakes indicating lake level fluctuations.

If atmospheric noble gases at the lake surface are always in equilibrium with the atmosphere, one would expect that in lakes located in temperate regions, noble gas concentrations and in particular the temperature sensitive Xe concentration should have strong vertical gradients during summer stratification. Assuming 25°C in the surface and 4°C in the deep water, the corresponding Xe concentration should differ by about 50%. Because the Xe flux at the lake surface due to gas exchange is limited and vertical transport would cause a flux of Xe from deep to shallow waters, Xe concentrations in the surface waters can be expected to be above atmospheric equilibrium in summer. Thus Xe and other atmospheric noble gases might be applied to study gas and deep-water exchange. To our knowledge, a profile of all atmospheric noble gases has not yet been measured in temperate lakes during periods of strong temperature stratification.

^{3}He and ^{4}He. Gas exchange between the atmosphere and the water at the lake surface is an important source or sink of ^3He and ^4He. Therefore the concentrations of ^3He and ^4He near the lake surface are usually close to atmospheric equilibrium (Fig. 11a,d). However, in addition to the atmosphere, He of terrigenic / radiogenic origin enters the lake via the sediments (Fig. 2). In most cases $^4He_{ter}$ stems from the Earth's crust but in some cases also from the Earth's mantle. If the contribution of the mantle component is significant, $^3He_{ter}$ can be important. However, in most lakes $^3He_{ter}$ is predominantly of crustal origin and is small compared to the other components contributing to the total concentration of ^3He. In contrast to $^3He_{ter}$, tritiogenic $^3He_{tri}$ is in most lakes an important source of ^3He which depends on the distribution of ^3H. The sources of ^4He and ^3He below the lake surface increase the contributions of $^4He_{ter}$, $^3He_{ter}$ and $^3He_{tri}$ to the total concentration of ^4He and ^3He, respectively, and thus lead to an increase in the concentration of both helium isotopes at larger depths. ^3He and ^4He concentrations

usually decrease towards the lake surface where the terrigenic and tritiogenic excess is lost to the atmosphere by gas exchange (see Fig. 11a,d).

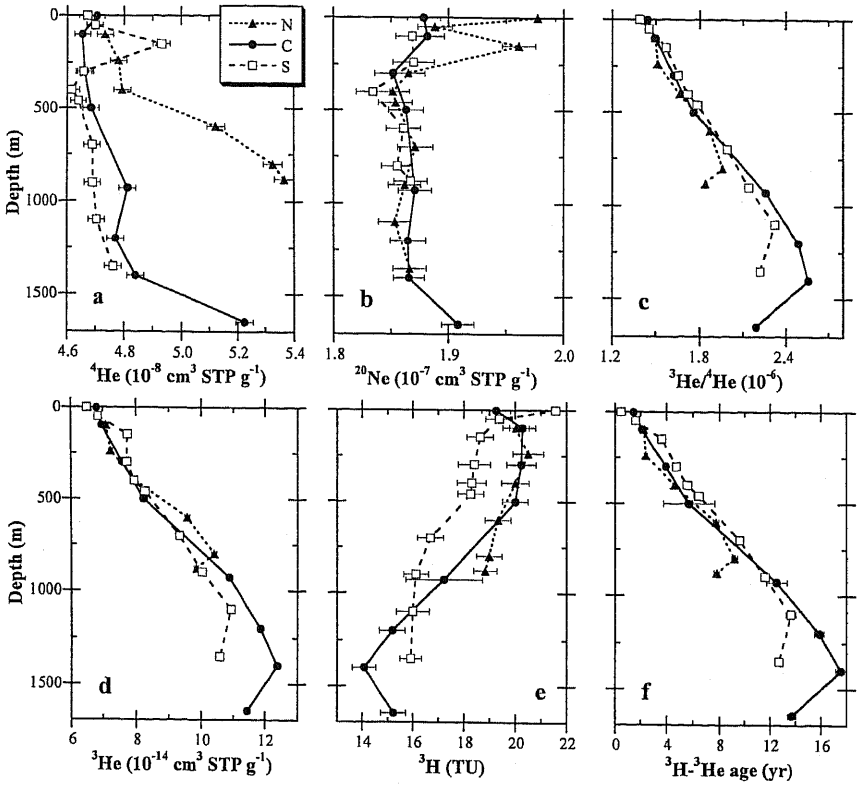

Figure 11. The vertical distribution of the ^{4}He, ^{20}Ne, ^{3}He and ^{3}H concentrations, the ^{3}He/^{4}He ratio and the ^{3}H-^{3}He water ages in the northern (N), central (C) and southern (N) basin of Lake Baikal in 1992 (data from Hohmann et al. 1998).

^{222}Rn. The noble gas isotope ^{222}Rn is of radiogenic origin and its concentration distribution is closely linked to the distribution of its mother element ^{226}Ra. In lakes, Ra is predominantly concentrated in the sediments and to a lesser extent adsorbed to particles suspended in the water. Therefore, the sediments are the most important source of ^{222}Rn and the ^{222}Rn concentrations are highest near the sediments, decreasing from there towards the lake surface. Because of the short half-life of ^{222}Rn (3.82 d) its concentration distribution has not only vertical but can also have large horizontal gradients which both depend on the location of ^{222}Rn release, i.e., on the slope of the sediments, and on the location of sampling with respect to lake morphometry. Therefore, the distribution of ^{222}Rn is affected by horizontal and vertical mixing processes. Although this enables an assessment of horizontal and vertical mixing processes from the distribution of ^{222}Rn, their quantification is non-trivial. In general, the estimation of mixing rates from the distribution of ^{222}Rn requires computation of transport in 2 or 3 dimensions (Imboden and Joller 1984).

Application of ^{3}H-^{3}He dating in lakes

Assuming that at the lake surface ^{3}He is in equilibrium with the atmosphere ^{3}He$_{tri}$, and consequently the ^{3}H-^{3}He age, should be zero. As soon as the water is moved away

from the lake surface and gas exchange stops, $^3He_{tri}$ accumulates and the ^3H-^3He age increases with time (Fig. 2). Thus the ^3H-^3He age is a measure of the 'isolation age', defined as the time elapsed since the water was last in contact with the atmosphere (Tolstikhin and Kamenskiy 1969; Torgersen et al. 1977). Note that water masses in lakes are usually mixtures and the isolation age of a sample must be understood as the volume weighted mean of the isolation age of the waters involved in the mixing. Because mixing leads to volume weighted mean concentrations of ^3H and ^3He and the ^3H-^3He age depends non-linearly on the concentrations of ^3H and ^3He, in mixed waters the ^3H-^3He age does not exactly agree with the isolation age (see Schlosser and Winckler 2002, this volume). In general, the ^3H-^3He water age of a mixture of water masses is biased towards the component with the larger ^3H concentration. However, in most lakes the simplified interpretation of the ^3H-^3He age as being equivalent to the isolation age can serve as a tool to study transport processes in a qualitative manner.

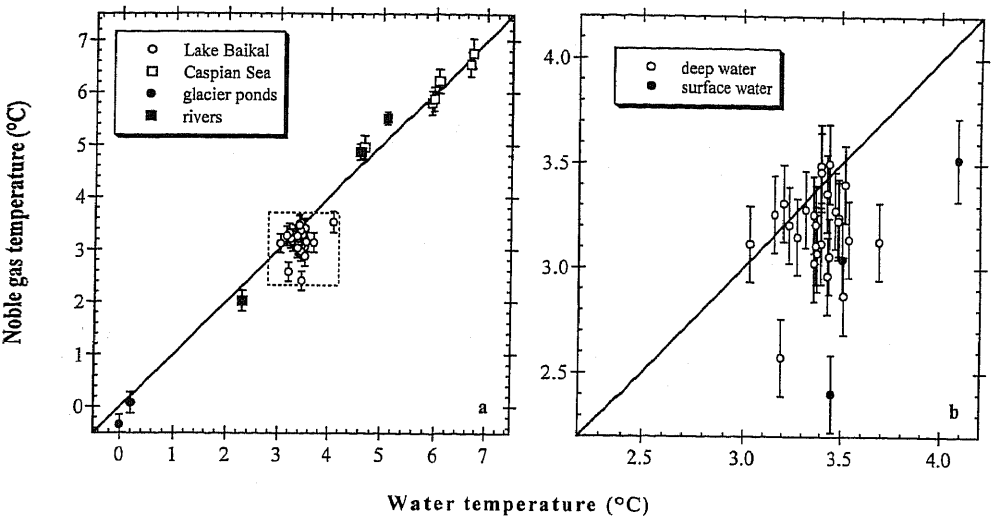

Figure 12. Comparison of temperatures derived from noble gas concentrations (NGT) with temperatures measured using thermistors (Aeschbach-Hertig et al. 1999b). Shown are several examples from surface waters including Lake Baikal and the Caspian Sea. In almost all cases the NGT agree very well with the data from temperature sensors.

For example: ^3H-^3He ages in the three basins of Lake Baikal are close to zero near the surface (Fig. 11f). With increasing depth the ^3H-^3He age increases, indicating that the deeper water was isolated from the surface for a longer period of time than the water at shallower depth. The increase of the ^3H-^3He age with depth is a measure of the intensity of vertical exchange. In the bottom 300 to 400 m, ^3H-^3He ages are about constant or even slightly decrease with increasing depth. In a one-dimensional interpretation it is impossible to explain younger water located below older water except by inflow of young water. However, inflow of young water from ground-water sources at great depths is unlikely, because typical ground-water flow is orders of magnitudes slower than vertical transport in lakes, deep ground waters generally have very large ages, and most ground-water inflow to lakes occurs near the edge of a lake, not in the middle. In Lake Baikal the young ages at largest depths originate from water of near surface regions which sinks advectively as density plumes along the basin boundaries to greatest depths where it spreads laterally (Peeters et al. 1996b; Hohmann et al. 1997). Because the ^3H-^3He age

near the surface is less than at greater depth the density plumes transport comparatively young water. Several processes causing such density plumes in Lake Baikal have been identified, e.g., river inflow, inter basin exchange, wind forcing, cabbeling (horizontal mixing of waters with temperature above and below the temperature of maximum density) and inflow of hydrothermal waters (Weiss et al. 1991; Shimaraev et al. 1993; Kipfer et al. 1996; Peeters et al. 1996a; Hohmann 1997; Hohmann et al. 1997).

In Lake Lucerne, which is a complex system of several basins separated by sills leaving 5 to 100 m water depth for inter basin exchange, ^{3}H-^{3}He age inversions indicate that horizontal water exchange between basins generates density plumes ventilating the bottom regions of the different basins. Aeschbach-Hertig et al. (1996a) estimated the horizontal and vertical exchange between neighboring basins responsible for deep-water renewal by a simple calculation of mixing ratios based on ^{3}H-^{3}He ages. During the winter in all basins the water deeper than the sills was exchanged more than once by water from above, whereas this exchange was close to zero in most basins during the summer.

As mentioned above ^{3}H-^{3}He age and isolation age unfortunately do not exactly agree in mixed waters. Nevertheless, direct application of ^{3}H-^{3}He age for quantification of water exchange is possible but limited to cases where (1) the ^{3}H concentration is approximately homogeneous, and (2) the water age is small compared to the half-life of tritium. The second condition is required because if ^{3}H-^{3}He ratios are small the water age can be linearized (Eqn. 34). If both conditions are fulfilled, mixing affects the ^{3}H-^{3}He age in the same way as ^{3}He$_{tri}$. Then, the ^{3}H-^{3}He age behaves as a bio-geochemically inert tracer with a constant source term increasing the age by 1 yr per yr and the ^{3}H-^{3}He age can be treated as an ideal tracer of the isolation age.

Today, in most seasonally mixed lakes, ^{3}H is nearly homogeneous because nowadays the external input from the atmosphere by river inflow and direct precipitation is nearly constant and the loss of ^{3}H by radioactive decay within the lake is small during a season (~ 6% yr^{-1}). In such lakes the ^{3}H-^{3}He age reliably reflects the isolation age and can be used for quantification of exchange rates, e.g., to determine horizontal exchange as in Lake Lucerne. However, it turns out that not only in seasonally mixed lakes but also in Lake Baikal (with water ages up to 18 yr) the ^{3}H-^{3}He water age is a good estimate of the isolation age. According to Hohmann et al. (1998) the ^{3}H concentrations in Lake Baikal vary by less than 15% and the effect of mixing leads to a deviation between the ^{3}H-^{3}He age and the isolation age of less than 10%, the ^{3}H-^{3}He age being generally larger than the isolation age of the mixed water. Even in the Caspian Sea, where ^{3}H-^{3}He ages reach up to 25 yrs and the ^{3}H concentration in the southern basin decreases with depth to about 50% of the surface value (Peeters et al. 2000a), the deviation between ^{3}H-^{3}He age and isolation age due to mixing is less than 10%.

Although the discussion above demonstrates that ^{3}H-^{3}He ages provide a reliable estimate of the isolation age in a wide range of lakes, this is not always the case, as has been demonstrated for Lake Lugano (Aeschbach-Hertig 1994). Therefore, it is advisable to complement the age estimates based on ^{3}H and ^{3}He concentrations by independent estimations based on other tracers such as CFC-12 or SF_6. Dating based on these tracers compares the concentration in the water sample with the historic atmospheric equilibrium concentration of the tracer at the lake surface to determine the apparent date of equilibration. The elapsed time between the sampling date and the apparent equilibration date gives the CFC-12 age or the SF_6 age, both measuring the time elapsed since the water was in last contact with the atmosphere, i.e., the isolation age. However, because the historic atmospheric concentrations of CFC-12 and SF_6 vary in a non-linear fashion, mixing of water masses also leads to a deviation between tracer age (CFC-12 age or SF_6 age) and isolation age. Because sources and transport of the transient tracers ^{3}He, ^{3}H, SF_6,

and CFC-12 differ, the deviation between tracer age and isolation age caused by mixing is different between the ^3H-^3He, SF_6, and CFC-12 dating techniques (Hofer et al. 2002).

In the Caspian Sea ^3H-^3He ages closely agree with the CFC-12 ages (Fig. 13; Peeters et al. 2000a). The agreement of the ages supports the reliability of the ages derived from the tracers and their interpretation as a reliable proxy for the isolation age. In Lake Issyk-Kul, ^3H-^3He ages closely agree with the SF_6 ages but are significantly smaller than the CFC-12 ages (Hofer et al. 2002; Vollmer et al. 2002). Hofer et al. (2002) demonstrated that mixing and the change in the atmospheric CFC-12 concentration since the 1990s leads to CFC-12 ages that significantly overestimate the isolation age. In Lake Lugano ^3H-^3He ages are significantly larger than SF_6 ages (Fig. 13; Holzner 2001). This indicates that mixing significantly affects the ^3H-^3He ages and that they do not agree with the isolation age.

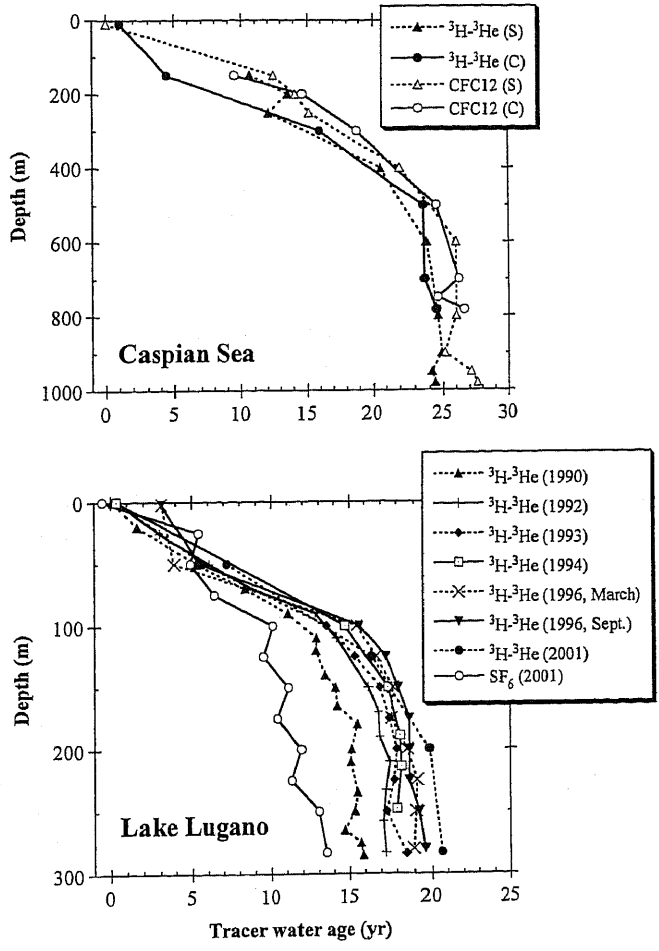

Figure 13. Comparison of ^3H-^3He ages with CFC-12 and SF_6 ages. (Upper panel) In case of the central and southern basin of the Caspian Sea (Peeters et al. 2000a), ^3H-^3He ages agree very well with CFC-12 ages indicating that the tracer water ages are a reliable proxy for the isolation age. (Lower panel) In case of Lake Lugano (Holzner 2001), ^3H-^3He ages are significantly larger than SF_6 ages suggesting that the isolation age in Lake Lugano cannot be described very reliably by ^3H-^3He ages.

Quantification of vertical exchange rates and vertical turbulent diffusivities

Budget methods. Vertical exchange rates and turbulent diffusivities K_z can be calculated from the heat balance or the mass balance of tracers for which transformation rates are known. Assuming horizontal homogeneity, the temporal change of tracer mass below a given depth z must be the sum of the net vertical mass flux through the cross-section at z and all sources and sinks of tracer mass below z. In the case of conservative tracers sources and sinks below z must be mass fluxes across the sediment-water interface. In the case of ^3H, radioactive decay is an additional sink. In the case of ^3He, tritium decay represents a source. If the increase of mass due to all sources and sinks, S_M, is known, the net mass flux can be calculated:

$$F \cdot A = -\left(\frac{dM_z}{dt} - S_M\right) \tag{39}$$

where A is the cross-sectional area at depth z,

$$M_z = \int_{z_{bot}}^{z} C(z')A(z')dz'$$

is the total tracer mass below z, z_{bot} is z at maximum depth and t is time. From F in Equations (37) and (39) turbulent diffusivities can be calculated if vertical concentration gradients and the change of tracer mass with time can be determined accurately:

$$K_z = \frac{\partial M_z/\partial t - S_M}{A \cdot \partial C/\partial z} \tag{40}$$

If only exchange rates in a 2-box model are of interest, F of Equations (38) and (39) can be used to estimate the volume exchange rates due to turbulent mixing between neighboring boxes using the concentration difference between the boxes:

$$Q_{ex} = \frac{\partial M_1/\partial t - S_{M,1}}{C_2 - C_1} \tag{41}$$

where M_1 is the volume weighted mean tracer mass in box 1, and the indices refer to the deep water box (i = 1) and the surface water box (i = 2). The exchange rate r and residence time τ_{res} for box 1 is then given by $r = 1/\tau_{res} = Q_{ex}/V_1$, where V_1 is the volume of box 1.

In the discussion above, river inflow and horizontal inter basin exchange at larger depth have been ignored, but could be incorporated in the source and sink terms if the water and mass fluxes are known.

The budget method outlined above has been introduced by Jassby and Powell (1975) and applied successfully to determine K_z in numerous studies using heat as conservative tracer that can be measured easily by temperature sensors. However, especially in deep waters, in the surface layer, and during turnover the heat budget method is not reliable because temperature variations are too small to be measured accurately. In these cases the combined mass balance of $^3He_{tri}$ and ^3H can be used to estimate exchange rates.

The mass balance of ^3H is usually not very sensitive to vertical mixing, because in many lakes ^3H gradients are small. Hence the ^3H flux is small and the change in ^3H content below a given depth is not significantly larger than the precision of the measurements. The mass balance of $^3He_{tri}$ is linearly dependent on the mass balance of ^3H, because $^3He_{tri}$ is coupled to ^3H via tritium decay. This problem could be overcome, if the estimation of exchange rates is based on the sum $^3H^* = {}^3H + {}^3He_{tri}$:

$$Q_{ex} = \frac{\partial M_{^3H^*,1}/\partial t}{^3H^*_2 - ^3H^*_1} \tag{42}$$

However, the experimental errors of ^3H concentrations are usually significantly larger than those of ^3He, making the error of $^3H^*$ rather large. Thus in the case of water bodies with long residence times and / or with a homogeneous ^3H concentration it can be advantageous to estimate volume exchange rates from ^3He concentrations

$$Q_{ex} = \frac{\partial M_{^3He_{tri},1}/\partial t - \lambda M_{^3H,1}}{^3He_{tri,2} - ^3He_{tri,1}} \tag{43}$$

because the error introduced by neglecting the transport and loss of ^3H due to decay during the observational period is small (Aeschbach-Hertig 1994).

In studies where the data are insufficient to calculate the temporal change of e.g., $^3He_{tri}$, water exchange can be estimated from the ^3H-^3He ages, provided that the ^3H-^3He ages agree with the isolation age. Then, the ^3H-^3He age can be treated as ideal tracer for water age τ which increases by 1 yr per yr. In case of steady state conditions, volume exchange between box 1 and box 2 can be calculated from the budget method (Eqn. 41):

$$Q_{ex} = \frac{V_1}{\tau_2 - \tau_1}. \tag{44}$$

Thus, if the assumptions underlying Equation (44) are fulfilled, the difference between volume weighted mean ^3H-^3He age of surface and deep water can be used as the residence time of the deep water (Peeters et al. 2000a). In Lake Baikal the exchange rates derived from this estimate of residence time can be highly inaccurate at times when ^3H gradients are large (e.g., close to 1963 during the atmospheric bomb peak) but agree reasonably well with exchange rates estimated from inverse modeling of several transient tracers if ^3H gradients are small (Peeters et al. 1997). In the case of the Caspian Sea the deep-water residence time was estimated based on the difference in ^3H-^3He ages and on the difference in CFC-12 ages between surface and deep water (Peeters et al. 2000a). Because mixing has a different effect on ^3H-^3He and on CFC-12 ages, the agreement of the residence times obtained supports the reliability of these estimates.

The two box models discussed above can be extended to a multibox model. In the limit of infinitely small boxes the multibox model corresponds to the continuous model of Jassby and Powell (1975). Using Equation (40), the vertical turbulent diffusivity as function of depth can be obtained from τ if τ is at steady state and can be treated as ideal tracer with source strength of 1yr/yr:

$$K_z = \frac{V}{A} \cdot \left(\frac{\partial \tau}{\partial z} \right)^{-1}. \tag{45}$$

Thus if the ^3H-^3He age closely agrees with the isolation age and is at steady state, K_z can be obtained directly from a vertical profile of ^3H-^3He ages. In Figure 14 measured ^3H-^3He ages in Lake Zug (Switzerland) are compared with the water age simulated by using Equation (45) and assuming that water age is at steady state and that mixing can be characterized by a diffusivity independent of depth and time. The latter assumption is unrealistic because mixing varies seasonally. Hence, the estimated diffusivity is a measure of the long-term mean effect of mixing on tracer distributions rather than the true vertical turbulent diffusivity. Model results and data agree reasonably well if a K_z betwen 6×10^{-5} m^2s^{-1} and 7×10^{-5} m^2s^{-1} is employed (Fig. 14). This range of K_z agrees well with the long-term mean K_z for Lake Zug derived from the budget of ^3He and from inverse numerical modeling of the temporal development of ^3He concentrations (Aeschbach-Hertig 1994).

Numerical modeling. In the deep water of very deep lakes such as Lake Baikal temporal changes in the concentration of ^{3}He or ^{3}H can be very small and a long time period must pass until changes can be determined with reasonable accuracy. In addition, in Lake Baikal river water sinks as density plumes from near surface regions to greatest depth and causes deep-water renewal (Hohmann et al. 1997). This process results in upwelling in the open water and thus contributes to the vertical transport of tracers. In such a case instead of the budget methods outlined above, 1-D numerical models are recommended to analyze deep-water exchange. The model must be capable of describing the vertical advective and vertical turbulent diffusive flux of the tracer at each depth and also simulate the input and loss of tracers by gas exchange, outflow and inflows at the lake surface. Because the atmospheric concentration of ^{3}He remains constant over time and the tritium concentration in precipitation can be reconstructed from the ^{3}H survey of the IAEA (IAEA/WMO 1998), it is possible to simulate ^{3}He and ^{3}H concentrations over long time periods and to predict values for ^{3}He and ^{3}H for the time of observation. By adjusting turbulent diffusivities and upwelling velocities such that data and model prediction agree, transport parameters can be determined (inverse fitting procedure). The constraint on the model parameters increases if data are available from different years and if several tracers are included. In the case of Lake Baikal the inverse fitting technique has been based on the combination of the tracers ^{3}He and ^{3}H with the gaseous tracers CFC-11 and CFC-12 (Peeters et al. 2000b). The transport rates estimated from the transient tracers can serve as the basis to estimate oxygen depletion in the deep water or the He flux from the sediments (see below).

Long term numerical modeling of the concentrations of ^{3}He and ^{3}H has also been successfully applied in smaller lakes that undergo strong seasonal changes (Aeschbach-Hertig 1994; Aeschbach-Hertig et al. 1999a, 2002a; Holzner 2001). However, in such

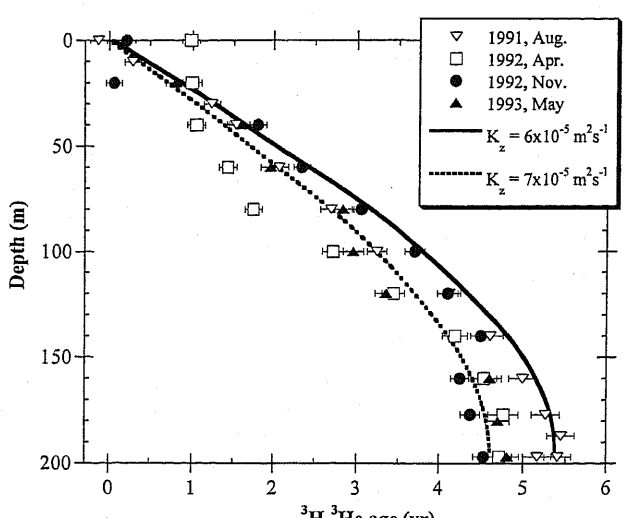

Figure 14. ^{3}H-^{3}He ages in Lake Zug determined from concentrations of noble gases and ^{3}H measured in water samples collected between 1991 to 1993 (Aeschbach-Hertig 1994) and isolation ages derived from a simplified exchange / mixing model. The model assumes that water ages are at steady state and that vertical transport can be described in analogy to Ficks law using a diffuivity of 6×10^{-5} m^{2}s^{-1} (solid line) and 7×10^{-5} m^{2}s^{-1} (dashed line) independent of depth and time.

lakes inverse fitting of the tracer data can only produce reliable results if the number of parameters describing the seasonal changes of the vertical distribution of K_z is small. Hence, a substantial amount of additional information must be available to describe the seasonally changing thickness of the surface layer and the vertical and temporal variation of K_z.

He flux from the continental crust and oxygen depletion

Estimation of the ^{4}He flux. In lakes, He emanates from the sediments and accumulates in the water column. The accumulation rate can be used to estimate the He flux from the sediments. Clarke et al. (1977) and Top and Clarke (1981) investigated the ^{4}He flux in several lakes in Labrador to localize zones of high ^{4}He fluxes that they assumed to be indicative of uranium and thorium deposits. However, Mamyrin and Tolstikhin (1984) demonstrated that the large ^{4}He flux observed in one of the lakes could also be explained by a ^{4}He flux from the deeper crust. O'Nions and Oxburgh (1988) have demonstrated that the radiogenic ^{4}He flux in lakes in Labrador is close to the steady state ^{4}He flux of 3×10^{10} atoms m^{-2} s^{-1} from the continental crust (O'Nions and Oxburgh 1983).

Assuming that the ^{4}He flux is constant in time and that the ^{4}He flux from the sediments does not vary within the typical depth range of lakes, the ^{4}He flux can be determined from the ^{4}He budget in a 2-box model:

$$F_{^4He,sed} \cdot A_1 \approx \frac{dM_{^4He_1}}{dt} - Q_{ex} \cdot \left(^4He_2 - ^4He_1\right) \tag{46}$$

where $F_{4He,sed}$ is the ^{4}He flux per sediment area and Q_{ex} can be determined from the balance of e.g., $^3He_{tri}$. In good approximation the total sediment area below a given depth z is equal to the cross-sectional area at depth z. Equation (46) states that the mass flux of ^{4}He introduced from the sediments below depth z corresponds to the change per unit time of the total mass of ^{4}He below z minus the ^{4}He lost by exchange with the upper layer. The boundary between upper and lower layer is somewhat arbitrary and the use of volume weighted mean ^{4}He concentrations in upper and lower layer to calculate ^{4}He exchange is an approximation. In seasonally mixed lakes with time varying ^{4}He profiles in which mixing across the thermocline is very small in the summer months, the accumulation over the summer season of ^{4}He in the deep water below the thermocline can be used directly to estimate $F_{4He,sed}$ (e.g., Laacher See Aeschbach-Hertig et al. 1996b).

In lakes where the ^{4}He profile is at steady state, $F_{4He,sed} = -Q_{ex}\cdot(^4He_2 - ^4He_1)/A_1$. If also the water age is at steady state, introducing the volume exchange estimated from water age differences (Eqn. 44) leads to

$$F_{4He,sed} = \frac{V_1}{A_1} \cdot \frac{^4He_2 - ^4He_1}{\tau_2 - \tau_1} \tag{47}$$

where τ_1 and τ_2 are the volume weighted mean water ages in box 1 and 2.

A simplified procedure to estimate $F_{4He,sed}$ directly compares the excess of ^{4}He above atmospheric equilibrium Δ^4He with the ^{3}H-^{3}He age (Mamyrin and Tolstikhin 1984). Assuming that the ^{3}H-^{3}He age measures the water residence time it can be interpreted as the time during which ^{4}He of terrestrial origin accumulates in a water parcel. Thus the ratio of Δ^4He to ^{3}H-^{3}He age gives the ingrowth of ^{4}He per unit volume and time. The total ^{4}He flux from the sediments can be obtained by multiplication with the lake volume V_o. Division by the surface area A_o gives the ^{4}He flux per unit area:

$$F_{4He,sed} \approx h_o \frac{\Delta^4He}{\tau} \tag{48}$$

where $h_o = V_o/A_o$ is the mean depth of the lake.

In Equation (48) the ratio Δ^4He/τ from an individual sample has been taken as representative for the entire lake. If several measurements are available the volume weighted mean values of Δ^4He and τ could be applied. This would correspond to the two box model (Eqn. 47) with box 2 representing surface water in equilibrium with the atmosphere. At the lake surface $^4He_2 = {}^4He_{equ}$ and $^3He_2 = {}^3He_{equ}$, implying $\tau_2 = 0$. Because $^4He_{equ}$ varies only very little with temperature $^4He_{equ}$ is approximately constant. Then $F_{4He,sed} = V_o/A_o \cdot \Delta^4He_1/\tau_1$ with Δ^4He_1 and τ being volume weighted mean values.

As an alternative, a representative value for Δ^4He/τ in Equation (48) can be obtained from all data simultaneously by using a regression of Δ^4He versus τ (e.g., Aeschbach-Hertig 1994; Hohmann et al. 1998). This technique implicitly assumes that the ratio Δ^4He/τ is the same for all samples. Figure 15 demonstrates that in many lakes a linear correlation between Δ^4He and τ is a reasonable approximation.

All methods outlined above are simplifications because mixing is assumed to have the same effect on ^3H-^3He age and ^4He, and, even more severely, the ^4He flux is treated as a volume source. In reality ^4He enters from the sediments and the accumulation of ^4He per unit volume should be largest near the lake bottom where the area to volume ratio $dA/dV = 1/A \cdot dA/dz$ is largest. In addition the ^3H-^3He age only approximates the true age. All these difficulties can be avoided if $F_{4He,sed}$ can be determined by inverse fitting of the ^4He concentrations using a 1-D vertical continuous model with known transport parameters. Assuming homogeneous conditions in the horizontal direction the equation describing the vertical transport of ^4He is:

$$\frac{\partial^4He}{\partial t} = \frac{1}{A}\frac{\partial}{\partial z}\left(A \cdot K_z \cdot \frac{\partial^4He}{\partial z}\right) + F_{4He,sed}\frac{1}{A}\frac{\partial A}{\partial z} \qquad (49)$$

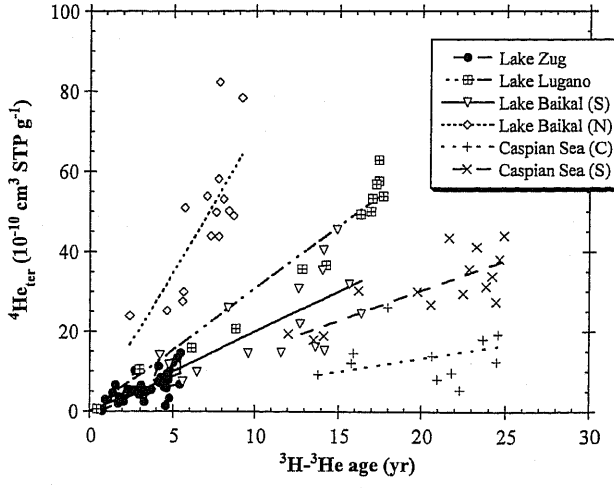

Figure 15. Δ^4He versus ^3H-^3He age in several lakes located on the Eurasian continent. A linear correlation (lines) between Δ^4He and ^3H-^3He age appears to be a reasonable approximation to the data from the different lakes. Data were compiled from several sources: Lake Zug and Lake Lugano (Aeschbach-Hertig 1994), central (C) and southern (S) basin of the Caspian Sea (Peeters et al. 2000a) and southern (S) and northern (N) basin of Lake Baikal (Hohmann et al. 1998).

The calculation of ^{4}He from Equation (49) requires as upper boundary condition a model describing the loss of ^{4}He by gas exchange at the lake surface. The best estimate of $F_{4He,sed}$ can be obtained by adjusting $F_{4He,sed}$ such that the squared deviation between simulated and measured ^{4}He normalised by the errors of the ^{4}He measurements becomes minimal (χ^2 minimisation). This technique has been applied to estimate $F_{4He,sed}$ in Lac Pavin (Aeschbach-Hertig et al. 1999a) and in Lake Lugano and Lake Zug (Aeschbach-Hertig 1994). Aeschbach-Hertig (1994) demonstrated for Lake Zug and Lake Lugano that $F_{4He,sed}$ obtained from inverse numerical modeling and from the Δ^4He versus ^{3}H-^{3}He age correlation technique agree reasonably well.

The flux of ^{4}He from the continental crust. The ^{4}He fluxes determined in several lakes in Swizerland and in the Caspian Sea using Equation (48) agree within a factor of 3, except for Urner basin of Lake Lucerne in which ^{4}He is possibly affected by ground-water sources (Table 4; Aeschbach-Hertig 1994). Ground-water inflow can introduce water with very high ^{4}He concentrations and thus increase the total ^{4}He flux into a lake. Vertical profiles of the ^{3}He and ^{4}He concentrations in the lakes considered suggest that the excess of ^{4}He is predominantly of crustal origin. Because inflow of ^{4}He-rich ground water leads to an increase in the total ^{4}He flux into a lake, the values given in Table 4 must be considered as an upper limit of the crustal ^{4}He flux.

The ^{4}He flux in the different basins of Lake Baikal is higher than the ^{4}He flux in the lakes mentioned above. The ^{3}He/^{4}He ratio measured in hot springs around Lake Baikal is about 2.2×10^{-7} indicating a small but significant contribution of mantle helium (Hohmann et al. 1996). In the northern basin of Lake Baikal Kipfer et al. (1996) observed substantial hydrothermal inflow accompanied by large ^{4}He concentrations. This explains that the ^{4}He flux in the northern basin is significantly larger than in the other basins of Lake Baikal (Hohmann et al. 1996). Hydrothermal inflows might also affect the ^{4}He flux in the central

Table 4. ^{4}He flux estimated in several lakes located on the Eurasian continent.

Lake	*Location*	*mean depth [m]*	*^{4}He accumulation rate [10^{-10} cm^3 STP g^{-1} yr^{-1}]*	*^{4}He flux [10^{10} atoms m^{-2} s^{-1}]*
Alpnach	Switzerland	22	5.7	1.1
Lucerne	Switzerland			
Vitznau basin		75	3.3	2.1
Gersau basin		146	1.8	2.2
Urner basin		144	12	14
Zug	Switzerland	84	2.3	1.6
Lugano	Switzerland	171	3.3	4.8
Baikal[1)]	Siberia			
Southern basin		844	1.9	14
Central basin		854	1.7	12
Northern basin		576	5.7	28
Caspian Sea[1)]	Middle Asia			
Southern basin		461	1.5	5.9
Central basin		259	0.8	1.9

[1)] Data and mean depth below 200 m.

Flux estimates were taken from Aeschbach-Hertig et al. (1996a: Lake Alpnach, Lake Lucerne, Lake Lugano, Lake Zug); Hohmann et al. (1998: Lake Baikal); Peeters et al. (2000a: Caspian Sea).

and southern basin, but direct evidence for hydrothermal activity in these basins does not exist. Additionally, the massive and up to 30 million year old sediments in Lake Baikal might release more ^4He than the host rock of the sediments (see hypothesis of Solomon et al. 1995). Hence, the ^4He flux obtained from the data of the southern and central basin of Lake Baikal can be expected to be higher than the common crustal flux and should therefore be considered as an upper limit of the ^4He flux from the continental crust.

The estimations of the crustal ^4He flux based on the experimental observations from the lakes located in Central Europe and Asia are of the same order of magnitude and range between 10^{10} and 10^{11} atoms m^{-2} s^{-1}. Based on these results one can speculate that the crustal ^4He flux over the Eurasian continent is approximately constant and agrees within a factor of 3 with the theoretical value of 3×10^{10} atoms m^{-2} s^{-1} (O'Nions and Oxburgh 1983). The range of the experimental values also agrees with the ^4He flux estimates derived from ground-water studies (Torgersen and Clarke 1985; Torgersen and Ivey 1985)

Oxygen depletion. By analogy to the estimation of the ^4He flux, oxygen consumption can also be estimated from a regression of concentration of dissolved oxygen versus ^3H-^3He age (Jenkins 1976). Dissolved oxygen is introduced into lakes by gas exchange at the lake surface and by biological production in the photic zone. In most lakes dissolved oxygen decreases below the photic zone with increasing depth and ^3H-^3He age, because O_2 is consumed by decomposition of organic material. In seasonally mixed lakes the rate of oxygen depletion can be estimated from the decrease with time of the concentration of dissolved oxygen during the period of stratification in summer and fall. If O_2 concentrations vary only very little with time, oxygen depletion can be estimated from the correlation between ^3H-^3He age and O_2 assuming that the decrease of oxygen per unit volume is constant in time. However, oxygen depletion comprises of two components: (1) a volume sink due to consumption in the open water and (2) an areal sink due to consumption at the sediment water interface. Especially in the deeper regions of lakes the latter may dominate the overall oxygen depletion. Nevertheless, the regression of O_2 concentration versus ^3H-^3He age provides a reasonable estimate of overall oxygen depletion which agrees with the values on oxygen depletion derived from traditional methods (Aeschbach-Hertig 1994). Especially in lakes where concentrations of dissolved oxygen remain the same over years (e.g., Lake Baikal) the regression of O_2 versus ^3H-^3He age is a comparatively simple method to estimate oxygen depletion. In the deep water of Lake Baikal oxygen depletion estimated in this manner is about 140 mg O_2 m^{-3} yr^{-1} (Hohmann et al. 1998) which is somewhat larger than the mean oxygen depletion of 80 mg O_2 m^{-3} yr^{-1} estimated from inverse numerical modeling (Peeters et al. 2000b). The inverse modeling approach has the advantage that a volume and an areal sink for oxygen can be distinguished. However, numerical modeling requires a substantial amount of information on the exchange processes and still can describe the transport of dissolved oxygen only in a very simplified manner.

Noble gases from the Earth's mantle

Lakes located in volcanically and tectonically active zones are suitable systems to obtain information on the noble gas composition in the Earth's mantle and to study mantle volatile fluxes because a lake can act as a collector of mantle fluids and gases (Fig. 2). The $^3He/^4He$ ratio has been employed as an indication of a mantle component (e.g., Sano et al. 1990; Collier et al. 1991; Giggenbach et al. 1991; Igarashi et al. 1992; Kipfer et al. 1994; Aeschbach-Hertig et al. 1996b, 1999a; Clark and Hudson 2001). In the lakes studied, the $^3He/^4He$ ratio varies between 7.4×10^{-6} and 10.3×10^{-6} (Table 5). The concentrations of ^3He and ^4He measured in several of the lakes mentioned above are shown in Figure 16. In the case of Laacher See the atomic ratios of additional gases in the

mantle component were also determined: $(^{20}Ne/^{3}He)_{man}$ = 1.8±0.3 and $(^{36}Ar/^{3}He)_{man} \leq$ 3.5±0.6 (Aeschbach-Hertig et al. 1996b). These ratios lie between the ratios calculated from Staudacher et al. (1989) for the upper and lower mantle.

Table 5. Helium fluxes, C/^{3}He and heat/^{3}He ratios in lakes located in volcanic or tectonically active regions (extended from Aeschbach-Hertig et al. 1996b).

Lake (country)	*Area [km^2]*	*^{4}He flux ×10^{-12} [atoms m^{-2} s^{-1}]*	*^{3}He/^{4}He [10^{-6}]*	*C/^{3}He [10^{9}]*	*heat/^{3}He [10^{-9} J atom^{-1}]*	*Reference*
Lake Nyos (Cameroon)	1.49	300±40	7.84±0.04	30±15	0.29±0.04	Sano et al. (1990)
Crater Lake (USA)	53	0.55	9.9	40	100	Collier et al. (1991)
Lake Mashu (Japan)	20	0.92	9.43±0.17	180	170	Igarashi et al. (1992)
Lake Nemrut (Turkey)	11	≤6	10.32±0.06	37±22 [a]	12±1	Kipfer et al. (1994)
Lake Van (Turkey)	3600	0.2-0.3	10.3 [b]	-	-	Kipfer et al. (1994)
Laacher See (Germany)	3.31	10±2	7.42±0.03	8.6±1.0	1.0±0.2	Aeschbach-Hertig et al. (1996b)
Lac Pavin (France)	0.44	0.6±0.2	9.1±0.01	13	6	Aeschbach-Hertig et al. (1999a, 2002a)

[a] Average of three gas samples from the Nemrut Caldera that were not discussed by Kipfer et al. (1994).

[b] Value taken from the nearby Lake Nemrut.

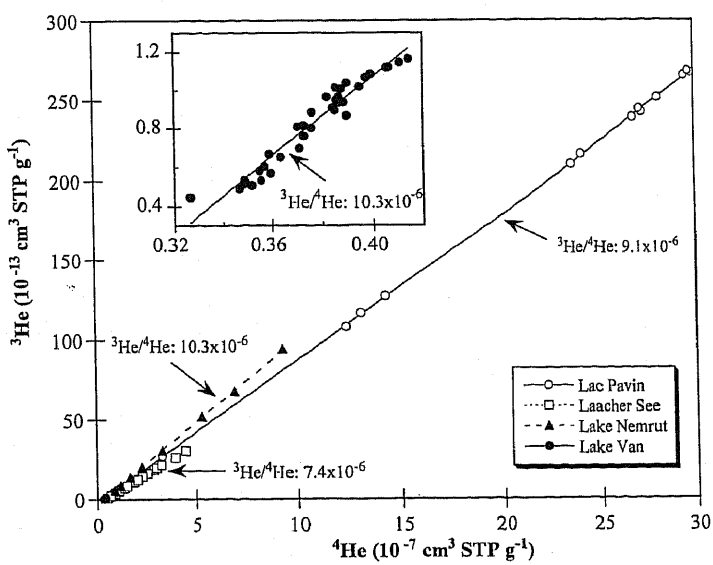

Figure 16. ^{3}He versus ^{4}He concentrations in several lakes affected by gas fluxes from the Earth's mantle. In all lakes shown, the ^{3}He/^{4}He ratios are more than two orders of magnitude higher than the ^{3}He/^{4}He ratio in the helium flux from the continental crust. Data from Kipfer et al. (1994: Lake Nemrut and Lake Van, Turkey), from Aeschbach-Hertig et al. (1996b: Laacher See, Germany; 1999a: Lac Pavin, France).

The estimation of the fluxes of the mantle component is complicated by the fact that in most cases ^3H-^3He dating cannot be employed in the presence of a significant mantle component because the separation of $^3He_{tri}$ and $^3He_{ter}$ becomes unreliable. In seasonally mixed lakes the accumulation of mantle derived gases in the deep water below the thermocline over the stratified period can be used to estimate fluxes. This technique gives a lower estimate of the mantle fluxes because it neglects the loss of gases due to transport through the thermocline. In addition, sources of mantle gases in near surface regions cannot be included. In lakes where gas concentrations are in steady state, the gas flux can be estimated from the gas exchange at the lake surface.

The local ^4He flux in volcanic lakes can be significantly higher than the ^4He flux from the continental crust. The ^3He flux in most volcanic lakes, e.g., 7.4×10^7 ^3He atoms m^{-2} s^{-1} (Laacher See, Aeschbach-Hertig et al. 1996b), is significantly larger than the mean oceanic flux of 4×10^4 ^3He atoms m^{-2} s^{-1} (Craig et al. 1975). Because of the comparatively small surface area of the lakes from tectonically active regions their overall contribution to the global ^3He flux is small (e.g., Laacher See 0.01%, Aeschbach-Hertig et al. 1996b, Lake Van 0.05%, Kipfer et al. 1994).

The flux ratio of heat to ^3He in volcanic lakes could be indicative of the type of volcanism involved. In Lac Pavin (France, Aeschbach-Hertig et al. 1999a), Laacher See (Germany, Aeschbach-Hertig et al. 1996b) and Lake Nyos (Cameroon, Sano et al. 1990) the heat/^3He flux ratio of 6×10^{-9} J atom^{-1}, 1×10^{-9} J atom^{-1} and 0.3×10^{-9} J atom^{-1}, respectively, is small compared to the heat/^3He flux ratio of 170×10^{-9} J atom^{-1} and 100×10^{-9} J atom^{-1} in Lake Mashu (Japan, Igarashi et al. 1992) and Crater Lake (USA, Collier et al. 1991), respectively. The former three lakes are maar lakes while the latter lakes are related to subduction volcanism at tectonic plate boundaries. For the three maar lakes, the C/^3He ratio appears to decrease with increasing formation age of the maar, whereas the heat/^3He flux ratio does not vary systematically with the formation age (Aeschbach-Hertig et al. 1999a)

Identification of gases of mantle origin in lakes can contribute to the understanding of the distribution of other gases and in particular of CO_2. The accumulation of CO_2 in Lake Nyos led to lethal gas bursts. Based on ^3He, ^4He, and Ne measurements it could be demonstrated that the high CO_2 concentrations were of mantle origin and that the CO_2 flux from the mantle leads to critical conditions in Lake Nyos within about 20 to 30 years (Sano and Wakita 1987; Sano et al. 1990).

APPLICATIONS IN GROUND WATER

The major application of the non-atmospheric noble gas components in ground water is dating, i.e., the determination of the residence time of the water in the subsurface. Dating applications fall into two major categories: (1) Young ground water with residence times of months to about 50 years can be studied with the ^3H-^3He technique as well as with the anthropogenic radioisotope ^{85}Kr. The natural radioisotope ^{222}Rn can be used to extend the age range to the study of very young ground water (up to 20 days). (2) Old ground water with residence times of thousands to millions of years is studied by using the accumulation of stable radiogenic ^4He and ^{40}Ar, or by the long-lived radioisotope ^{81}Kr. Another radioisotope, ^{39}Ar, covers the time range between about 100 and 1000 years that otherwise is very difficult to access.

An understanding and quantification of fluxes of terrigenic noble gases into aquifers is a prerequisite to their use for dating purposes. Conversely, the study of non-atmospheric He and Ar isotopes in ground water contributes to our understanding of the degassing of the Earth's mantle and crust. At this point, the field of noble gases in ground water is strongly linked to the noble gas geochemistry of other crustal fluids and the solid

Earth (see Ballentine et al. 2002 and Ballentine and Burnard 2002 in this volume).

The major application of the atmospheric noble gas components in ground water is paleotemperature reconstruction, i.e., determination of the temperature at which the infiltrating ground water equilibrated with the atmosphere in the past. This method offers a unique possibility to derive paleotemperatures based on simple physical principles. However, the atmospheric noble gases not only yield information about recharge temperatures, but also on the excess air component, and thus on the processes of gas-water exchange during ground-water infiltration. Some recent studies suggest that excess air may yield valuable paleoclimate information, but this is still a young field that leaves many open questions to be investigated.

Dating of young ground waters

In this section, applications of several tracer methods used for dating of ground waters with ages up to about 50 yr are presented. It is discussed how the resulting data are being used to derive hydraulic quantities such as recharge rates or flow velocity, to quantify mixing of different water components, and even to calibrate numerical ground-water models. More comprehensive reviews of these methods may be found in Cook and Solomon (1997) and Cook and Herczeg (2000).

^{3}H-^{3}He. Starting in the early 1950s, tritium (^{3}H) from anthropogenic sources (mainly atmospheric nuclear weapon tests) was added to the atmosphere in significant amounts (Fig. 6). After oxidation to $^1H^3HO$, tritium participates in the global hydrological cycle. ^{3}H concentrations in precipitation have been monitored by an international network of stations beginning in the 1950s, and the delivery of ^{3}H to surface waters, ground water, and the oceans is reasonably well known (Doney et al. 1992). ^{3}H has been used extensively as a dye for better understanding the dynamics of ground-water flow systems (e.g., Kaufman and Libby 1954; Begemann and Libby 1957; Brown 1961; Münnich et al. 1967; see Schlosser 1992 for additional references on early tritium applications). However, as a consequence of ^{3}H decay and mixing, it has become increasingly difficult to quantify ground-water flow dynamics by relating measured ^{3}H concentrations to the ^{3}H input functions. The simultaneous measurement of ^{3}H and its decay product ^{3}He allows us to compensate radioactive decay and to determine ground-water ^{3}H concentrations as if ^{3}H were a stable isotope. In addition, we can determine an apparent age based on the concentration ratio of radioactive mother (^{3}H) and daughter ($^3He_{tri}$), the ^{3}H-^{3}He age τ (Eqn. 33).

This method, originally proposed by Tolstikhin and Kamenskiy (1969), has found many applications in hydrogeology during the past twenty years (e.g., Torgersen et al. 1979; Takaoka and Mizutani 1987; Weise and Moser 1987; Poreda et al. 1988; Schlosser et al. 1988, 1989; Solomon and Sudicky 1991; Solomon et al. 1992, 1993; Ekwurzel et al. 1994; Szabo et al. 1996; Beyerle et al. 1999a). While ground water percolates through the unsaturated zone, all produced ^{3}He escapes fairly rapidly into the atmosphere. However, just below the water table the loss of ^{3}He is limited considerably (Schlosser et al. 1989), and ^{3}He begins to accumulate and the ^{3}H-^{3}He age to increase. Tritiogenic ^{3}He can be fairly easily separated if the other He components are dominated by atmospheric sources with only small additions of radiogenic or mantle He (see Eqns. 29-31). Dispersion (including molecular diffusion) affects ^{3}H-^{3}He ages in a systematic way by mixing ^{3}H and ^{3}He from the bomb test peak into younger and older water and thus shifting ^{3}H-^{3}He ages somewhat towards the early 1960s (Fig. 17).

^{3}H-^{3}He ages have been used to determine ground-water flow velocities in different situations. Vertical ^{3}H-^{3}He profiles allowed determination of ground-water recharge rates (e.g., Schlosser et al. 1988; Solomon and Sudicky 1991; Solomon et al. 1993). Horizontal

transects of ^3H-^3He ages with increasing distance from rivers served to quantify river infiltration (Stute et al. 1997; Beyerle et al. 1999a). ^3H-^3He data have also been used for

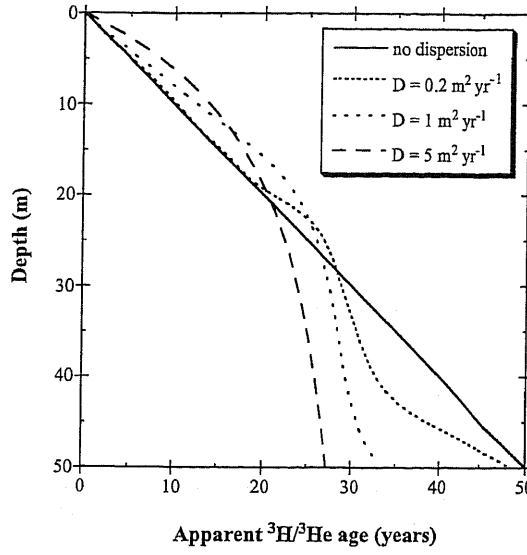

Figure 17. Effect of dispersion on the ^3H-^3He age in a system dominated by vertical water movement. A ^3H input function typical for the north-eastern United States was used and a vertical flow velocity of 1 m yr^{-1} assumed. The calculation was conducted for the year 1992. Similar one-dimensional models were published by Schlosser et al. (1989), Solomon and Sudicky (1991), Ekwurzel et al. (1994), and others.

the estimation of hydraulic conductivity, effective porosity, and dispersivity on a range of scales (Solomon et al. 1995). Another important application of the method is to provide chronologies for records of past environmental change, in particular histories of groundwater contamination (Böhlke et al. 1997; Aeschbach-Hertig et al. 1998; Johnston et al. 1998; Schlosser et al. 1998; Dunkle Shapiro et al. 1999). ^3H-^3He data can also provide constraints on mixing of different water components, e.g., in aquifers affected by river infiltration (Plummer et al. 1998b; Plummer et al. 2000; Holocher et al. 2001).

^3H-^3He dating has also been applied in fractured rock aquifers (Cook et al. 1996; Aeschbach-Hertig et al. 1998). Typical problems encountered in fractured systems are their extreme heterogeneity, double porosity causing differences between hydrodynamic and ^3H-^3He age, and geochemical complications due to the presence of other He sources.

From the beginning, other environmental tracers such as chlorofluorocarbons (CFC-11, CFC-12), ^{85}Kr, and more recently SF_6 have been used in parallel with ^3H and ^3He. Because of the different shape of their input functions, sources and sinks, the combination of these tracers provides better constraints on the ground-water flow regime than the use of a single method alone. In the following, two ^3H-^3He case studies are discussed in some more detail.

^3H-^3He, CFCs, and ^{85}Kr were studied in a sandy, unconfined aquifer on the Delmarva Peninsula in the eastern USA by Ekwurzel et al. (1994). ^3H and ^3H+^3He depth-profiles show peak-shaped curves that correspond to the time series of ^3H concentration precipitation, smoothed by dispersion (Fig. 18a). The peak occuring at a depth of about 8m below the water table therefore most likely reflects the ^3H peak in precipitation that occurred in 1963 (Fig. 6). The ^3H-^3He ages show a linear increase with depth, reaching a maximum of about 32 years. The ^3H-^3He ages are also supported by CFC-11, CFC-12, and ^{85}Kr tracer data (Fig. 18b). The latter tracers are used here as 'dyes' and their concentrations are converted into residence times by using the known history of the atmospheric concentrations and their solubility in water. From the vertical ^3H-^3He age profile at well nest 4 at the Delmarva site, the vertical flow velocity can be

estimated as 0.5 m yr^{-1}. Assuming a porosity of 0.3, this is equivalent to a recharge rate of 0.15 m yr^{-1}.

An example for the use of ^3H-^3He data to determine the origin and spreading rate of pollutants is the extensive study of a sewage plume spreading in an unconfined aquifer in Cape Cod, Massachusetts (USA) by Dunkle Shapiro et al. (1999). ^3H-^3He ages at the center of the plume were found to increase linearly as a function of distance from the source (Fig. 19). Similar to the Delmarva study, the ^3H+^3He depth profiles resemble the ^3H precipitation input curves. The resulting distribution of ^3H-^3He ages was found to be consistent with the beginning of the use of detergents and their expected history in sewage. The ages also compared well with those from particle-tracking simulations.

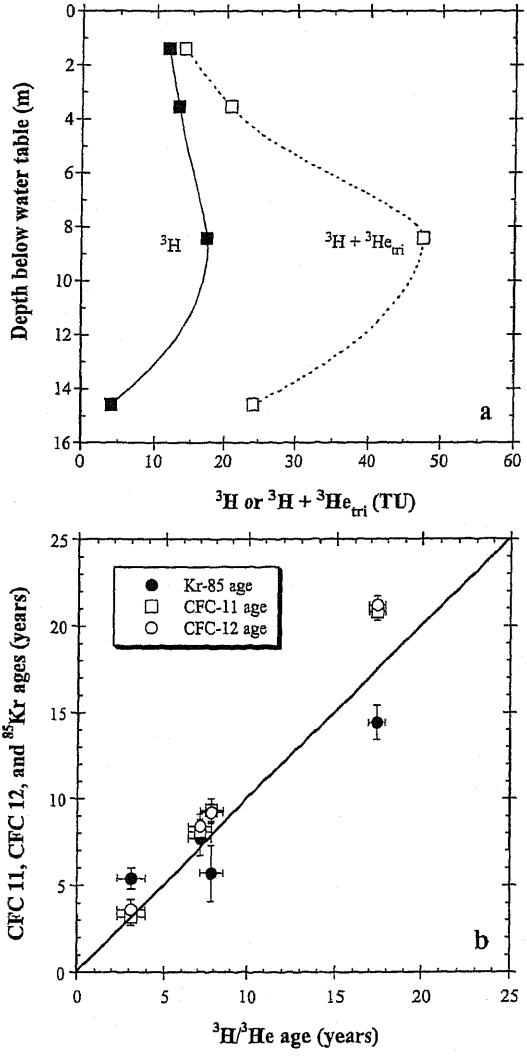

Figure 18. Results from a multi-tracer study, Delmarva Peninsula, USA. (a) ^3H and $^3H + ^3He_{tri}$ versus depth for well nest 4. (b) Comparison of ^3H-^3He, CFC-11, CFC-12, and ^{85}Kr ages (after Ekwurzel et al. 1994).

^{85}Kr. Although ^{85}Kr is radioactive, the age information is not derived from the radioactive decay itself, but from the increase of the atmospheric concentrations since the 1950s. In this regard, the method has strong similarities with the transient tracer methods based on ^3H, CFCs, and SF_6. In comparison with these related techniques, the ^{85}Kr-method has several advantages: (1) The input function is still steadily increasing today; (2) locally enhanced atmospheric concentrations occur only near the sources (nuclear fuel reprocessing plants e.g., in Europe, Weiss et al. 1992); (3) local contamination is unlikely and subsurface production is usually small; (4) conservative behavior can be taken for granted, as usual for noble gases; and (5) the ^{85}Kr method is unaffected by excess air and recharge temperature, because only the ^{85}Kr/Kr ratio and not the absolute concentration is relevant.

The reason why ^{85}Kr has not been applied as widely as ^3H, ^3H-^3He, or CFCs lies in the technical difficulties of detecting its minute concentrations in natural waters. Sampling large volumes of water is time-consuming and not always feasible. Laser-based resonance ionization mass spectrometry for ^{85}Kr analysis is currently being developed (Thonnard et al. 1997),

which should reduce the sample size to a few liters. If such techniques can be established, ^{85}Kr could become a major tool for dating shallow ground waters.

Up to the present, ^{85}Kr studies of shallow ground waters are rare and limited to small numbers of samples. An early assessment of the feasibility of the method with a few examples was presented by Rozanski and Florkowski (1979). In a study of ground-water flow based exclusively on ^{85}Kr conducted in the Borden aquifer in Canada a monotonic increase of the ^{85}Kr age along the ground-water flow path was found and compared with the results of a two-dimensional advection dispersion model of ^{85}Kr transport (Smethie et al. 1992). It was found that the modeled ^{85}Kr distribution was insensitive to dispersion and that therefore ^{85}Kr could be used in a straightforward manner to estimate the ground-water residence time.

More commonly, ^{85}Kr has been combined with other dating tracers, in particular with tritium. This tracer combination is particulary useful because the two isotopes have similar half-lives but experienced completely different input histories (Fig. 6). The basic idea in the interpretation of ^{3}H-^{85}Kr data, which can be generalised to all multi-tracer approaches, is to calculate the expected concentrations of ^{3}H and ^{85}Kr for different mean ground-water residence times and/or different models of mixing in the aquifer, and to compare the measured concentrations with the model predictions (Loosli 1992; Loosli et al. 2000). This approach has been used successfully to derive mean residence times and to quantify admixing of old, tracer-free ground water, which is identified by concentrations of ^{3}H and ^{85}Kr below those predicted by the models (Purtschert 1997; Mattle 1999).

Comparable in many respects to the ^{3}H-^{3}He method, the tracer pair ^{3}H-^{85}Kr removes many of the difficulties inherent to the use of ^{3}H alone. However, in contrast to the ^{3}H-^{3}He method, a knowledge of the ^{3}H-input function is always needed, because ^{85}Kr is not linked to the ^{3}H-decay. Another difference between ^{3}He and ^{85}Kr lies in their transport behavior through the unsaturated zone. Weise et al. (1992a) showed that while the fast diffusing ^{3}He was at the atmospheric level in the soil air down to 25 m depth, the ^{85}Kr activity in the soil gas decreased significantly at depths larger than about 10 m. A time lag between the atmospheric input function and the concentrations in the soil air at the water table in deep unsaturated zones affects not only ^{85}Kr but also the dating methods based on CFCs (Cook and Solomon 1995) and SF_6 (Zoellmann et al. 2001).

^{222}Rn. Due to its short half-life (3.8 d), the use of ^{222}Rn for dating is restricted to the study of the first few weeks after ground-water infiltration. This age range is hardly accessible by other methods but nicely complements the range of the ^{3}H-^{3}He method. In addition, ^{222}Rn can also be used in older ground water and in surface water as a tracer to study hydrological and geochemical processes. For a more comprehensive review of the ^{222}Rn-method in subsurface hydrology, we refer to Cecil and Green (2000).

As a dating tracer, ^{222}Rn has in particular been applied to study the infiltration of river water into alluvial aquifers. Such aquifers are often exploited because of their high yield, but the quality of the ground water can be threatened by the possibility of break through of contaminated river water. In this context, the water components with very short residence times are of central interest. Hoehn and von Gunten (1989) were able to monitor the increase of the ^{222}Rn concentration in freshly infiltrated water as it moved away from the rivers in two alluvial sites in Switzerland. The concentration increase could be converted to residence times of up to about 15 days and the ground-water flow velocity could be derived.

A difficulty of the ^{222}Rn dating method is to distinguish between changes of the ^{222}Rn concentration that are due to actual aging of a water parcel and variations that

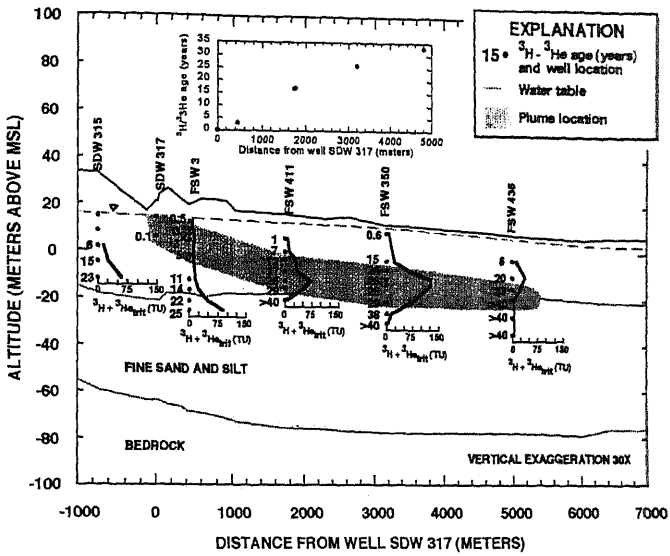

Figure 19. Distribution of ^{3}H-^{3}He ages across a sewage plume (shaded) for an unconfined aquifer in Cape Cod, Massachusetts. Depth profiles in piezometer clusters along the plume are shown. The inset shows the increase of ^{3}H-^{3}He ages along a single flowline through the core of the plume where sewage (boron, detergents) concentrations have maximum values (adapted from Dunkle Shapiro et al. 1999).

merely reflect different mixing ratios between Rn-rich ground water and virtually Rn-free surface water. To solve this problem, Bertin and Bourg (1994) used chloride as an additional tracer to quantify the mixing ratios. On the other hand, the large contrast in ^{222}Rn concentrations between ground and surface water renders this isotope useful for the study of interaction between ground water and surface water. For example, Cable et al. (1996) used ^{222}Rn in conjunction with CH_4 to quantify ground-water discharge to the coastal ocean. Ellins et al. (1990) applied ^{222}Rn to study the discharge of ground water into a river. In these cases, the ^{222}Rn concentrations were interpreted in terms of mixing between surface and ground water, rather than in terms of age.

In ground waters with residence times above about 20 days, the concentration of ^{222}Rn is at equilibrium with the production rate in the aquifer matrix. Instead of age information, ^{222}Rn then conveys information about the characteristics of the aquifer matrix, such as U content, porosity, grain size distribution, and release efficiency for ^{222}Rn (Andrews and Lee 1979). Because both radiogenic ^{4}He and ^{222}Rn originate from the U decay series, the study of ^{222}Rn may support the application of ^{4}He as a dating tool (Torgersen 1980). ^{222}Rn data from ground water in the Stripa granite in conjunction with data and production rate calculations of other noble gas radioisotopes (^{37}Ar, ^{39}Ar, ^{85}Kr) were used to draw conclusions about the distribution of U and the release and transport mechanisms for these isotopes (Loosli et al. 1989). In this case all investigated isotopes were found to be in equilibrium with their local subsurface production.

A relatively new and promising application of ^{222}Rn is its use as partitioning tracer in studies of aquifers contaminated by non-aqueous-phase liquids (NAPLs). Hunkeler et al. (1997) demonstrated in laboratory and field studies that Rn partitions strongly into the NAPL phase, resulting in a corresponding decrease in the water phase. By observation of

the decrease of the ^{222}Rn concentration upon passing of a zone of diesel fuel contamination in an aquifer, the authors were able to estimate the mean diesel fuel saturation in this zone.

CFCs and SF_6. Although not noble gases, CFCs and SF_6 behave often practically as conservative tracers and are frequently used in conjunction with noble gas based dating techniques in the study of young ground water. A comprehensive review of the literature on CFCs in ground water is beyond the scope of this work, but has recently been given by Plummer and Busenberg (2000).

Although proposed already in the 1970s (Thompson and Hayes 1979), large-scale applications of CFCs in ground-water hydrology began not before the early 1990s, when methods developed for oceanographic studies were adapted for the use in ground-water studies. Busenberg and Plummer (1992) and later Hofer and Imboden (1998) presented methods for collecting and preserving ground-water samples for CFC analysis and demonstrated first successful applications. The reliability of the CFC-method was demonstrated in two studies of shallow Coastal Plain aquifers of the Delmarva Peninsula (USA), by comparison with data on ^{3}H (Dunkle et al. 1993), as well as ^{3}He and ^{85}Kr (Ekwurzel et al. 1994). Another verification of the method in comparison with ^{3}H-^{3}He ages and flow modeling was provided by Szabo et al. (1996).

Applications of CFCs include the study of leakage from a sinkhole lake into the nearby ground water (Katz et al. 1995) and the recharge of a karstic limestone aquifer from a river (Plummer et al. 1998a; Plummer et al. 1998b). In the latter case, ^{3}H-^{3}He ages were used to reconstruct the initial CFC concentration in the river water fraction. Conversely, Modica et al. (1998) used CFCs to constrain the source and residence time of ground-water seepage into a gaining stream. Detailed vertical CFC profiles and tracking of the ^{3}H peak were used to assess vertical recharge velocities to within ±10% in a shallow, silty sand aquifer (Cook et al. 1995). Vertical profiles of CFCs as well as ^{3}H and ^{3}He were also used to infer shallow ground-water flow in fractured rock (Cook et al. 1996). Important applications of ground-water dating techniques are related to the source and history of ground-water contaminations. For example, Böhlke and Denver (1995) and Johnston et al. (1998) used CFCs in combination with ^{3}H or ^{3}H-^{3}He dating to reconstruct the recharge history of nitrate in agricultural watersheds.

Complications of the CFC-method are increased atmospheric concentrations near industrial source regions, degradation of at least CFC-11 under anoxic conditions, and contamination of ground and surface waters. The 'urban air' problem was assessed by Oster et al. (1996) for the case of western Europe, whereas Ho et al. (1998) provide data from a large urban area in eastern North America. Microbial degradation of CFC-11 under anaerobic conditions has been observed in several studies (e.g., Lovley and Woodward 1992; Cook et al. 1995; Oster et al. 1996). Local contamination is a serious and widespread, but still not fully understood problem (Thompson and Hayes 1979; Busenberg and Plummer 1992; Böhlke et al. 1997; Beyerle et al. 1999a). A fundamental problem for the CFC-method is the nearly constant atmospheric mixing ratios in recent years, making alternatives such as SF_6 attractive for dating of very young ground water.

SF_6 is just emerging as a new tracer in ground-water hydrology. A detailed assessment of the method including first applications and comparisons with ages derived from CFCs, ^{3}H-^{3}He, ^{85}Kr, as well as radiogenic ^{4}He accumulation, has been presented by Busenberg and Plummer (2000). Zoellmann et al. (2001) used SF_6 together with ^{3}H to calibrate a transport model that was used to predict nitrate levels in wells for different land-use scenarios. Bauer et al. (2001) found evidence for CFC-113 retardation in comparison to SF_6, ^{3}H, and ^{85}Kr. Plummer et al. (2001) found SF_6 and ^{3}H-^{3}He to be the most reliable dating methods in a multi-tracer study including also CFCs, ^{35}S, and stable

isotopes of water.

Multitracer studies and modeling. A straightforward interpretation of any tracer concentration in terms of ground-water age is only possible under the assumption that the sampled water parcel has not been affected by mixing along its way between the points of recharge and sampling. This assumption is often referred to as the plug flow or piston flow model. It is obviously a simplification of the real flow conditions in aquifers, where dispersion always creates some degree of mixing.

To improve the interpretation of tracer data, simple input-output models of the effect of mixing on tracer concentrations have been developed since the early years of tracer hydrology (Erikson 1958; Vogel 1967; Maloszewski and Zuber 1982; Zuber 1986a; b) and applied up to the present (Cook and Böhlke 2000; Plummer et al. 2001). These 'lumped-parameter' models view the ground-water system as a 'black box', which transfers the tracer input curve into a time-dependent output concentration that can be compared to the observations. The transfer functions that characterize the different types of models specify the fraction of the input of each year that is present in the mixed output water. The transfer function of the piston flow model is a delta function that picks the input concentration of a single year and yields the respective output without any mixing. Mixing is often described by the 'exponential' or the 'dispersion' model. The transfer function of the exponential model prescribes an exponential decrease of the fraction of each input year with increasing elapsed time, which is equivalent to modeling the ground-water reservoir as a mixed reactor. The dispersion model weighs the fraction of the different input years by a Gauss-type distribution.

The more recent development of sophisticated ground-water flow and transport modeling software and the availability of powerful computers allow a much more detailed modeling of the tracer evolution in ground-water systems. Consequently, applications of tracer data in conjunction with multi-dimensional flow and transport models began to show up in the 1990s (Reilly et al. 1994; Szabo et al. 1996; Sheets et al. 1998). Despite the undisputable power of this approach, it should be noted that in cases with few tracer data and little knowledge about the ground-water system, the simple lumped-parameter models still have their justification (Richter et al. 1993). In any case, it is clear that the full potential of the tracer methods can only be exploited by simultaneous application of several tracer methods and by interpretation of the data in the framework of a model.

The combination of several independent tracer methods has a great potential in identifying mixing or other disturbing effects in a ground-water system. Close agreement between the apparent (piston-flow) ages derived from different tracers , as found in some comparative studies (Ekwurzel et al. 1994; Szabo et al. 1996), indicate that mixing and dispersion are of minor importance. Many of the early tracer studies were aimed at verifying the methods and were therefore conducted in homogeneous, sandy aquifers with relatively simple and uniform flow fields. In more complex settings, larger deviations between the different tracer ages are to be expected and also have been observed (Cook et al. 1996; Plummer et al. 1998a).

Within the framework of the lumped-parameter models, it is relatively simple to derive information about the mixing regime from multi-tracer data. As discussed above for the ^{3}H-^{85}Kr tracer pair, the predicted concentrations for any tracer can be calculated for different lumped-parameter models with various parameter values, and the model that best fits the data can be found. This inverse modeling procedure can be illustrated by plotting the predicted output concentrations for any pair of tracers versus each other (Fig. 20). By plotting the measured concentrations in such a figure containing a series of curves that represent different models and parameter values, the curve that best fits the

data can easily be found (Loosli 1992; Plummer et al. 2001). A more rigorous approach to solve the problem involves least square fitting, analogous to the inverse techniques to derive model parameters from the data on atmospheric noble gases. A first example of this approach was presented by Purtschert et al. (1999). Such an approach can go beyond classical lumped-parameter models by including effects such as binary mixing, in particular with a component of old, tracer-free water. Under favorable conditions, the combination of different tracers can even be used to decompose mixed samples into the primary components (Beyerle et al. 1998).

Of course, inverse-modeling approaches can also be used to determine the parameters of numerical ground-water transport models from fits to observed tracer data. Estimates of residence times for a number of locations in an aquifer provide a powerful calibration target for numerical ground-water transport models. If enough data are available to constrain the numerous unknowns in such models, this is presumably the most effective way to extract useful information from tracer data, in particular because the numerical models can be used to make predictions for the future development of the investigated system. Such predictions may become much more constrained and trustworthy if the model has been calibrated against tracer data.

Typically, tracer data are used to calibrate certain model parameters, such as recharge rate, hydraulic conductivity, or (effective) porosity (Reilly et al. 1994). Solomon et al. (1992) compared the spatial distribution of ^{3}H-^{3}He ages with a previously calibrated ground-water transport model of the Borden aquifer (Canada). Although the ^{3}H-^{3}He age profiles were vertically offset from the modeled travel times, the gradients in travel time and ^{3}H-^{3}He age compared very well. In a study of a sandy aquifer in the southern New Jersey coastal plain, ^{3}H-^{3}He ages were compared to two-dimensional ground-water flow models that were calibrated without using information from large-scale tracer measurements (Szabo et al. 1996). Steady-state finite difference ground-water flow models were calibrated at three sites by adjusting horizontal and vertical hydraulic conductivities to match measured hydraulic heads. Travel times were then calculated using particle tracking codes and compared to the measured ^{3}H-^{3}He (and CFC) ages. The agreement between ^{3}H-^{3}He, CFC, and particle tracking ages indicated that the influence of dispersion was very small at this site and that, with few exceptions, the ground-water flow model did not require major adjustments. Comparison of a water bound tracer such as ^{3}H with gaseous tracers such as ^{85}Kr or SF_6 provides constraints on the thickness of the unsaturated zone and its field capacity (Bauer et al. 2001; Zoellmann et al. 2001). In a study of river infiltration by means of a three-dimensional transport model, Mattle et al. (2001) found the hydraulic conductance of the riverbed to be the decisive parameter that could be calibrated by using data on tritiogenic ^{3}He.

In recent studies, attempts have been made to merge hydrogeological models and ^{3}H-^{3}He data in more complex systems. Particle tracking ages derived from independently calibrated three-dimensional flow models for two sites in a hydrogeologically complex buried-valley aquifer in Ohio (Sheets et al. 1998) compared reasonably well with ^{3}H-^{3}He ages (Dunkle Shapiro et al. 1998). The agreement decreased with depth. Selected conceptual and parameter modifications (porosity, transmissivity) to the models resulted in improved agreement between ^{3}H-^{3}He ages and simulated travel times. The first attempts to calibrate fractured rock ground-water flow models using ^{3}H-^{3}He ages demonstrate some of the difficulties encountered in these even more complex environments (e.g., Cook et al. 1996).

It is important to note that in some cases environmental tracer data not only help to constrain model parameters, but also can indicate weaknesses of the conceptual model that underlies a numerical model. Reilly et al. (1994) and Sheets et al. (1998) showed that

by changing their conceptual assumptions about the distribution of recharge, the

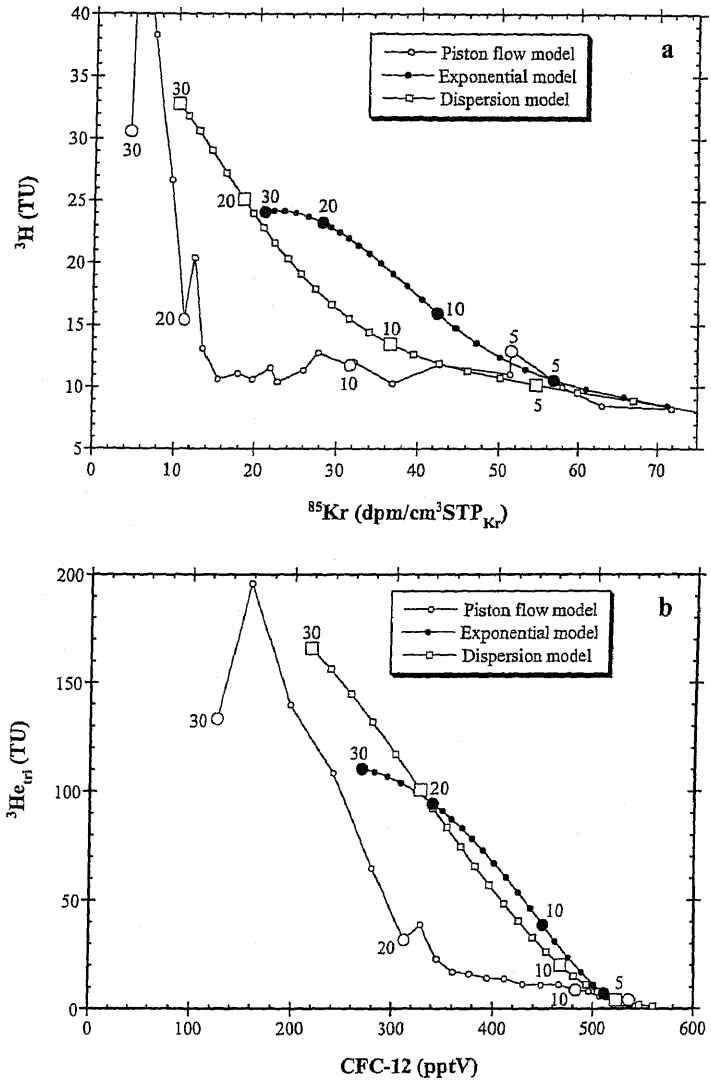

Figure 20. Expected concentrations of several tracers used for dating of young ground waters as functions of mean water residence time for different lumped-parameter models. (a) ^{3}H (in tritium units, TU) versus ^{85}Kr (in decay per minutes per cm^{3}STP of Kr); (b) ^{3}He$_{tri}$ (in TU) versus CFC-12 (in equivalent atmospheric volume fractions, pptV). All output concentrations were calculated for the year 2000 and mean residence times between 1 and 30 yr, using the lumped-parameter models (see Maloszewski and Zuber 1982) 'piston flow', 'exponential' and 'dispersion' (with a value of 0.2 for the dimensionless dispersion parameter) and input functions typical for central Europe. Selected values of the mean residence time (5, 10, 20, 30 yr) are highlighted by larger symbols and labels. By comparing measured concentrations with these diagrams, the appropriate model can be selected. Mixtures with old, tracer-free ground water lie on mixing lines toward the origin.

agreement between the modeled and measured tracer concentrations as well as the hydraulic heads and fluxes could be improved.

Dating of old ground waters

The most common method to date ground waters in the age range of 10^3 to 10^4 yr is ^{14}C-dating of the dissolved inorganic carbon in the water. However, due to the complexity of the geochemistry of carbon in aquifer systems, this method is difficult and not always reliable. The situation is probably even worse for ^{36}Cl, which has been explored as a dating tool in the range of 10^5 to 10^6 yr. Therefore, noble gases are very welcome as additional tracers that help to constrain long ground-water residence times.

Radiogenic ^4He. Due to its strong production in crustal rocks, radiogenic ^4He is ubiquitous in ground water and has been detected in numerous studies. It has generally been observed that ^4He concentrations increase with ground-water travel time (e.g., Andrews and Lee 1979; Heaton 1984; Torgersen and Clarke 1985; Stute et al. 1992b; Castro et al. 2000). If the rate of accumulation of radiogenic ^4He in an aquifer can be determined, the ^4He concentrations can be used to derive ground-water ages over a wide time range. Unfortunately, the transport of He through the crust and its accumulation in ground water are very complex and much debated issues. We only give a brief overview of this topic here, with emphasis on the practical use of radiogenic ^4He for ground-water dating. For a more detailed discussion the reader is referred to the reviews given by Ballentine and Burnard (2002) and Ballentine et al. (2002) in this volume.

Marine (1979) and Andrews and Lee (1979) showed how the accumulation rate due to *in situ* production of radiogenic ^4He in the aquifer matrix can be calculated (Eqn. 36). However, it was soon realized (e.g., Andrews and Lee 1979; Heaton 1984) that the ^4He accumulation ages derived in this way were significantly larger than ^{14}C ages, indicating the presence of additional sources of ^4He. Several different origins for the excess ^4He in ground water have since then been postulated.

The most prominent and controversial explanation for higher than *in situ* ^4He accumulation rates is the hypothesis of a steady state whole crustal degassing flux, i.e., the assumption that the ^4He production of the entire crust is balanced by a uniform flux to the surface (Torgersen and Clarke 1985). Torgersen and Ivey (1985) estimated the whole crustal flux to $2.7 \cdot 10^{10}$ atoms m^{-2} s^{-1}, similar to the value derived from a global heat and He budget (O'Nions and Oxburgh 1983). Comparable fluxes of ^4He have been reported for several aquifers (e.g., Heaton 1984; Martel et al. 1989; Castro et al. 1998a; Beyerle et al. 1999a) as well as for lakes (see above). However, other studies found significantly lower ^4He fluxes (e.g., Andrews et al. 1985; Stute et al. 1992b; Castro et al. 2000).

Despite its elegance, the hypothesis of a whole crustal flux is far from being universally accepted. Mazor and Bosch (1992) strongly advocated that *in situ* ^4He accumulation ages should be trusted more than hydraulic ages, and that the large ^4He ages correctly reflect the trapped and immobilised situation of many deep ground waters. Even more important are conceptual objections against the idea of a whole crustal flux. Andrews (1985) showed that only the uppermost part of the crust should be affected by a diffusive ^4He flux. Solomon (2000) as well as Ballentine and Burnard (2002) argue that the high diffusivity of ^4He required to support the typical whole crustal flux is unlikely to be valid for the bulk crust.

Between the extreme views of *in situ* production and whole crustal flux, there are alternative explanations for the observed ^4He concentrations in ground water. Andrews and Lee (1979) and Tolstikhin et al. (1996) suggested that diffusion from the adjacent confining layers constituted the major source of ^4He. This hypothesis is supported by the widespread correlation between ^4He and Cl^- in ground waters, since both species could

originate from the pore water of the aquitards (Lehmann et al. 1996). Another possible He source is the release of ^{4}He stored in the minerals of the aquifer matrix over geologic time by weathering or diffusion. Heaton (1984) discussed the He release due to chemical weathering, but considered it unlikely to represent an important source in two aquifers in southern Africa. Solomon et al. (1996) explained the occurrence of significant concentrations of radiogenic ^{4}He in young, shallow ground water by diffusion of ^{4}He from sediment grains, which only relatively recently had been produced by erosive fragmentation of old, ^{4}He-rich rocks. This mechanism may be important in shallow aquifers consisting of relatively recent sediment (e.g., Beyerle et al. 1999a) or in lake sediments, but is hardly relevant for deep ground water hosted by old sediments.

From a practical point of view, with respect to the applicability of ^{4}He as a dating tool, it can be stated that *in situ* production is rarely the only source of ^{4}He in ground water, but that the origin and in particular the strength of the additional sources is uncertain. This uncertainty has practically prevented the application of ^{4}He accumulation as a quantitative dating tool. Quantitative dating using ^{4}He requires calibration with another dating tool, such as ^{14}C, as suggested by Andrews and Lee (1979). Such a calibration was used in a study in Niger to date ground water beyond the limit of the ^{14}C method (Beyerle et al. submitted). Beyerle et al. (1999b) used the age information from the four first examples of successful ^{81}Kr-dating (see below) to calibrate a ^{4}He age scale for part of the GAB. Even if calibration of the ^{4}He age is not possible, ^{4}He may still provide a useful qualitative chronology, e.g., for noble gas paleotemperature records (Clark et al. 1997).

In some aquifers, or at least in some parts of them (upstream and uppermost layers), it may be possible to rule out major contributions from He sources other than *in situ* production. Significant diffusive release of stored He from sand grains can occur at most for 50 million years after deposition of the sediments (Solomon et al. 1996). The crustal He flux may be shielded by underlying aquifers that flush the He out of the system before it can migrate across them (Torgersen and Ivey 1985; Castro et al. 2000). Such favorable conditions enabled Aeschbach-Hertig et al. (2002b) to calculate ^{4}He accumulation ages from the U- and Th-concentrations in the Aquia aquifer (USA). The resulting ages were consistent with the paleoclimate information provided by the atmospheric noble gases and made it possible to construct a paleotemperature record (Fig. 21) despite the lack of reliable ^{14}C ages due to the complex carbonate chemistry at this site.

Apart from its potential use as dating tool, the study of terrigenic He in aquifers contributes to our understanding of the degassing of the Earth's crust and mantle, as discussed by Ballentine and Burnard (2002) and Ballentine et al. (2002) in this volume. Although crustal (radiogenic) He dominates in most aquifers, mantle He has occasionally been observed in ground water. Strong and unambiguous mantle He signatures can be observed in springs in volcanic areas, such as the Eifel and Rhine Graben regions of Germany (Griesshaber et al. 1992; Aeschbach-Hertig et al. 1996b), the Massif Central in France (Matthews et al. 1987; O'Nions and Oxburgh 1988), or western Turkey (Gülec 1988). Away from point sources, the contribution of a mantle-derived component to the non-atmospheric He in ground water has to be inferred from ^{3}He/^{4}He ratios that are elevated compared to typical crustal values. A large-scale flux of mantle He may be found in zones of active extension, such as the Great Hungarian Plain, where Stute et al. (1992b) found a mantle-contribution of 6 to 9%. Such findings show that vertical transport of He through the crust can occur at least in active regions. Quite surprising in this context is the detection of a mantle He component in ground water of the Mirror Lake Basin (New Hampshire, USA), in an area that is neither tectonically nor volcanically active (Torgersen et al. 1994; Torgersen et al. 1995).

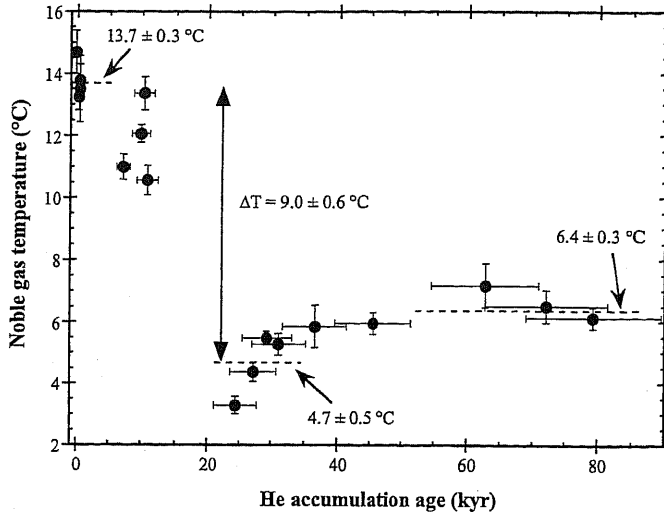

Figure 21. Noble gas temperature record from the Aquia aquifer, Maryland (USA), modified from Aeschbach-Hertig et al. (2002b). The chronology for this record could be established by ^{4}He accumulation ages based on the assumption of pure in-situ production. Only data from Aquia aquifer wells that could consistently be interpreted are shown. Mean noble gas temperatures for selected groups of samples, thought to best represent the Holocene, last glacial maximum (LGM), and preceding last glacial period are indicated, as well as the derived Holocene–LGM temperature difference.

^{40}Ar and ^{21}Ne. Although ^{40}Ar is produced from ^{40}K in similar amounts as $^{4}He_{rad}$ from U and Th in crustal rocks, the detection of radiogenic $^{40}Ar_{rad}$ is much less frequent than that of radiogenic He. The main reason is the much higher atmospheric abundance of Ar, but also the better retention of Ar in minerals may play a role. Ballentine et al. (1994) discussed the thermal constraints on the release of ^{4}He and ^{40}Ar, showing that preferential release of ^{4}He is expected in the upper part of the crust. In a large study of He and Ar isotopes in rocks and ground water, Tolstikhin et al. (1996) found that the ratio $(^{4}He/^{40}Ar)_{rad}$ in the ground water was higher than the production ratio in the aquifer matrix, whereas the opposite was true for the rock and mineral samples.

Torgersen et al. (1989) found a large variation in the $(^{4}He/^{40}Ar)_{rad}$ ratio in ground water from the GAB with a mean value close to their estimate of the whole crustal $^{4}He/^{40}Ar$ production ratio of 4.5. From these findings it was concluded that the overall degassing flux of both ^{40}Ar and ^{4}He was close to steady state with the whole crustal production. In contrast, Beyerle et al. (2000b) reported data from another part of the GAB that indicated a rather uniform $(^{4}He/^{40}Ar)_{rad}$ ratio of 50, an order of magnitude larger than the production ratio. Thus, the existence of a whole crustal degassing flux appears less likely for ^{40}Ar than for ^{4}He.

A method to date very old pore waters in impermeable rocks using radiogenic ^{4}He and ^{40}Ar has been developed by Osenbrück et al. (1998). In their case study in a cap rock above a salt dome, large $^{40}Ar_{rad}$ concentrations were found, but it appeared that they originated from the K-rich salts in the salt deposits and entered the cap rock by diffusion, rather than from *in situ* production. Therefore, ^{40}Ar dating was not possible in this case.

The only other radiogenic noble gas isotope that has some potential for ground-water dating is ^{21}Ne. Kennedy et al. (1990) noticed a very uniform radiogenic $^{21}Ne/^{4}He$ ratio of about 5×10^{-8} in crustal fluids. Bottomley et al. (1984) were able to detect radiogenic ^{21}Ne

in granitic rocks, whereas Weise et al. (1992b) for the first time reported a ^{21}Ne excess in a sedimentary aquifer. Although the applicability of ^{21}Ne has been demonstrated by these studies, this method is likely to remain a specialty that may help to improve the interpretation of ^{4}He data in some cases.

^{39}Ar. With its half-life of 269 yr, ^{39}Ar covers a very important age range between the ranges accessible by ^{3}H-^{3}He, ^{85}Kr, CFCs and SF_6 (younger than 50 yr) and by ^{14}C (older than about 1 kyr). It also has quite ideal properties, similar to those of ^{85}Kr, with the exception that subsurface production cannot *a priori* be neglected and may in some cases lead to deviations of the evolution of the ^{39}Ar concentration from the pure radioactive decay. In crystalline rocks, dating may even be impossible, but ^{39}Ar may then be used to study water-rock interactions (Loosli et al. 1989; Loosli et al. 1992). As for ^{85}Kr, the reason why ^{39}Ar has not been applied more widely lies in the difficulty of its analysis.

The applicability of ^{39}Ar for ground-water dating was demonstrated by Andrews et al. (1984) in a multi-isotope study of the East Midlands Triassic sandstone aquifer (UK), where subsurface production was found to be unimportant and ^{39}Ar activities were consistent with those of ^{14}C, ^{3}H, and ^{85}Kr. ^{39}Ar ages from 25 up to 240 yr could be calculated for wells in or near the recharge area, whereas for some wells further downstream only a lower limit of 1300 yr could be assigned. Some further examples of ^{39}Ar dating of ground water were discussed by Loosli (1992). ^{39}Ar data played an important role in a multi-tracer study of a confined aquifer in the Glatt Valley, Switzerland (Beyerle et al. 1998; Purtschert et al. 2001). In between young waters in the recharge area (^{3}H and ^{85}Kr active) and late Pleistocene waters downstream (^{39}Ar in production equilibrium, ^{14}C low), some samples were found for which ^{39}Ar indicated significantly younger ages than ^{14}C. By using the water chemistry (mainly Cl^- concentrations) as additional constraint, these samples could be decomposed into an old and a relatively young (^{39}Ar active, but ^{3}H and ^{85}Kr dead) component.

^{81}Kr. Among the noble gas radioisotopes with the potential for application in hydrology, ^{81}Kr is certainly the most exotic. Due to the enormous effort of ^{81}Kr analysis, there are so far only two examples of actual ^{81}Kr-measurements on ground-water samples. Lehmann et al. (1991) were able to determine the $^{81}Kr/Kr$ ratio in one sample from the Milk River aquifer (Canada) to be (82±18)% of the modern atmospheric ratio. The measurement was done by laser resonance spectroscopy following an elaborate multi-step isotope enrichment procedure. In view of the achieved accuracy, which yielded only an upper limit of 140 kyr for the age of the sample, this first measurement was hardly more than a demonstration of the feasibility of ^{81}Kr-dating.

The first real application of ^{81}Kr was conducted recently on four samples from the GAB by using accelerator mass spectrometry on a cyclotron (Collon et al. 2000). In this study, ages between 220 and 400 kyr could be determined with reasonable uncertainties of 40 to 50 kyr. These reliable ages offered a unique opportunity to interpret ^{36}Cl, ^{4}He, and noble gas data that were analyzed in the framework of the same study on timescales of 10^5 yr (Beyerle et al. 1999b; Lehmann et al. 1999). Except for the difficulty of measurement, ^{81}Kr appears to be an almost ideal dating tracer for ground water in this age range, which is appropriate for deep ground waters in large sedimentary basins.

Noble gas recharge temperatures

The possibility to derive paleotemperature records from dissolved noble gases in ground water, on the basis of the temperature dependency of their solubilities in water, is probably the application of noble gases in subsurface hydrology that received most attention in recent years. A large number of ground-water studies over the past 40 years used this approach to reconstruct paleoclimate conditions.

Method and historic development. Water percolating through the unsaturated zone equilibrates continuously with ground air until it reaches the capillary fringe and the quasi-saturated zone where entrapped air resides and excess air is formed. Model calculations and field observations have shown that after correcting for excess air formation, noble gas temperatures closely reflect the mean ground temperature at the water table, except in cases where the water table is very close (1 to 2 m) to the surface, or the recharge rates are very high (exceeding several hundred mm yr^{-1}; Stute and Schlosser 1993). Unless the water table is very deep (>30 m), the noble gas temperatures are usually found to be within 1°C of the ground (soil) temperature at the surface. Ground temperatures are typically slightly (1±1°C) warmer than mean annual air temperatures, although larger temperature differences may occur under extreme climate conditions (Smith et al. 1964; Beyerle et al. submitted). The conversion of noble gas temperatures into air temperatures should therefore be based on local relationships between ground and air temperature or calibrated locally by analysing young ground water that infiltrated under known climate conditions.

After leaving the water table, ground water moves towards the discharge area carrying information imprinted in the recharge area in the form of atmospheric noble gas concentrations. Mixing occurring in the aquifer or induced by sampling through wells with long screens tends to result in smoothing the variability of the recorded signals (Stute and Schlosser 1993). Due to this smoothing and also the difficulties of dating old ground waters, the noble gas method cannot be used to study short-term climate fluctuations, but it is well-suited to derive quantitative estimates of mean temperatures during major climate states, and in particular the difference between the last glacial maximum (LGM, about 21 kyr BP) and the Holocene.

The earliest applications of the noble gas thermometer include a study by Oana (1957), who found that N_2 and Ar concentrations in precipitation followed the seasonal temperature cycle whereas the concentrations in ground water were fairly constant and on average slightly higher than in precipitation. Sugisaki (1961) used the seasonal cycle of N_2 and Ar in ground water recharged by a stream to determine ground-water flow velocities. Mazor (1972) found that dissolved atmospheric noble gases in thermal ground waters of the Jordan Rift Valley in Israel reflected the modern air temperature in the recharge areas. He suggested that ground water could be used as an archive of paleoclimate, because it appears to retain the dissolved gases over many thousands of years.

The first glacial–interglacial paleotemperature record was established for the Bunter Sandstone in England (Andrews and Lee 1979). Ground water with a ^{14}C age between 20,000 and 35,000 years was characterized by noble gas temperatures 4 to 7°C lower than ground water of Holocene (0-10,000 years) origin. The gap in the record between 10,000-20,000 years was explained by the absence of recharge due to permafrost conditions in England during the last glacial maximum (Fig. 22). Heaton (1981) derived paleotemperatures from N_2 and Ar concentrations in ground water in southern Africa and found a systematic temperature difference between recent and glacial ground water. Similar patterns were found in confined aquifers in Germany and northern Africa, not only in the noble gas temperatures but also in stable isotope ($\delta^{18}O$, δD) records (Rudolph et al. 1984). Since these early studies many paleoclimate studies were conducted using the concentrations of atmospheric noble gases (and N_2-Ar) to reconstruct climate conditions for the last ~30,000 years (e.g., Heaton et al. 1986; Stute et al. 1992a, 1995a,b; Clark et al. 1997, 1998; Dennis et al. 1997; Beyerle et al. 1998; Clark et al. 1998; Weyhenmeyer et al. 2000).

Besides paleoclimate reconstructions, noble gas temperatures are also useful in

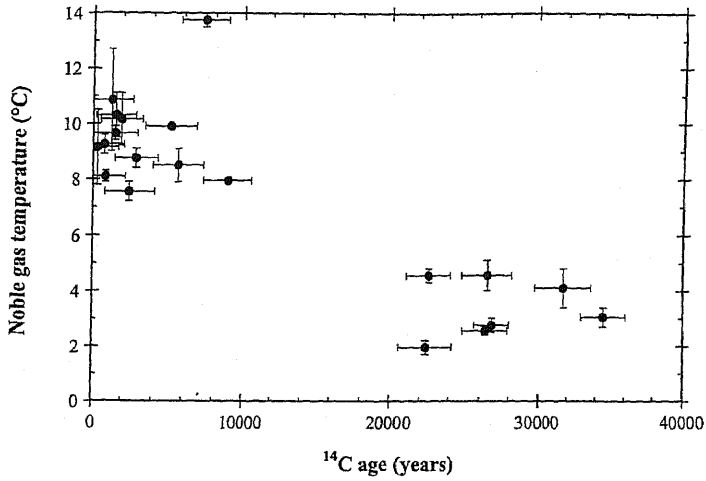

Figure 22. Noble gas temperature record from the Bunter Sandstone in the United Kingdom (modified from Andrews and Lee 1979).

helping to constrain ground-water flow regimes. For example, in cases where radiocarbon ages have large uncertainties due to complicated hydrochemical conditions, the glacial–interglacial temperature transition in the noble gas temperatures can be used as a stratigraphic marker to check the derived ages (e.g., Clark et al. 1997; Aeschbach-Hertig et al. 2002b). Commonly used dating techniques for shallow ground water (^3H-^3He, CFCs, SF_6) require knowledge of the recharge temperature and the amount of excess air, in order to separate the contributing mechanisms or to relate the concentrations of dissolved gases to atmospheric input functions. Dissolved noble gas concentrations can provide this information.

Paleoclimatic implications. The presently available noble gas paleotemperature records may be divided into two groups: those from northern temperate latitudes and those from tropical and sub-tropical areas. A major question in studies from higher latitudes is whether a complete record was obtained or whether the coldest periods, namely the LGM, may be missing because glaciation or permafrost prevented recharge during this period. Such a gap, first suggested by Andrews and Lee (1979) and later confirmed by Beyerle et al. (1998), may also be present in other European records (e.g., Rudolph et al. 1984; Andrews et al. 1985; Bertleff et al. 1993) from locations which may have cooled below the freezing point during the LGM. Therefore, estimates of 5 to 7°C glacial cooling obtained in such records may not represent the maximum cooling. Two noble gas records from northern latitudes appear to be complete and indicate a maximum LGM cooling of ~9°C (Fig. 21, Stute and Deák 1989; Aeschbach-Hertig et al. 2002b).

The first reliable tropical noble gas paleotemperature record found a LGM cooling of about 5°C (Stute et al. 1995b), a finding that received considerable attention in the ongoing debate about the magnitude of the glacial cooling in the tropics (e.g., Broecker 1996; Crowley 2000). The result of this particular study was challenged on grounds of insufficient modelling of the excess air fractionation by Ballentine and Hall (1999), but later confirmed by using the CE-model for excess air (Aeschbach-Hertig et al. 2000). Other noble gas studies from tropical sites also yielded similar coolings (Andrews et al. 1994; Edmunds et al. 1998; Weyhenmeyer et al. 2000), suggesting that the tropics and subtropics (Stute et al. 1992a; Clark et al. 1997; Stute and Talma 1998) cooled rather

uniformly by around 5°C during the LGM.

The noble gas thermometer has increasingly been accepted as a climate proxy in the framework of integrated reconstructions of climate conditions during the glacial period (e.g., Farrera et al. 1999; Pinot et al. 1999). Crowley and Baum (1997) and Crowley (2000) relied heavily on noble gas paleotemperature data in comparing model results with climate proxy data. These data are of particular interest in low geographical latitudes where undisrupted ground-water records can be obtained, and where the discrepancies between proxy data and models are particularly large.

Another important aspect of ground-water paleoclimate records is the possibility to relate the absolute temperature estimates obtained from the noble gases to the relative temperature indicator provided by the stable isotope composition of the water ($\delta^{18}O$ and $\delta^{2}H$). In most noble gas paleotemperature studies, stable isotopes ratios have also been determined, and in many cases clear relationships between the two climate proxys were found (e.g., Heaton et al. 1986; Stute and Deák 1989; Beyerle et al. 1998; Huneau et al. 2001). Such relationships offer the chance to derive local slopes for the long-term $\delta^{18}O$/T-relationship.

A case study. As an example of the application of the noble gas paleothermometer, we discuss a study conducted on the Stampriet artesian aquifer in Namibia. This confined sandstone aquifer is located in southeastern Namibia and has been extensively studied since the 1970s (e.g., Vogel et al. 1981; Heaton et al. 1983; Heaton 1984; Stute and Talma 1998). The noble gas temperature record was re-evaluated applying the CE-model and the inverse method developed by Aeschbach-Hertig et al. (1999b).

The average noble gas temperature of ground water less than 10,000 years is about 26°C (Fig. 23a), in close agreement with today's mean ground temperature in the region as determined from the temperature of shallow ground water (26.7°C). The average noble gas temperature of water samples 15,000 years and older, i.e., of glacial origin, is 21°C, indicating that the mean annual ground temperature in Namibia was about 5°C lower during the last glacial maximum as compared to today. This estimate of the temperature change is consistent with the the 5.5°C cooling obtained with the N_2/Ar technique at the Uitenhage aquifer (Heaton et al. 1986) and a maximum cooling of 6°C derived from a speleothem in Cango Caves in South Africa (Talma and Vogel, 1992). The glacial period is also characterized by an increased $\delta^{18}O$ (Fig. 23b), suggesting that the dominating moisture source shifted from the Atlantic to the Indian Ocean at the transition from the Pleistocene (>10,000 years) to the Holocene (<10,000 years). The noble gas record of the aquifer also shows a clear trend in the concentrations of excess air (Fig. 23c). The peak in ΔNe reaches values of up to 225% around 6,000 radiocarbon years ago, indicating a transition from a drier to a wetter climate, which probably caused the water table to rise and consequently to trap and dissolve air. Such a transition is also indicated by independent paleoclimatic evidence. The concentrations of non-atmospheric He show an increase as a function of radiocarbon age which is initially dominated by in situ production and later by the accumulation of a crustal He flux (Fig. 23d, Heaton 1984; Castro et al. 2000).

In summary, the studies of the Stampriet aquifer highlight all main features of noble gas paleoclimate studies: (1) The noble gas temperatures in conjunction with a ^{14}C timescale provide a quantitative record of the glacial/interglacial temperature change, (2) the local long-term relationship between $\delta^{18}O$ and noble gas temperature can be quantified, (3) the excess air record appears to provide additional climatic information related to precipitation, and iv) the accumulation of He provides a qualitative age scale and information on the crustal He flux.

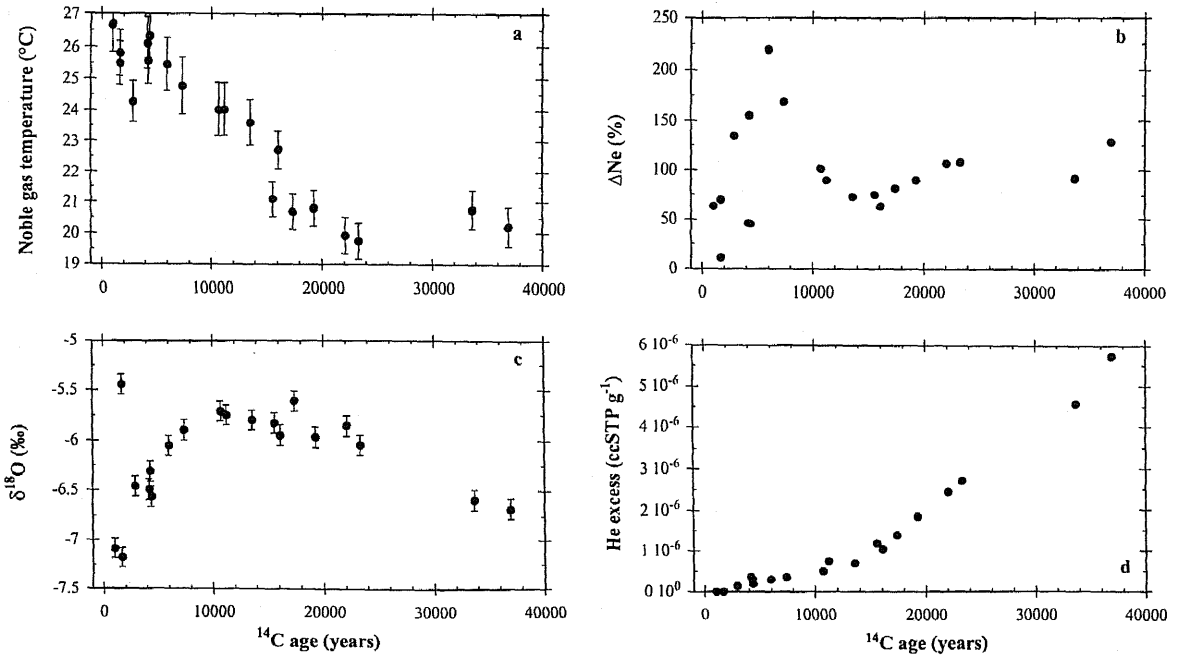

Figure 23. Noble gas temperatures, ΔNe, $\delta^{18}O$, and He excess as a function of radiocarbon ages derived from ground water in the Stampriet aquifer, Namibia (after Stute and Talma 1998). The noble gas data were re-evaluated using the CE-model for excess air (Aeschbach-Hertig et al. 2000).

Excess air

Herzberg and Mazor (1979) found significant amounts of excess air only in some karstic springs, suggesting that excess air was a characteristic feature of karstic systems. However, both Andrews and Lee (1979) and Heaton and Vogel (1981) found excess air also in sedimentary aquifers, which had different lithologies and were located in different climate zones. Since then, excess air has been found in virtually all noble gas studies of ground water, clearly showing that an excess of atmospheric gases is a real and ubiquitous feature of ground water. Heaton and Vogel (1981) were the first to focus explicitly on the excess air phenomenon and to suggest possible hydrological applications.

If excess air is viewed as a potentially useful tool rather than a disturbing effect in the calculation of noble gas temperatures, any corruption of the signal by potential air contamination during sampling has to be avoided. Manning et al. (2000) presented a sampling method based on passive diffusion samplers that supposedly yielded smaller concentrations of excess air than the traditional method using copper tube samplers. However, copper tube samplers have extensively been used without significant air contamination in oceans and lakes. In our experience, duplicate ground-water samples usually reproduce within experimental uncertainty (e.g., Aeschbach-Hertig et al. 2002b) and sample series taken at different times from the same wells usually reproduce within a few percent (e.g., unpublished data from Beyerle et al. 1998). Thus, the copper tube method yields reliable results if appropriate sampling procedures are applied.

Heaton and Vogel (1981) found varying amounts of excess air up to 10^{-2} cm^3 STP g^{-1} in several aquifers of South Africa, representing different lithologic, hydrologic, and climatic environments. They argued that excess air was formed by complete dissolution of air bubbles entrapped in the capillary fringe and carried down to sufficient depth to force dissolution due to the increased hydrostatic pressure. They discussed the possibility that the physical structure of the unsaturated zone might influence the formation of excess air, which therefore might be useful to distinguish between different recharge areas. Last but not least, they suggested that the semi-arid climate of southern Africa, characterized by intermittent recharge in response to sporadic but heavy rainfalls might favor the formation of excess air.

In confined aquifers in the Western Kalahari, Heaton et al. (1983) found even larger concentrations of excess air than in South Africa, in particular in the Nossob aquifer. Their most important finding, however, were systematic variations of excess air with ground-water age in the Stampriet Auob aquifer. They observed peaks of excess air at ages of around 10 and 30 kyr, coinciding with independently reconstructed periods of more humid climate and flooding. This finding strongly supported the suggestion that heavy but intermittent recharge might create high concentrations of excess air.

Despite these promising early indications of the potential of excess air as a tool for hydrologic and even paleoclimatic investigations, later noble gas paleoclimate studies mostly treated excess air as a disturbance for which the measured data had to be corrected. A reason for this lack of interest may be that systematic variations of excess air have not been observed in aquifers from temperate climate zones (Stute and Sonntag 1992; Stute and Schlosser 2000; Aeschbach-Hertig et al. 2001). Only in recent years, the interest in the excess air signal has been revived.

In an aquifer in a semi-arid region of tropical Brazil, Stute et al. (1995b) found large concentrations of clearly fractionated excess air. They noted that ΔNe was roughly two to three times higher in the glacial than in the Holocene waters but did not interpret this

finding any further. In contrast, in the case study of the Stampriet Auob aquifer, Stute and Talma (1998) confirmed the existence of an excess air peak in this aquifer (Fig. 23c) and interpreted it in terms of a climatic transition.

Wilson and McNeill (1997) compared the Ne excess from aquifers in different lithologies and climates. Their main conclusion was that lithology had a strong influence on the Ne excess, which was found to increase from granites over sandstones to limestones. Notably, they found no excess air in ground water from granites of southwest England. Relating the Ne excess to the recharge temperature, Wilson and McNeill (1997) found no relationship for limestone aquifers of the UK, a certain decrease of the Ne excess with temperature for a sandstone aquifer in the UK, and a strong decrease for a sandstone aquifer in Niger (data from Andrews et al. 1994). The strong difference of excess air between the warmer Holocence and the cooler Pleistocene waters, the latter having unusually high Ne excesses, in semi-arid tropical Niger is fully consistent with the findings of Heaton et al. (1983), Stute et al. (1995b), and Stute and Talma (1998). Wilson and McNeill (1997) noted that not temperature itself, but rather other climatic factors such as precipitation or frequency of flooding were likely to influence the excess air content of ground water. Indeed they found an increase of the Ne excess with mean annual precipitation when comparing different aquifers, but ascribed this effect to different lithologies and inferred a decrease of the Ne excess with precipitation when comparing data from the same lithologies.

In the light of the new approaches for a physical interpretation of the excess air component provided by the CE-model, Aeschbach-Hertig et al. (2001) made another attempt to find systematical patterns in the excess air data from several aquifers. In a comparison of three aquifers from temperate, humid climates and three aquifers from tropical, semi-arid regions (one of them being the Brazilian aquifer of Stute et al. 1995b), they found systematic differences between the two groups. In agreement with previous studies, the tropical aquifers exhibited higher mean values of ΔNe and a strong negative correlation between ΔNe and the noble gas temperature (Fig. 24).

The CE-model suggests that in general not the amount of entrapped air (A_e), but the pressure acting on this entrapped reservoir (q) determines the final excess (ΔNe). This argues against a major influence of lithology, unless very fine pores cause the surface tension to become a major source of excess pressure on the trapped bubbles, or very low porosity severely limits air entrapment. Otherwise, ΔNe is expected to depend mainly on the hydrostatic pressure. Persistent bubbles of entrapped air, which exist long enough to allow complete equilibration between water and gas phase are likely bound to certain sites in the porous medium, and cannot easily be transported up- or down-wards. Increasing the hydrostatic pressure in order to dissolve more gas therefore requires an increase of the water table. As a result, ΔNe is thought to be related mainly to the amplitude of water table fluctuations, and thus to depend on the variability of precipitation rather than on its mean value. In semi-arid climates with a distinct rainy season, and strong intermittent recharge events, this variability is likely higher than in humid climates with more continuous recharge. An additional factor that favors relatively high excess air in semi-arid regions are deep unsaturated zones, offering the potential for water table increases of many meters.

However, laboratory and field studies under defined conditions are needed to firmly establish the relationships between excess air parameters and environmental conditions during infiltration. Early laboratory experiments with sand columns designed to create and study excess air used somewhat artificial constructions to increase the hydrostatic pressure in the column and facilitate the dissolution of bubbles (Gröning 1989; Osenbrück 1991). More recent laboratory studies have demonstrated that excess air can

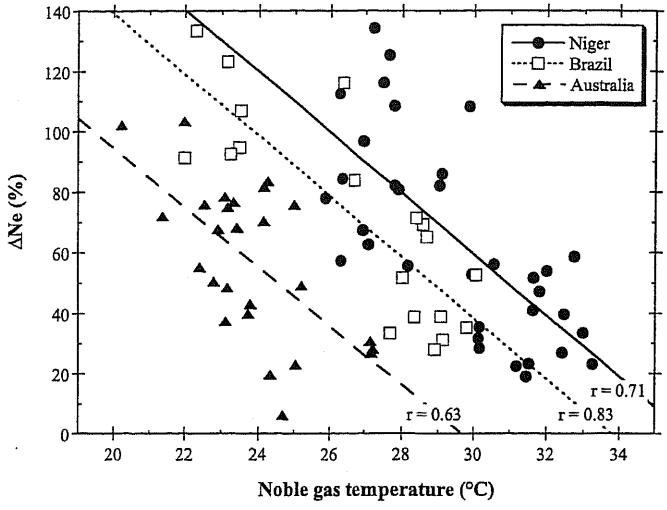

Figure 24. Excess air (expressed by the relative Ne excess ΔNe) in relation to noble gas temperature for three aquifers from tropical, semi-arid sites. Data are from (Beyerle et al. submitted) for Niger, (Stute et al. 1995b) for Brazil, and (Beyerle et al. 1999b) for Australia. Despite a large scatter, all three aquifers show strong and very similar decreasing trends of ΔNe with temperature (about -10 % per °C), which presumably reflect a change in infiltration condition (e.g. variability of recharge) between the Pleistocene and the Holocene.

be generated by simple water table fluctuations of less than 1 m amplitude, and that the size of the excess depends mainly on the hydrostatic pressure (Holocher et al. 2000, 2002). Complete dissolution of entrapped air was only achieved if the sand column was continuously flushed with air-saturated water at relatively high flow rates. Numerical modeling of the kinetics of gas exchange between entrapped gas and water enabled an understanding of the mechanisms that lead to different type of excess air fractionations depending on the experimental setup. Both the numerical model and the data showed that after a water table increase a new equilibrium between water and entrapped air was quickly achieved, although in the first phase complete dissolution of the smallest bubbles is possible.

In summary, there is little evidence for systematic variations of excess air in aquifers from temperate, humid climate zones (Wilson and McNeill 1997; Aeschbach-Hertig et al. 2001). In contrast, past periods of strongly increased excess air contents have been identified in five aquifer systems from warm, semi-arid climates: the Stampriet Auob aquifer in Namibia (Heaton et al. 1983; Stute and Talma 1998), the Serra Grande and Cabecas aquifer in Brazil (Stute et al. 1995b), the Continental Intercalaire aquifer in the Irhazer Plain in Niger (Andrews et al. 1994; Wilson and McNeill 1997); the Continental Terminal aquifers in the Iullemeden Basin in Niger (Aeschbach-Hertig et al. 2001; Beyerle et al. submitted), and the Great Artesian Basin in Australia (Beyerle et al. 1999b; Aeschbach-Hertig et al. 2001). In several of these studies, the periods of enhanced excess air could be correlated to known periods of more humid climate. These findings provide strong support for the hypothesis that excess air is a proxy for infiltration conditions, in particular the intensity and variability of recharge in semi-arid regions. The questions related to excess air are of central importance for the contemporary research on paleoclimate reconstruction based on noble gases in ground water.

NOBLE GASES IN ICE

The polar ice sheets constitute one of the most important archives of past environmental conditions. A prominent example is the reconstruction of the atmospheric composition in the past, in particular with respect to the greenhouse gases CO_2 and CH_4, based on air trapped in polar ice (e.g., Raynaud et al. 1993). No major changes of the atmospheric abundances of the noble gases are to be expected over the timescale of several 100 kyr accessible by the ice archive. Therefore, the isotopic and elemental composition of the noble gases in trapped air provides a tool to study physical processes acting during the entrapment of air in ice.

Gravitational separation

Atmospheric gases trapped in polar ice are enriched in the heavy species due to gravitational separation. This fractionation takes place in the thick firn layer (up to around 100 m) where the pore space is still connected. Below this layer, air bubbles are closed off in the ice and henceforth essentially preserved. The change in the ratio of any two gases from the initial atmospheric value f_0 to the value f in the trapped gas depends on the absolute mass difference ΔM between the two gases, the depth Z of the firn layer, and temperature T, as follows (Craig and Wiens 1996):

$$\frac{f}{f_0} = e^{\frac{g \cdot Z \cdot \Delta M}{R \cdot T}} \tag{50}$$

where g is the gravitational acceleration and R the gas constant.

Craig et al. (1988) demonstrated the occurrence of gravitational fractionation in polar firn based mainly on the isotopic composition of nitrogen and oxygen, but also on the elemental ratios O_2/N_2 and Ar/N_2. Craig and Wiens (1996) used the $^{84}Kr/^{36}Ar$ ratio in trapped air to confirm the dominance of gravitational separation over kinetic fractionation by processes such as effusion from compressed air bubbles, which depend on the relative mass difference $\Delta M/M$ rather than the absolute difference ΔM. The large ΔM between Kr and Ar allowed a clear distinction between different processes. Graf and Craig (1997) presented both Kr/Ar and Xe/Ar data that clearly confirmed the presence of gravitational separation.

However, elemental ratios can be fractionated due to gas loss from the samples through microfractures or crystal imperfections, which is governed by differences in molecular volumes (Craig et al. 1988; Bender et al. 1995). This process does not significantly affect isotope ratios. For this reason, much of the work on fractionation of trapped gases in ice has focused on high-precision isotope ratio measurements.

Because the magnitude of the gravitational fractionation depends on the thickness of the firn layer, which in turn is correlated to ambient temperature during firn accumulation, Craig and Wiens (1996) suggested the use of noble gas ratios in ice as a paleothermometer. Indeed, isotope ratios of N_2 and Ar in trapped air have recently been successfully employed to quantify past temperature changes, yet based on an additional fractionating effect, namely thermal diffusion.

Thermal diffusion

Thermal diffusion denotes an effect derived from kinetic gas theory, which predicts that a gas mixture subjected to a temperature gradient tends to unmix, producing an enrichment of the heavier species in the colder regions (Grew and Ibbs 1952; Chapman and Cowling 1970). A rapid temperature change at the surface of an ice sheet will lead t a temperature gradient in the firn column, which will cause the gases to separate b thermal diffusion. Heavier isotopes or elements will preferentially migrate towards th

cooler regions. This separation will continue until it is balanced by diffusion along the concentration gradient in the opposite direction.

The fractional difference δ (in per mil) of the isotope ratio f at temperature T to the ratio f_0 at temperature T_0 is given by (Chapman and Cowling 1970):

$$\delta = \left(\frac{f}{f_0} - 1\right) \cdot 10^3 = \left(\left[\frac{T_0}{T}\right]^{\alpha} - 1\right) \cdot 10^3 \qquad (51)$$

where α is the thermal diffusion factor characteristic for the investigated pair of gases.

The occurrence of thermal diffusion in nature was first observed by Severinghaus et al. (1996) for soil gas in sand dunes. The fractionation of soil air by water vapor diffusion, gravitational settling, and thermal diffusion studied by these authors may also have a small effect on dissolved noble gases in ground water, and hence the calculation of noble gas paleotemperatures. However, these comparatively minor effects have not yet been further studied in the soil–air–ground-water system.

Severinghaus et al. (1998) demonstrated that thermal fractionation of the air in polar firn layers can be detected and separated from the gravitational effect by high precision analysis of $^{15}N/^{14}N$ and $^{40}Ar/^{36}Ar$ ratios. Rapid temperature changes at the surface induce a transient temperature gradient in the upper part of the firn, which by way of thermal diffusion induces an isotopic signal that propagates downwards and is recorded in the trapped air in the ice. The resulting isotopic anomaly can directly be compared to other changes in the trapped air record. In this way, Severinghaus et al. (1998) showed that the increase of atmospheric methane at the end of the Younger Dryas cold period (about 12 kyr BP) began within 0 to 30 years after the warming event. This finding provides important constraints on the mechanisms of climate change at that time.

Moreover, by relating the isotopic anomaly in the trapped air as a marker of warming to the corresponding change of $\delta^{18}O$ in the ice, the age difference between ice and trapped air can be determined. This gas-age-ice-age difference can then be translated into a paleotemperature estimate using an empirical model of the snow densification process, which slows with decreasing temperature. For the Younger Dryas in central Greenland, Severinghaus et al. (1998) deduced 15°C lower than present temperatures. This estimate is in good agreement with values obtained from borehole temperature profiles, but significantly larger than inferred previously from the $\delta^{18}O$ paleothermometer calibrated by the modern spatial $\delta^{18}O$/temperature relationship.

Further studies have confirmed the usefulness of the thermal diffusion signal stored in polar ice cores. Severinghaus and Brook (1999) investigated the termination of the last glacial period (about 15 kyr BP), with similar results as in the previous study of the termination of the Younger Dryas. Lang et al. (1999) studied the abrupt warming at the start of a Dansgaard-Oeschger event about 70 kyr BP, whereas Leuenberger et al. (1999) focused on the largest temperature excursion during the Holocene, a cool period around 8.2 kyr BP. The latter studies were based on N_2 isotopes only and focused on the calibration of the $\delta^{18}O$ paleothermometer.

Severinghaus et al. (2001) directly observed thermal fractionation of the present-day firn air in response to seasonal temperature gradients. Elemental and isotopic ratios of N_2, O_2, Ar, Kr, and Xe analyzed in the air of the top 15 m of the firn at two Antarctic sites were found to match a model without adjustable parameters reasonably well. Relative thermal diffusion sensitivities for different gas pairs could be derived.

Analytical methods. Detection of the small thermal fractionation signals requires high precision isotope ratio mass spectrometry, which differs substantially from the

methods used to analyze noble gases in water samples as discussed earlier in this chapter. The most prominent difference is the use of dynamic rather than static mass spectrometry. Severinghaus et al. (2002) discuss in detail their methods used to measure $^{40}Ar/^{36}Ar$ and $^{84}Kr/^{36}Ar$ ratios in ice samples.

Ice samples are put into pre-cooled extraction vessels for evacuation. The ice is then melted and a gas extraction and purification similar to that used for water samples is performed. Because dynamic analysis requires far more sample than the static mode, ultrapure N_2 is added to increase bulk pressure by a factor of 10. The mass spectrometric analysis follows conventional procedures of dynamic isotope ratio mass spectrometry, with modifications designed to avoid any fractionating effects, such as thermal diffusion during volume splitting steps. An external precision of the order of ±0.01‰ for $^{40}Ar/^{36}Ar$ is achieved, yielding a good resolution of signals associatied with abrupt climate change that are about 0.4‰ in Greenland ice cores. The reproducibility of $^{84}Kr/^{36}Ar$ ratios is about ±1‰ for ice core samples. The $^{84}Kr/^{36}Ar$ ratio is primarily measured to identify samples that have experienced argon leakage out of the bubbles, e.g., during storage.

Helium isotopes

Helium isotopes have also been analyzed in polar ice cores, although very few results have been published so far. The first data showed a strong depletion of He in trapped air relative to atmospheric air (Craig and Chou 1982; Jean-Baptiste et al. 1993). The $^3He/^4He$ ratio was also found to be somewhat depleted compared to air. These findings clearly indicate loss of helium, presumably due to upward diffusion through the ice in response to increasing compression of the trapped air bubbles. However, some uncertainty remained as to what extent He loss during sampling influenced the results. The high diffusivity of He in ice clearly complicates its use in this archive.

Radiogenic He. Strong signals of crustal He have been found near the base of the ice sheets. Craig and Scarsi (1997) observed an approximately constant and slightly lower than atmospheric $^3He/^4He$ ratio in the upper 2.8 km, but a clearly radiogenic signature in the lowermost 250 m of the GISP2 ice core. The profile showed sharp peaks of radiogenic ^4He, indicating a disturbed stratigraphy of the deepest section of the core.

In the Vostok ice core, Jean-Baptiste et al. (2001) found a very sharp transition both in He concentration as well as in the isotopic ratio at a depth of 3539 m, the boundary between glacier ice and accreted ice from re-freezing of water of the underlying Lake Vostok. In the glacier ice, the He concentration was found to be nearly constant although depleted relative to the atmosphere, and the isotopic ratio was close to the air value. In the accreted ice, the He content was higher by a factor of more than three, and the $^3He/^4He$ ratio was correspondingly lowered ($R/R_a = 0.25 \pm 0.04$). Apparently, radiogenic He that had accumulated in the lake water was incorporated into the ice during freezing. Jean-Baptiste et al. (2001) used the assumption of a whole crustal He flux to estimate the water renewal time of the lake to about 5000 yr. Given the uncertainties related to the crustal He flux, this result must be regarded with caution, although it is in reasonable agreement with geophysical inferences.

Extraterrestrial ^3He. Polar ice also archives the influx of extraterrestrial matter in the form of interplanetary dust particles (IDPs), similar to the ocean sediments (see Schlosser and Winckler 2002 in this volume). Ice cores may provide less ambiguous results for the IDP flux than ocean sediments, as accumulation rates and time scales are well known in this archive. By analyzing He isotopes in particles separated from polar ice, Brook et al. (2000) demonstrated the utility of the ice core record to study the IDP flux and found similar results as obtained from marine sediments.

REFERENCES

Aeschbach-Hertig W (1994) Helium und Tritium als Tracer für physikalische Prozesse in Seen. PhD dissertation, ETH Zürich, Zürich

Aeschbach-Hertig W, Beyerle U, Holocher J, Peeters F, Kipfer R (2001) Excess air in ground water as a potential indicator of past environmental changes. *In* Intl Conf on the Study of Environmental Change Using Isotope Techniques (IAEA-CN-80). IAEA, Vienna, p 34-36

Aeschbach-Hertig W, Hofer M, Kipfer R, Imboden DM, Wieler R (1999a) Accumulation of mantle gases in a permanently stratified volcanic Lake (Lac Pavin, France). Geochim Cosmochim Acta 63: 3357-3372

Aeschbach-Hertig W, Hofer M, Schmid M, Kipfer R, Imboden DM (2002a) The physical structure and dynamics of a deep, meromictic crater lake (Lac Pavin, France). Hydrobiol (in press)

Aeschbach-Hertig W, Kipfer R, Hofer M, Imboden DM, Baur H (1996a) Density-driven exchange between the basins of Lake Lucerne (Switzerland) traced with the ^{3}H-^{3}He method. Limnol Oceanogr 41: 707-721

Aeschbach-Hertig W, Kipfer R, Hofer M, Imboden DM, Wieler R, Signer P (1996b) Quantification of gas fluxes from the subcontinental mantle: The example of Laacher See, a maar lake in Germany. Geochim Cosmochim Acta 60:31-41

Aeschbach-Hertig W, Peeters F, Beyerle U, Kipfer R (1999b) Interpretation of dissolved atmospheric noble gases in natural waters. Water Resour Res 35:2779-2792

Aeschbach-Hertig W, Peeters F, Beyerle U, Kipfer R (2000) Palaeotemperature reconstruction from noble gases in ground water taking into account equilibration with entrapped air. Nature 405:1040-1044

Aeschbach-Hertig W, Schlosser P, Stute M, Simpson HJ, Ludin A, Clark JF (1998) A $^{3}H/^{3}He$ study of ground-water flow in a fractured bedrock aquifer. Ground Water 36:661-670

Aeschbach-Hertig W, Stute M, Clark J, Reuter R, Schlosser P (2002b) A paleotemperature record derived from dissolved noble gases in ground water of the Aquia Aquifer (Maryland, USA). Geochim Cosmochim Acta 66:797-817

Andrews JN (1985) The isotopic composition of radiogenic helium and its use to study ground-water movement in confined aquifers. Chem Geol 49:339-351

Andrews JN, Balderer W, Bath AH, Clausen HB, Evans GV, Florkowski T, Goldbrunner JE, Ivanovich M, Loosli H, Zojer H (1984) Environmental isotope studies in two aquifer systems: A comparison of ground-water dating methods. *In* Isotope Hydrology 1983 (IAEA-SM-270). IAEA, Vienna, p 535-577

Andrews JN, Davis SN, Fabryka-Martin J, Fontes J-C, Lehmann BE, Loosli HH, Michelot J-L, Moser H, Smith B, Wolf M (1989) The in situ production of radioisotopes in rock matrices with particular reference to the Stripa granite. Geochim Cosmochim Acta 53:1803-1815

Andrews JN, Fontes J-C, Aranyossy J-F, Dodo A, Edmunds WM, Joseph A, Travi Y (1994) The evolution of alkaline ground waters in the continental intercalaire aquifer of the Irhazer Plain, Niger. Water Resour Res 30:45-61

Andrews JN, Goldbrunner JE, Darling WG, Hooker PJ, Wilson GB, Youngman MJ, Eichinger L, Rauert W, Stichler W (1985) A radiochemical, hydrochemical and dissolved gas study of ground waters in the Molasse basin of Upper Austria. Earth Planet Sci Lett 73:317-332

Andrews JN, Lee DJ (1979) Inert gases in ground water from the Bunter Sandstone of England as indicators of age and palaeoclimatic trends. J Hydrol 41:233-252

Ballentine CJ, Burgess R, Marty B (2002) Tracing fluid origin, transport and interaction in the crust. Rev Mineral Geochem 47:539-614

Ballentine CJ, Burnard PG (2002) Production, release and transport of noble gases in the continental crust. Rev Mineral Geochem 47:481-538

Ballentine CJ, Hall CM (1999) Determining paleotemperature and other variables by using an error-weighted, nonlinear inversion of noble gas concentrations in water. Geochim Cosmochim Acta 63:2315-2336

Ballentine CJ, Mazurek M, Gautschi A (1994) Thermal constraints on crustal rare gas release and migration: Evidence from Alpine fluid inclusions. Geochim Cosmochim Acta 58:4333-4348

Bauer S, Fulda C, Schäfer W (2001) A multi-tracer study in a shallow aquifer using age dating tracers ^{3}H, ^{85}Kr, CFC-113 and SF_6—indication for retarded transport of CFC-113. J Hydrol 248:14-34

Bayer R, Schlosser P, Bönisch G, Rupp H, Zaucker F, Zimmek G (1989) Performance and Blank Components of a Mass Spectrometric System for routine measurement of helium isotopes and tritium by the ^{3}he ingrowth method. *In* Sitzungsberichte der Heidelberger Akademie der Wissenschaften. 5:241-279

Begemann F, Libby WF (1957) Continental water balance, ground-water inventory and storage times, surface ocean mixing rates and world-wide water circulation patterns from cosmic-ray and bomb tritium. Geochim Cosmochim Acta 12:277-296

Benson BB, Krause D (1976) Empirical laws for dilute aqueous solutions of nonpolar gases. J Chem Phys 64:689-709

Benson BB, Krause D (1980) Isotopic fractionation of helium during solution: A probe for the liquid state. J Solution Chem 9:895-909

Bender M, Sowers T, Lipenkov V (1995) On the concentrations of O_2, N_2, and Ar in trapped gases from ice cores. J Geophys Res 100:18651-18660

Bertin C, Bourg ACM (1994) Radon-222 and chloride as natural tracers of the infiltration of river water into an alluvial aquifer in which there is significant river/ground-water mixing. Environ Sci Technol 28:794-798

Bertleff B, Ellwanger D, Szenkler C, Eichinger L, Trimborn P, Wolfendale N (1993) Interpretation of hydrochemical and hydroisotopical measurements on palaeoground waters in Oberschwaben, south German alpine foreland, with focus on quanternary geology. *In* Isotope techniques in the study of past and current environmental changes in the hydrosphere and the atmosphere (IAEA-SM-329). IAEA, Vienna, p 337-357

Beyerle U, Aeschbach-Hertig W, Hofer M, Imboden DM, Baur H, Kipfer R (1999a) Infiltration of river water to a shallow aquifer investigated with $^3H/^3He$, noble gases and CFCs. J Hydrol 220:169-185

Beyerle U, Aeschbach-Hertig W, Imboden DM, Baur H, Graf T, Kipfer R (2000a) A mass spectrometric system for the analysis of noble gases and tritium from water samples. Environ Sci Technol 34: 2042-2050

Beyerle U, Aeschbach-Hertig W, Peeters F, Kipfer R (2000b) Accumulation rates of radiogenic noble gases and noble gas temperatures deduced from the Great Artesian Basin, Australia. Beyond 2000—New Frontiers in Isotope Geoscience 1:21

Beyerle U, Aeschbach-Hertig W, Peeters F, Kipfer R, Purtschert R, Lehmann B, Loosli HH, Love A (1999b) Noble gas data from the Great Artesian Basin provide a temperature record of Australia on time scales of 10^5 years. *In* Isotope techniques in water resources development and management (IAEA-SM-361, IAEA-CSP-C/2). IAEA, Vienna, p 97-103

Beyerle U, Purtschert R, Aeschbach-Hertig W, Imboden DM, Loosli HH, Wieler R, Kipfer R (1998) Climate and ground water recharge during the last glaciation in an ice-covered region. Science 282:731-734

Beyerle U, Rüedi J, Aeschbach-Hertig W, Peeters F, Leuenberger M, Dodo A, Kipfer R (2002) Evidence for periods of wetter and cooler climate in the Sahel between 6 and 40 kyr. Geophys Res Lett (submitted)

Bieri RH (1971) Dissolved Noble Gases in Marine Waters. Earth Planet Sci Lett 10:329-333

Böhlke JK, Denver JM (1995) Combined use of ground water dating, chemical, and isotopic analyzes to resolve the history and fate of nitrate contamination in two agricultural watersheds, Atlantic coastal plain, Maryland. Water Resour Res 31:2319-2339

Böhlke JK, Révész K, Busenberg E, Deak J, Deseö E, Stute M (1997) Ground water record of halocarbon transport by the Danube river. Environ Sci Technol 31:3293-3299

Bottomley DJ, Ross JD, Clarke WB (1984) Helium and neon isotope geochemistry of some ground waters from the Canadian Precambrian Shield. Geochim Cosmochim Acta 48:1973-1985

Brennwald MS, Peeters F, Beyerle U, Rüedi J, Hofer M, Kipfer R (2001) Modeling the transport of CFCs and 3H through the unsaturated zone. Geophys Res Abstr EGS HSA6

Broecker W (1996) Glacial climate in the tropics. Science 272:1902-1903

Brook EJ, Kurz MD, Curtice J, Cowburn S (2000) Accretion of interplanetary dust in polar ice. Geophys Res Lett 27:3145-3148

Brown RM (1961) Hydrology of tritium in the Ottawa Valley. Geochim Cosmochim Acta 21:199-216

Busenberg E, Plummer LN (1992) Use of chlorofluorocarbons (CCl_3F and CCl_2F_2) as hydrologic tracers and age-dating tools: The alluvium and terrace system of central Oklahoma. Water Resour Res 28:2257-2284

Busenberg E, Plummer NL (2000) Dating young ground water with sulfur hexafluoride: Natural and anthropogenic sources of sulfur hexafluoride. Water Resour Res 36:3011-3030

Busenberg E, Weeks EP, Plummer LN, Bartholomay RC (1993) Age dating ground water by use of chlorofluorocarbons (CCl_3F and CCl_2F_2), and distribution of chlorofluorocarbons in the unsaturated zone, Snake River plain aquifer, Idaho National Engineering Laboratory, Idaho. U S Geol Surv 93-4054 93:1-47

Cable JE, Bugna GC, Burnett WC, Chanton JP (1996) Application of ^{222}Rn and CH_4 for assessment of ground water discharge to the coastal ocean. Limnol Oceanogr 41:1347-1353

Castro MC, Goblet P, Ledoux E, Violette S, de Marsily G (1998a) Noble gases as natural tracers of water circulation in the Paris Basin, 2. Calibration of a ground water flow model using noble gas isotope data. Water Resour Res 34:2467-2483

Castro MC, Jambon A, de Marsily G, Schlosser P (1998b) Noble gases as natural tracers of water circulation in the Paris Basin, 1. Measurements and discussion of their origin and mechanisms of vertical transport in the basin. Water Resour Res 34:2443-2466

Castro MC, Stute M, Schlosser P (2000) Comparison of ^{4}He ages and ^{14}C ages in simple aquifer systems: implications for ground water flow and chronologies. Appl Geochem 15:1137-1167

Chapman S, Cowling TG (1970) The mathematical theory of non-uniform gases. Cambridge University Press, Cambridge, London, New York

Cecil LD, Green JR (2000) Radon-222. *In* Environmental tracers in subsurface hydrology. Cook P, Herczeg AL (eds) Kluwer Academic Publishers, Boston, p 175-194

Christiansen JE (1944) Effect of entrapped air upon the permeability of soils. Soil Sci 58:355-365

Clark JF, Davisson ML, Hudson GB, Macfarlane PA (1998) Noble gases, stable isotopes, and radiocarbon as tracers of flow in the Dakota aquifer, Colorado and Kansas. J Hydrol 211:151-167

Clark JF, Hudson GB (2001) Quantifying the flux of hydrothermal fluids into Mono Lake by use of helium isotopes. Limnol Oceanogr 46:189-196

Clark JF, Stute M, Schlosser P, Drenkard S, Bonani G (1997) A tracer study of the Floridan aquifer in southeastern Georgia: Implications for ground water flow and paleoclimate. Water Resour Res 33: 281-289

Clarke WB, Jenkins WJ, Top Z (1976) Determination of tritium by mass spectrometric measurement of ^{3}He. Intl JAppl Radiat Isotopes 27:515-522

Clarke WB, Top Z, Beavan AP, Gandhi SS (1977) Dissolved helium in lakes: Uranium prospecting in the precambrian terrain of Central Labrador. Econ Geol 72:233-242

Clever HL (ed) (1979a) Helium and neon-gas solubilities. Solubility Data Series. Vol 1. Pergamon Press, Oxford, New York, Toronto, Sydney, Paris, Frankfurt

Clever HL (ed) (1979b) Krypton, xenon and radon-gas solubilities. Solubility Data Series. Vol 2. Pergamon Press, Oxford, New York, Toronto, Sydney, Paris, Frankfurt

Clever HL (ed) (1980) Argon. Solubility Data Series. Vol 4. Pergamon Press, Oxford, New York, Toronto, Sydney, Paris, Frankfurt

Collier RW, Dymond J, McManus J (1991) Studies of hydrothermal processes in Crater Lake, OR. College of Oceanography, Oregon State University, Report #90-7:1:201

Collon P, Kutschera W, Loosli HH, Lehmann BE, Purtschert R, Love A, Sampson L, Anthony D, Cole D, Davids B, Morrissey DJ, Sherrill BM, Steiner M, Pardo RC, Paul M (2000) ^{81}Kr in the Great Artesian Basin, Australia: a new method for dating very old ground water. Earth Planet Sci Lett 182:103-113

Colman JA, Armstrong DE (1987) Vertical eddy diffusivity determined with Rn-222 in the benthic boundary-layerof ice-covered lakes. Limnol Oceanogr 32:577-590

Cook PG, Böhlke J-K (2000) Determining timescales for ground water flow and solute transport. *In* Environmental tracers in subsurface hydrology. Cook P, Herczeg AL (eds) Kluwer Academic Publishers, Boston, p 1-30

Cook PG, Herczeg AL (eds) (2000) Environmental tracers in subsurface hydrology. Kluwer Academic Publishers, Boston

Cook PG, Solomon DK (1995) Transport of atmospheric trace gases to the water table: Implications for ground water dating with chlorofluorocarbons and krypton 85. Water Resour Res 31:263-270

Cook PG, Solomon DK (1997) Recent advances in dating young ground water: chlorofluorocarbons, ^{3}H/^{3}He and ^{85}Kr. J Hydrol 191:245-265

Cook PG, Solomon DK, Plummer LN, Busenberg E, Schiff SL (1995) Chlorofluorocarbons as tracers of ground water transport processes in a shallow, silty sand aquifer. Water Resour Res 31:425-434

Cook PG, Solomon DK, Sanford WE, Busenberg E, Plummer LN, Poreda RJ (1996) Inferring shallow ground water flow in saprolite and fractured rock using environmental tracers. Water Resour Res 32:1501-1509

Craig H, Chou CC (1982) Helium isotopes and gases in Dye 3 ice cores. EOS Trans Am Geophys Union 63:298

Craig H, Clarke WB, Beg MA (1975) Excess ^{3}He in deep water on the East Pacific Rise. Earth Planet Sci Lett 26:125-132

Craig H, Dixon F, Craig VK, Edmond J, Coulter G (1974) Lake Tanganyika geochemical and hydrographic study: 1973 expedition. Scripps Institution of Oceanography Series 75-5:1-83

Craig H, Horibe Y, Sowers T (1988) Gravitational separation of gases and isotopes in polar ice caps. Science 242:1675-1678

Craig H, Scarsi P (1997) Helium isotope stratigraphy in the GISP2 ice core. EOS Trans Am Geophys Union 78:F7

Craig H, Weiss RF (1971) Dissolved gas saturation anomalies and excess helium in the ocean. Earth Planet Sci Lett 10:289-296

Craig H, Wiens RC (1996) Gravitational enrichment of $^{84}Kr/^{36}Ar$ ratios in polar ice caps: a measure of firn thickness and accumulation temperature. Science 271:1708-1710

Crovetto R, Fernandez-Prini R, Japas ML (1982) Solubilities of inert gases and methane in H_2O and in D_2O in the temperature range of 300 to 600 K. J Chem Phys 76:1077-1086

Crowley TJ (2000) CLIMAP SSTs re-revisited. Clim Dyn 16:241-255

Crowley TJ, Baum SK (1997) Effect of vegetation on an ice-age climate model simulation. J Geophys Res 102:16463-16480

Cunnold DM, Fraser PJ, Weiss RF, Prinn RG, Simmonds PG (1994) Global trends and annual releases of CCl_3F and CCl_2F_2 estimated from ALE/GAGE and other measurements from July 1978 to June 1991. J Geophys Res 99:1107-1126

Dennis F, Andrews JN, Parker A, Poole J, Wolf M (1997) Isotopic and noble gas study of Chalk ground water in the London Basin, England. Appl Geochem 12:763-773

Doney SC, Glover DM, Jenkins WJ (1992) A model function of the global bomb tritium distribution in precipitation, 1960-1986. J Geophys Res 97:5481-5492

Dunkle SA, Plummer LN, Busenberg E, Phillips PJ, Denver JM, Hamilton PA, Michel RL, Coplen TB (1993) Chlorofluorocarbons (CCl_3F and CCl_2F_2) as dating tools and hydrologic tracers in shallow ground water of the Delmarva Peninsula, Atlantic Coastal Plain, United States. Water Resour Res 29:3837-3860

Dunkle Shapiro S, LeBlanc D, Schlosser P, Ludin A (1999) Characterizing a sewage plume using the ^3H-^3He dating technique. Ground Water 37:861-878

Dunkle Shapiro S, Rowe G, Schlosser P, Ludin A, Stute M (1998) Tritium–helium-3 dating under complex conditions in hydraulically stressed areas of a buried-valley aquifer. Water Resour Res 34:1165-1180

Edmunds WM, Fellman E, Goni IB, McNeill G, Harkness DD (1998) Ground water, palaeoclimate and palaeorecharge in the southwest Chad Basin, Borno State, Nigeria. *In* Isotope techniques in the study of environmental change (IAEA-SM-349). IAEA, Vienna, p 693-707

Ekwurzel B, Schlosser P, Smethie WM, Plummer LN, Busenberg E, Michel RL, Weppernig R, Stute M (1994) Dating of shallow ground water: Comparison of the transient tracers $^3H/^3He$, chlorofluorocarbons, and ^{85}Kr. Water Resour Res 30:1693-1708

Ellins KK, Roman-Mas A, Lee R (1990) Using ^{222}Rn to examine ground water/surface discharge interaction in the Rio Grande de Manati, Puerto Rico. J Hydrol 115:319-341

Erikson E (1958) The possible use of tritium for estimating ground water storage. Tellus 10:472-478

Farrera I, Harrison SP, Prentice IC, Ramstein G, Guiot J, Bartlein PJ, Bonnefille R, Bush M, Cramer W, von Grafenstein U, Holmgren K, Hooghiemstra H, Hope G, Jolly D, Lauritzen SE, Ono Y, Pinot S, Stute M, Yu G (1999) Tropical climates at the Last Glacial Maximum: a new synthesis of terrestrial palaeoclimate data. I. Vegetation, lake levels and geochemistry. Clim Dyn 15:823-856

Faybishenko BA (1995) Hydraulic behavior of quasi-saturated soils in the presence of entrapped air: Laboratory experiments. Water Resour Res 31:2421-2435

Fayer MJ, Hillel D (1986) Air encapsulation: 1. Measurement in a field soil. Soil Sci Soc Am J 50:568-572

Frei MW (1999) Entwicklung und erster Feldeinsatz einer neuen massenspektrometrischen Methode zur Echtzeitbestimmung der Hauptgaskomponenten in Bodenluft. Diploma thesis, ETH-Zürich / EAWAG, Zürich / Dübendorf

Giggenbach WF, Sano Y, Schmincke HU (1991) CO_2-rich gases from Lakes Nyos and Monoun, Cameroon; Laacher See, Germany; Dieng, Indonesia, and Mt. Gambier, Australia—variations on a common theme. J Volcanol Geotherm Res 45:311-323

Gill AE (1982) Atmosphere-Ocean Dynamics. Academic Press, San Diego

Graf T, Craig H (1997) GISP2: Gravitational enrichment of Kr/Ar and Xe/Ar ratios. EOS Trans Am Geophys Union 78:F7

Graham DW (2002) Noble gas isotope geochemistry of mid-ocean ridge island basalts: characterization of mantle source reservoirs. Rev Mineral Geochem 47:247-318

Grew KE, Ibbs TL (1952) Thermal Diffusion in Gases. Cambridge University Press, Cambridge, London, New York

Griesshaber E, O'Nions RK, Oxburgh ER (1992) Helium and carbon isotope systematics in crustal fluids from the Eifel, the Rhine Graben and Black Forest, F.R.G. Chem Geol 99:213-235

Gröning M (1989) Entwicklung und Anwendung einer neuen Probenahmetechnik für Edelgasmessungen an Grundwasser und Untersuchungen zum Luftüberschuss im Grundwasser. Diploma thesis, Universität Heidelberg, Heidelberg

Gröning M (1994) Edelgase und Isotopentracer im Grundwasser: Paläo-Klimaänderungen und Dynamik regionaler Grundwasserfliesssysteme. PhD dissertation, Universität Heidelberg, Heidelberg

Gülec N (1988) Helium-3 distribution in Western Turkey. Mineral Res. Expl. Bull. 108:35-42

Heaton THE (1981) Dissolved gases; some applications to ground water research. Trans Geol Soc South Africa 84:91-97

Heaton THE (1984) Rates and sources of ^{4}He accumulation in ground water. Hydrol Sci J 29:29-47
Heaton THE, Talma AS, Vogel JC (1983) Origin and history of nitrate in confined ground water in the western Kalahari. J Hydrol 62:243-262
Heaton THE, Talma AS, Vogel JC (1986) Dissolved gas paleotemperatures and ^{18}O variations derived from ground water near Uitenhage, South Africa. Quat Res 25:79-88
Heaton THE, Vogel JC (1979) Gas concentrations and ages of ground waters in Beaufort Group sediments, South Africa. Water SA 5:160-170
Heaton THE, Vogel JC (1981) "Excess air" in ground water. J Hydrol 50:201-216
Herzberg O, Mazor E (1979) Hydrological applications of noble gases and temperature measurements in underground water systems: Examples from Israel. J Hydrol 41:217-231
Ho DT, Schlosser P, Smethie WM, Simpson HJ (1998) Variability in atmospheric chlorofluorocarbons (CCl_3F and CCl_2F_2) near a large urban area: Implications for ground water dating. Environ Sci Technol 32:2377-2382
Hoehn E, von Gunten HR (1989) Radon in ground water: A tool to assess infiltration from surface waters to aquifers. Water Resour Res 25:1795-1803
Hofer M, Imboden DM (1998) Simultaneous determination of CFC-11, CFC-12, N_2 and Ar in water. Analyt Chem 70:724-729
Hofer M., Peeters F, Aeschbach-Hertig W, Brennwald M, Holocher J, Livingstone DM., Romanovski V, and Kipfer R (2002) Rapid deep-water renewal in lake Issyk-Kul (Kyrgyzstan) indicated by transient tracers. Limnol Oceanogr 47:1210-1216
Hohmann R (1997) Deep-Water Renewal in Lake Baikal. PhD dissertation, ETH-Zürich, Zürich
Hohmann R, Hofer M, Kipfer R, Peeters F, Imboden DM (1998) Distribution of helium and tritium in Lake Baikal. J Geophys Res 103:12823-12838
Hohmann R, Kipfer R, Peeters F, Piepke G, Imboden DM, Shimaraev MN (1997) Processes of deep water renewal in Lake Baikal. Limnol Oceanogr 42:841-855
Holocher J, Matta V, Aeschbach-Hertig W, Beyerle U, Hofer M, Peeters F, Kipfer R (2001) Noble gas and major element constraints on the water dynamics in an alpine floodplain. Ground Water 39:841-852
Holocher J, Peeters F, Aeschbach-Hertig W, Beyerle U, Brennwald M, Hofer M, Kipfer R (2000) New insights into the mechanisms controlling the formation of excess air in ground water. EOS Trans Am Geophys Union 81:F441
Holocher J, Peeters F, Aeschbach-Hertig W, Beyerle U, Hofer M, Brennwald M, Kinzelbach W, Kipfer R (2002) Experimental investigations on the formation of excess air in quasi-saturated porous media. Geochim Cosmochim Acta (in press)
Holzner C (2001) Untersuchung der Tiefenwassererneuerung in meromiktischen Seen mittels transienter Tracer und numerischer Modellierung. Diploma thesis, ETH-Zürich / EAWAG-Zürich-Dübendorf
Huneau F, Blavoux B, Aeschbach-Hertig W, Kipfer R (2001) Palaeoground waters of the Valréas Miocene aquifer (Southeastern France) as archives of the LGM/Holocene climatic transition in the Western Mediterranean region. *In* Intl Conf Study of Environmental Change Using Isotope Techniques (IAEA-CN-80). IAEA, Vienna, p 27-28
Hunkeler D, Hoehn E, Höhener P, Zeyer J (1997) ^{222}Rn as a partitioning tracer to detect diesel fuel contamination in aquifers: laboratory study and field observations. Environ Sci Technol 31:3180-3187
IAEA/WMO (1998) Global Network of Isotopes in Precipitation. The GNIP Database www.iaea.or.at/programs/ri/gnip/gnipmain.htm. IAEA, Vienna
Igarashi G, Ozima M, Ishibashi J, Gamo T, Sakai H, Nojiri Y, Kawai T (1992) Mantle helium flux from the bottom of Lake Mashu, Japan. Earth Planet Sci Letters 108:11-18
Imboden DM (1977) Natural radon as a limnological tracer for the study of vertical and horizontal eddy diffusion. *In* Isotopes in lake studies. IAEA, Vienna p 213-218
Imboden DM, Emerson S (1978) Natural radon and phosphorus as limnologic tracers: Horizontal and vertical eddy diffusion in Greifensee. Limnol Oceanogr 23:77-90
Imboden DM, Joller T (1984) Turbulent mixing in the hypolimion of Baldeggersee (Switzerland) traced by natural radon-222. Limnol Oceanogr 29:831-844
Jassby A, Powell T (1975) Vertical patterns of eddy diffusion during stratification in Castle Lake, California. Limnol Oceanogr 20:530-543
Jean-Baptiste P, Petit JR, Lipenkov VY, Raynaud D, Barkov N (2001) Constraints on hydrothermal processes and water exchange in Lake Vostok from helium isotopes. Nature 411:460-462
Jean-Baptiste P, Raynaud D, Mantisi F, Sowers T, Barkov N (1993) Measurement of helium isotopes in Antarctic ice: preliminary results from Vostok. C R Acad Sci Paris 316:491-497
Jenkins WJ (1976) Tritium-helium dating in the Sargasso Sea: A measurement of oxygen utilization rates. Science 196:291-292
Johnston CT, Cook PG, Frape SK, Plummer LN, Busenberg E, Blackport RJ (1998) Ground water age and nitrate distribution within a glacial aquifer beneath a thick unsaturated zone. Ground Water 36:171-180

Juillard-Tardent M (1999) Gasübersättigung an Paläogrundwässern in Estland. Diploma thesis, Universität Bern, Bern

Katz BG, Lee TM, Plummer LN, Busenberg E (1995) Chemical evolution of ground water near a sinkhole lake, northern Florida -1. Flow patterns, age of ground water, and influence of lake water leakage. Water Resour Res 31:1549-1564

Kaufman S, Libby WF (1954) The natural distribution of tritium. Phys Rev 93:1337-1344

Kennedy BM, Hiyagon H, Reynolds JH (1990) Crustal neon: a striking uniformity. Earth Planet Sci Lett. 98:277-286

Kipfer R, Aeschbach-Hertig W, Baur H, Hofer M, Imboden DM, Signer P (1994) Injection of mantle type helium into Lake Van (Turkey): The clue for quantifying deep water renewal. Earth Planet. Sci Lett 125:357-370

Kipfer R, Aeschbach-Hertig W, Beyerle U, Goudsmit G, Hofer M, Peeters F, Klerkx J, Plisnier J-P, Kliembe EA, Ndhlovu R (2000) New evidence for deep water exchange in Lake Tanganyika. EOS Trans Am Geophys Union 80:OS239

Kipfer R, Aeschbach-Hertig W, Hofer M, Hohmann R, Imboden DM, Baur H, Golubev V, Klerkx J (1996) Bottomwater formation due to hydrothermal activity in Frolikha Bay, Lake Baikal, eastern Siberia. Geochim Cosmochim Acta 60:961-971

Lang C, Leuenberger M, Schwander J, Johnsen S (1999) 16°C rapid temperature variation in central Greenland 70,000 years ago. Science 286:934-937

Lehmann BE, Davis S, Fabryka-Martin J (1993) Atmospheric and subsurface sources of stable and radioactive nuclides used for ground-water dating. Water Resour Res 29:2027-2040

Lehmann BE, Loosli HH (1991) Isotopes formed by underground production. *In* Applied Isotope Hydrogeology, a Case Study in Northern Switzerland. Pearson FJ, Balderer W, Loosli HH, Lehmann BE, Matter A, Peters T, Schmassmann H, Gautschi A (eds) Elsevier, Amsterdam, p 239-296

Lehmann BE, Loosli HH, Purtschert R, Andrews JN (1996) A comparison of chloride and helium concentrations in deep ground waters. *In* Isotopes in water resources management (IAEA-SM-336). IAEA, Vienna, p 3-17

Lehmann BE, Loosli HH, Rauber D, Thonnard N, Willis RD (1991) ^{81}Kr and ^{85}Kr in ground water, Milk River aquifer, Alberta, Canada. Appl Geochem 6:419-423

Lehmann BE, Purtschert R (1997) Radioisotope dynamics—the origin and fate of nuclides in ground water. Appl Geochem 12:727-738

Lehmann BE, Purtschert R, Loosli HH, Love A, Sampson L, Collon P, Kutschera W, Beyerle U, Aeschbach-Hertig W, Kipfer R (1999) ^{81}Kr-, ^{36}Cl- and ^{4}He-dating in the Great Artesian Basin, Australia. *In* Isotope techniques in water resources development and management (IAEA-SM-361). IAEA, Vienna, p 98

Leuenberger M, Lang C, Schwander J (1999) Delta^{15}N measurements as a calibration tool for the paleothermometer and gas-ice age differences: A case study for the 8200 B.P. event on GRIP ice. J Geophys Res 104:22163-22170

Loosli HH (1983) A dating method with ^{39}Ar. Earth Planet Sci Lett 63:51-62

Loosli HH (1992) Applications of ^{37}Ar, ^{39}Ar and ^{85}Kr in hydrology, oceanography and atmospheric studies. *In* Isotopes of noble gases as tracers in environmental studies. IAEA, Vienna, p 73-85

Loosli HH, Lehmann BE, Balderer W (1989) Argon-39, argon-37 and krypton-85 isotopes in Stripa ground waters. Geochim Cosmochim Acta 53:1825-1829

Loosli HH, Lehmann BE, Smethie WM (2000) Noble gas radioisotopes: ^{37}Ar, ^{85}Kr, ^{39}Ar, ^{81}Kr. *In* Environmental tracers in subsurface hydrology. Cook P, Herczeg AL (eds) Kluwer Academic Publishers, Boston, p 379-396

Loosli HH, Lehmann BE, Thalmann C, Andrews JN, Florkowski T (1992) Argon-37 and argon-39: Measured concentrations in ground water compared with calculated concentrations in rock. *In* Isotope techniques in water resources development (IAEA-SM-319). IAEA, Vienna, p 189-201

Lovley DR, Woodward JC (1992) Consumption of freons CFC-11 and CFC-12 by anaerobic sediments and soils. Environ Sci Technol 26:925-929

Lucas LL, Unterweger MP (2000) Comprehensive review and critical evaluation of the half-life of Tritium. J Res Natl Inst Stand Technol 105:541-549

Ludin A, Wepperning R, Bönisch G, Schlosser P (1997) Mass spectrometric measurement of heli isotopes and tritium in water samples. Techn Report Lamont-Doherty Earth Observatory, Palisad New York

Ludin AI, Lehmann BE (1995) High-resolution diode-laser spectroscopy on a fast beam of metasta atoms for detecting very rare krypton isotopes. Appl Phys B61:461-465

Maloszewski P, Zuber A (1982) Determining the turnover time of ground water systems with the aid of environmental tracers, I. Models and their applicability. J Hydrol 57:207-231

Mamyrin BA, Tolstikhin IN (1984) Helium isotopes in nature. Elsevier, Amsterdam, Oxford, New York, Tokyo

Manning AH, Sheldon AL, Solomon DK (2000) A new method of noble gas sampling that improves excess air determinations. EOS Trans Am Geophys Union 81:F449

Marine IW (1979) The use of naturally occurring helium to estimate ground water velocities for studies of geologic storage of radioactive waste. Water Resour Res 15:1130-1136

Martel DJ, Deak J, Horvath F, O'Nions RK, Oxburgh ER, Stegena L, Stute M (1989) Leakage of Helium from the Pannonian Basin. Nature 342:908-912

Matthews A, Fouillac C, Hill R, O'Nions RK, Oxburgh ER (1987) Mantle-derived volatiles in continental crust: the Massif Central of France. Earth Planet Sci Lett 85:117-128

Mattle N (1999) Interpretation von Tracermessungen mittels Boxmodellen und numerischen Strömungs-/Transportmodellen. PhD dissertation, Universität Bern, Bern

Mattle N, Kinzelbach W, Beyerle U, Huggenberger P, Loosli HH (2001) Exploring an aquifer system by integrating hydraulic, hydrogeologic and environmental tracer data in a three-dimensional hydrodynamic transport model. J Hydrol 242:183-196

Mazor E (1972) Paleotemperatures and other hydrological parameters deduced from gases dissolved in ground waters, Jordan Rift Valley, Israel. Geochem Cosmochim Acta 36:1321-1336

Mazor E, Bosch A (1992) Helium as a semi-quantitative tool for ground water dating in the range of 10^4-10^8 years. *In* Isotopes of noble gases as tracers in environmental studies. IAEA, Vienna, p 163-178

Modica E, Burton HT, Plummer LN (1998) Evaluating the source and residence times of ground water seepage to streams, New Jersey Coastal Plain. Water Resour Res 34:2797-2810

Münnich KO, Roether W, Thilo L (1967) Dating of ground water with tritium and ^{14}C. *In* Isotopes in Hydrology (IAEA-SM-83). IAEA, Vienna, p 305-320

O'Nions RK, Oxburgh ER (1983) Heat and helium in the earth. Nature 306:429-431

O'Nions RK, Oxburgh ER (1988) Helium, volatile fluxes and the development of continental crust. Earth Planet Sci Lett 90:331-347

Oana S (1957) Bestimmung von Argon in besonderem Hinblick auf gelöste Gase in natürlichen Gewässern. J Earth Sci Nagoya Univ 5:103-105

Osenbrück K (1991) Laborversuche zur Bildung des Luftüberschusses im Grundwasser. Diploma thesis, Universität Heidelberg, Heidelberg

Osenbrück K, Lippmann J, Sonntag C (1998) Dating very old pore waters in impermeable rocks by noble gas isotopes. Geochim Cosmochim Acta 62:3041-3045

Oster H, Sonntag C, Münnich KO (1996) Ground water age dating with chlorofluorocarbons. Water Resour Res 32:2989-3001

Oxburgh ER, O'Nions RK (1987) Helium loss, tectonics, and the terrestrial heat budget. Science 237: 1583-1588

Ozima M, Podosek FA (1983) Noble gas geochemistry. Cambridge Univ. Press, Cambridge, London, New York

Peeters F, Beyerle U, Aeschbach-Hertig W, Holocher J, Brennwald MS, Kipfer R (2002) Improving noble gas based paleoclimate reconstruction and ground water dating using $^{20}Ne/^{22}Ne$ ratios. Geochim Cosmochim Acta in press

Peeters F, Kipfer R, Achermann D, Hofer M, Aeschbach-Hertig W, Beyerle U, Imboden DM, Rozanski K, Fröhlich K (2000a) Analysis of deep-water exchange in the Caspian Sea based on environmental tracers. Deep-Sea Res I 47:621-654

Peeters F, Kipfer R, Hofer M, Imboden DM, Domysheva VM (2000b) Vertical turbulent diffusion and upwelling in Lake Baikal estimated by inverse modeling of transient tracers. J Geophys Res 105:14283 and 3451-3464

Peeters F, Kipfer R, Hohmann R, Hofer M, Imboden DM, Kodenev GG, Khozder T (1997) Modelling transport rates in Lake Baikal: gas exchange and deep water renewal. Environ Sci Technol 31: 2973-2982

Peeters F, Piepke G, Kipfer R, Hohmann R, Imboden DM (1996a) Description of stability and neutrally buoyant transport in freshwater lakes. Limnol Oceanogr 41:1711-1724

Peeters F, Piepke G, Kipfer R, Hohmann R, Imboder DM (1996b) Neutrally buoyant transport in deep freshwater systems: the case of Lake Baikal (Siberia). Am Soc Limnology Oceanography 73

Pinot S, Ramstein G, Harrison SP, Prentice IC, Guiot J, Stute M, Joussaume S (1999) Tropical paleoclimates at the Last Glacial Maximum: comparison of Paleoclimate Modeling Intercomparison Project (PMIP) simulations and paleodata. Clim Dyn 15:857-874

Pinti DL, Van Drom E (1998) PALEOTEMP: a MATHEMATICA program for evaluating paleotemperatures from the concentration of atmosphere-derived noble gases in ground water. Computers & Geosci 24:33-41

Plummer LN, Busenberg E (2000) Chlorofluorocarbons. *In* Environmental tracers in subsurface hydrology. Cook P, Herczeg AL (eds) Kluwer Academic Publishers, Boston, p 441-478

Plummer LN, Busenberg E, Böhlke JK, Nelms DL, Michel RL, Schlosser P (2001) Ground water residence times in Shenandoah National Park, Blue Ridge Mountains, Virginia, USA: a multi-tracer approach. Chem Geol 179:93-111

Plummer LN, Busenberg E, Drenkard S, Schlosser P, Ekwurzel B, Weppernig R, McConnell JB, Michel RL (1998a) Flow of river water into a karstic limestone aquifer—2. Dating the young fraction in ground water mixtures in the Upper Floridan aquifer near Valdosta, Georgia. Appl Geochem 13: 1017-1043

Plummer LN, Busenberg E, McConnell JB, Drenkard S, Schlosser P, Michel RL (1998b) Flow of river water into a Karstic limestone aquifer. 1. Tracing the young fraction in ground water mixtures in the Upper Floridan Aquifer near Valdosta, Georgia. Appl Geochem 13:995-1015

Plummer LN, Rupert MG, Busenberg E, Schlosser P (2000) Age of irrigation water in ground water from the eastern Snake River Plain Aquifer, South-Central Idaho. Ground Water 38:264-283

Poreda RJ, Cerling TE, Solomon DK (1988) Tritium and helium isotopes as hydrologic tracers in a shallow unconfined aquifer. J Hydrol 103:1-9

Purtschert R (1997) Multitracer-Studien in der Hydrologie, Anwendungen im Glattal, am Wellenberg und in Vals. PhD dissertation, Universität Bern, Bern

Purtschert R, Beyerle U, Aeschbach-Hertig W, Kipfer R, Loosli HH (2001) Palaeowaters from the Glatt Valley, Switzerland. *In* Palaeowaters in Coastal Europe: evolution of ground water since the late Pleistocene. Vol 189. Edmunds WM, Milne CJ (eds) Geological Soc London, London, p 155-162

Purtschert R, Loosli HH, Beyerle U, Aeschbach-Hertig W, Imboden D, Kipfer R, Wieler R (1999) Dating of young water components by combined application of $^{3}H/^{3}He$ and ^{85}Kr measurements. *In* Isotope techniques in water resources development and management (IAEA-SM-361). IAEA, Vienna, p 59-60

Reilly TE, Plummer LN, Phillips PJ, Busenberg E (1994) The use of simulation and multiple environmental tracers to quantify ground water flow in a shallow aquifer. Water Resour Res 30: 421-433

Richter J, Szymczak P, Abraham T, Jordan H (1993) Use of combinations of lumped parameter models to interpret ground water isotopic data. J Contam Hydrol 14:1-13

Raynaud D, Jouzel J, Barnola JM, Chappellaz J, Delmas RJ, Lorius C (1993) The ice record of greenhouse gases. Science 259:926-934

Rozanski K, Florkowski T (1979) Krypton-85 dating of ground water. *In* Isotope Hydrology 1978 (IAEA-SM-228/2). IAEA, Vienna, p 949-961

Rudolph J (1981) Edelgastemperaturen und Heliumalter ^{14}C-datierter Paläowässer. PhD dissertation, Universität Heidelberg, Heidelberg

Rudolph J, Rath HK, Sonntag C (1984) Noble gases and stable isotopes in ^{14}C-dated palaeowaters from central Europa and the Sahara. *In* Isotope Hydrology 1983 (IAEA-SM-270). IAEA, Vienna, p 467-477

Sano Y, Kusakabe M, Hirabayashi J, Nojiri Y, Shinohara H, Njine T, Tanyileke G (1990) Helium and carbon fluxes in Lake Nyos, Cameroon: Constraint on next gas burst. Earth Planet Sci Lett 99:303-314

Sano Y, Wakita H (1987) Helium isotope evidence for magmatic gases in Lake Nyos, Cameroon. Geophys Res Lett 14:1039-1041

Schlosser P (1992) Tritium/^{3}He dating of waters in natural systems. *In* Isotopes of noble gases as tracers in environmental studies. IAEA, Vienna, p 123-145

Schlosser P, Shapiro SD, Stute M, Aeschbach-Hertig W (1998) Tritium/^{3}He measurements in young ground water: Chronologies for environmental records. *In* Isotope techniques in the study of environmental change (IAEA-SM-349). IAEA, Vienna, p 165-189

Schlosser P, Stute M, Dörr C, Sonntag C, Münnich KO (1988) Tritium/^{3}He-dating of shallow ground water. Earth Planet Sci Lett 89:353-362

Schlosser P, Stute M, Sonntag C, Münnich KO (1989) Tritiogenic ^{3}He in shallow ground water. Earth Planet Sci Lett 94:245-256

Schlosser P, Winckler G (2002) Noble gases in the ocean and ocean floor. Rev Mineral Geochem 47: 701-730

Schwarzenbach RP, Gschwend PM, Imboden DM (1993) Environmental organic chemistry. John Wiley & Sons, New York

Severinghaus JP, Bender ML, Keeling RF, Broecker WS (1996) Fractionation of soil gases by diffusion water vapor, gravitational settling, and thermal diffusion. Geochim Cosmochim Acta 60:1005-1018

Severinghaus JP, Brook EJ (1999) Abrupt climate change at the end of the last glacial period inferred trapped air in polar ice. Science 286:930-934

Severinghaus JP, Grachev A, Battle M (2001) Thermal fractionation of air in polar firn by seas temperature gradients. Geochem Geophys Geosyst 2:2000GC000146

Severinghaus JP, Luz B, Caillon N (2002) A method for precise measurement of argon 40/36 and krypton/argon ratios in trapped air in polar ice with applications to past firn thickness and abrupt climate change. Geochim Cosmochim Acta (in press)

Severinghaus JP, Sowers T, Brook EJ, Alley RB, Bender ML (1998) Timing of abrupt climate change at the end of the Younger Dryas interval from thermally fractionated gases in polar ice. Nature 391: 141-146

Sheets RA, Bair ES, Rowe GL (1998) Use of $^{3}H/^{3}He$ ages to evaluate and improve ground water flow models in a complex buried-valley aquifer. Water Resour Res 34:1077-1089

Shimaraev MN, Granin NG, Zhadanov AA (1993) Deep ventilation of Lake Baikal due to spring thermal bars. Limnol Oceanogr 38:1068-1072

Smethie WMJ, Solomon DK, Schiff SL, Mathieu G (1992) Tracing ground water flow in the Borden aquifer using krypton-85. J Hydrol 130:279-297

Smith GD, Newhall F, Robinson LH, Swanson D (1964) Soil temperature regimes: Their characteristics and predictability. U S Dept Agricul , Soil Conservation Service Report SCS-TP-144

Smith SP, Kennedy BM (1983) Solubility of noble gases in water and in NaCl brine. Geochim Cosmochim Acta 47:503-515

Solomon DK (2000) ^{4}He in ground water. *In* Environmental tracers in subsurface hydrology. Cook P, Herczeg AL (eds) Kluwer Academic Publishers, Boston, p 425-439

Solomon DK, Cook PG (2000) ^{3}H and ^{3}He. *In* Environmental tracers in subsurface hydrology. Cook P, Herczeg AL (eds) Kluwer Academic Publishers, Boston, p 397-424

Solomon DK, Hunt A, Poreda RJ (1996) Source of radiogenic helium 4 in shallow aquifers: Implications for dating young ground water. Water Resour Res 32:1805-1813

Solomon DK, Poreda RJ, Cook PG, Hunt A (1995) Site characterization using $^{3}H/^{3}He$ ground-water ages, Cape Cod, MA. Ground Water 33:988-996

Solomon DK, Poreda RJ, Schiff SL, Cherry JA (1992) Tritium and helium 3 as ground water age tracers in the Borden aquifer. Water Resour Res 28:741-755

Solomon DK, Schiff SL, Poreda RJ, Clarke WB (1993) A validation of the $^{3}H/^{3}He$-method for determining ground water recharge. Water Resour Res 29:2591-2962

Solomon DK, Sudicky EA (1991) Tritium and helium 3 isotope ratios for direct estimate of spatial variations in ground water recharge. Water Resour Res 27:2309-2319

Staudacher T, Sarda P, Richardson SH, Allègre CJ, Sagna I, Dmitriev LV (1989) Noble gases in basalt glasses from a Mid-Atlantic Ridge topographic high at 14°N: geodynamic consequences. Earth Planet Sci Lett 96:119-133

Stonestrom DA, Rubin J (1989) Water content dependence of trapped air in two soils. Water Resour Res 25:1947-1958

Stute M (1989) Edelgase im Grundwasser—Bestimmung von Paläotemperaturen und Untersuchung der Dynamik von Grundwasserfliesssystemen. PhD dissertation, Universität Heidelberg, Heidelberg

Stute M, Clark JF, Schlosser P, Broecker WS (1995a) A 30'000 yr continental paleotemperature record derived from noble gases dissolved in ground water from the San Juan Basin, New Mexico. Quatern Res 43:209-220

Stute M, Deák J (1989) Environmental isotope study (^{14}C, ^{13}C, ^{18}O, D, noble gases) on deep ground water circulation systems in Hungary with reference to paleoclimate. Radiocarbon 31:902-918

Stute M, Deák J, Révész K, Böhlke JK, Deseö É, Weppernig R, Schlosser P (1997) Tritium/^{3}He dating of river infiltration: An example from the Danube in the Szigetkös area, Hungary. Ground Water 35: 905-911

Stute M, Forster M, Frischkorn H, Serejo A, Clark JF, Schlosser P, Broecker WS, Bonani G (1995b) Cooling of tropical Brazil (5°C) during the Last Glacial Maximum. Science 269:379-383

Stute M, Schlosser P (1993) Principles and applications of the noble gas paleothermometer. *In* Climate Change in Continental Isotopic Records. Vol 78. Swart PK, Lohmann KC, McKenzie J, Savin S (eds) American Geophysical Union, Washington, DC, p 89-100

Stute M, Schlosser P (2000) Atmospheric noble gases. *In* Environmental tracers in subsurface hydrology. Cook P, Herczeg AL (eds) Kluwer Academic Publishers, Boston, p 349-377

Stute M, Schlosser P, Clark JF, Broecker WS (1992a) Paleotemperatures in the Southwestern United States derived from noble gases in ground water. Science 256:1000-1003

Stute M, Sonntag C (1992) Paleotemperatures derived from noble gases dissolved in ground water and in relation to soil temperature. *In* Isotopes of noble gases as tracers in environmental studies. IAEA, Vienna, p 111-122

Stute M, Sonntag C, Déak J, Schlosser P (1992b) Helium in deep circulating ground water in the Great Hungarian Plain Flow dynamics and crustal and mantle helium fluxes. Geochim Cosmochim Acta 56:2051-2067

Stute M, Talma AS (1998) Glacial temperatures and moisture transport regimes reconstructed from noble gases and delta ^{18}O, Stampriet aquifer, Namibia. *In* Isotope techniques in the study of environmental change (IAEA-SM-349). IAEA, Vienna, p 307-318

Suckow A, Sonntag C (1993) The influence of salt on the noble gas thermometer. *In* Isotope techniques in the study of past and current environmental changes in the hydrosphere and the atmosphere (IAEA-SM-329). IAEA, Vienna, p 307-318

Sugisaki R (1961) Measurement of effective flow velocity of ground water by means of dissolved gases. Am J Sci 259:144-153

Szabo Z, Rice DE, Plummer LN, Busenberg E, Drenkard S, Schlosser P (1996) Age dating of shallow ground water with chlorofluorocarbons, tritium/helium 3, and flow path analysis, southern New Jersey coastal plain. Water Resour Res 32:1023-1038

Takaoka N, Mizutani Y (1987) Tritiogenic ^{3}He in Ground water in Takaoka. Earth Planet Sci Letters 85:74-78

Talma AS, Vogel JC (1992) Late Quaternary paleotemperatures derived from a speleothem from Cango Caves, Cape Province, South Africa. Quat Res 37:203-213

Thompson GM, Hayes JM (1979) Trichloroflouromethan in ground water—a possible tracer and indicator of ground water age. Water Resour Res 15:546-554

Thonnard N, McKay LD, Cumbie DH, Joyner CF (1997) Status of laser-based krypton-85 analysis development for dating of young ground water. Geol Soc Am Abstr 29(6):A-78

Tolstikhin I, Lehmann BE, Loosli HH, Gautschi A (1996) Helium and argon isotopes in rocks, minerals, and related ground waters: A case study in northern Switzerland. Geochim Cosmochim Acta 60: 1497-1514

Tolstikhin IN, Kamenskiy IL (1969) Determination of ground-water ages by the T-^{3}He Method. Geochem Intl 6:810-811

Top Z, Clarke WB (1981) Dissolved helium isotopes and tritium in lakes: Further results for uranium prospecting in Central Labrador. Econ Geol 76:2018-2031

Top Z, Eismont WC, Clarke WB (1987) Helium isotope effect and solubility of helium and neon in distilled water and seawater. Deep-Sea Res 34:1139-1148

Torgersen T (1980) Controls on pore-fluid concentration of ^{4}He and ^{222}Rn and the calculation of $^{4}He/^{222}Rn$ ages. J Geochem Explor 13:57-75

Torgersen T (1989) Terrestrial degassing fluxes and the atmospheric helium budget: Implications with respect to the degassing processes of continental crust. Chem Geol 79:1-14

Torgersen T, Clarke WB (1985) Helium accumulation in ground water, I: An evaluation of sources and the continental flux of crustal ^{4}He in the Great Artesian Basin, Australia. Geochim Cosmochim Acta 49:1211-1218

Torgersen T, Clarke WB, Jenkins WJ (1979) The tritium/helium-3 method in hydrology. *In* Isotope Hydrology 1978 (IAEA-SM-228/2). IAEA, Vienna, p 917-930

Torgersen T, Drenkard S, Farley K, Schlosser P, Shapiro A (1994) Mantle helium in the ground water of the Mirror Lake Basin, New Hampshire, U.S.A. *In* Noble Gas Geochemistry and Cosmochemistry. Matsuda J (ed) Terra Scientific Publishing Company, Tokyo, p 279-292

Torgersen T, Drenkard S, Stute M, Schlosser P, Shapiro A (1995) Mantle helium in ground waters of eastern North America: Time and space constraints on sources. Geology 23:675-678

Torgersen T, Hammond DE, Clarke WB, Peng T-H (1981) Fayetteville, Green Lake, New York: ^{3}H-^{3}He water mass ages and secondary chemical structure. Limnol Oceanogr 26:110-122

Torgersen T, Ivey GN (1985) Helium accumulation in ground water, II: A model for the accumulation of the crustal ^{4}He degassing flux. Geochim Cosmochim Acta 49:2445-2452

Torgersen T, Kennedy BM, Hiyagon H, Chiou KY, Reynolds JH, Clark WB (1989) Argon accumulatio and the crustal degassing flux of ^{40}Ar in the Great Artesian Basin, Australia. Earth Planet. Sci Le 92:43-56

Torgersen T, Top Z, Clarke WB, Jenkins WJ, Broecker WS (1977) A new method for physical limnol —tritium-helium-3 ages: Results for Lakes Erie, Huron and Ontario. Limnol Oceanogr 22:181-193

Vollmer MK, Weiss RF, Schlosser P, Williams RT (2002) Deep-water renewal in Lake Issyk-Ku Geophys Res Lett 29:124/1-124/4

Vogel JC (1967) Investigation of ground-water flow with radiocarbon. *In* Isotopes in Hydrology (IAEA-SM-83). IAEA, Vienna, p 355-369

Vogel JC, Talma AS, Heaton THE (1981) Gaseous nitrogen as evidence for denitrification in ground water. J Hydrol 50:191-200

Weise S, Eichinger L, Forster M, Salvamoser J (1992a) Helium-3 and krypton-85 dating of shallow ground waters: diffusive loss and correlated problems. *In* Isotopes of noble gases as tracers in environmental studies. IAEA, Vienna, p 147-162

Weise S, Moser H (1987) Ground water dating with helium isotopes. *In* Isotope techniques in water resources development. IAEA, Vienna, p 105-126

Weise SM, Faber P, Stute M (1992b) Neon-21—a possible tool for dating very old ground waters? *In* Isotope techniques in water resources development (IAEA-SM-319). IAEA, Vienna, p 179-188

Weiss RF (1970) The solubility of nitrogen, oxygen and argon in water and seawater. Deep-Sea Res 17:721-735

Weiss RF (1971) Solubility of helium and neon in water and seawater. J Chem Eng Data 16:235-241

Weiss RF, Carmack EC, Koropalov VM (1991) Deep-water renewal and biological production in Lake Baikal. Nature 349:665-669

Weiss RF, Kyser TK (1978) Solubility of krypton in water and seawater. J Chem Eng Data 23:69-72

Weiss W, Sartorius H, Stockburger H (1992) Global distribution of atmospheric ^{85}Kr: A database for the verification of transport and mixing models. *In* Isotopes of noble gases as tracers in environmental studies. IAEA, Vienna, p 29-62

Weiss W, Zapf T, Baitter M, Kromer B, Fischer KH, Schlosser P, Roether W, Münnich KO (1984) Subsurface horizontal water transport and vertical mixing in Lake Constance traced by radon-222, tritium, and other physical and chemical tracers. *In* Isotope Hydrology 1983 (IAEA-SM-270). IAEA, Vienna, p 43-54

Weyhenmeyer CE, Burns SJ, Waber HN, Aeschbach-Hertig W, Kipfer R, Loosli HH, Matter A (2000) Cool glacial temperatures and changes in moisture source recorded in Oman ground waters. Science 287:842-845

Wilson GB, McNeill GW (1997) Noble gas recharge temperatures and the excess air component. Appl Geochem 12:747-762

Wüest A, Aeschbach-Hertig W, Baur H, Hofer M, Kipfer R, Schurter M (1992) Density structure and tritium-helium age of deep hypolimnetic water in the northern basin of Lake Lugano. Aquat Sci 54:205-218

Zenger A, Ilmberger J, Heinz G, Schimmele M, Schlosser P, Imboden D, Münnich KO (1990) Behavior of a medium-sized basin connected to a large lake. *In* Large Lakes: Ecological Structure and Function. Tilzer MM, Serruya C (eds) Springer-Verlag, Berlin, Heidelberg, p 133-155

Zoellmann K, Kinzelbach W, Fulda C (2001) Environmental tracer transport (^{3}H and SF_6) in the saturated and unsaturated zones and its use in nitrate pollution management. J Hydrol 240:187-205

Zuber A (1986a) Mathematical models for the interpretation of environmental radioisotopes in ground water systems. *In* Handbook of Environmental Geochemistry. Vol 2. Fritz P, Fontes JC (eds) Elsevier, Amsterdam, p 1-59

Zuber A (1986b) On the interpretation of tracer data in variable flow systems. J Hydrol 86:45-57